UNIVERSITÀ
DI SIENA
1240

UNIVERSITY OF SIENA

Department of Biotechnology, Chemistry and Pharmacy

PHD SCHOOL IN BIOCHEMISTRY AND MOLECULAR BIOLOGY, XXXIII CYCLE

PhD coordinator: Prof. Lorenza Trabalzini

Recovery of rare cells and single cells analysis : different opportunities and challenging applications

S.S.D: BIO/10

Tutor:
Prof.ssa Ottavia Spiga
Dott.ssa Cristina Tinti
Prof.ssa Paola Ricciardi-Castagnoli

PhD student:
Rebecca Maiocchi
Rebecca Maiocchi

Academic year: 2019/2020

Vivere momento per momento, volgersi interamente alla luna, alla neve, ai fiori di ciliegio e alle foglie rosse degli aceri, cantare canzoni, bere sake*, consolarsi dimenticando la realtà, non preoccuparsi della miseria che ci sta di fronte, non farsi scoraggiare, essere come una zucca vuota che galleggia sulla corrente dell'acqua: questo, io chiamo* ukiyo*.*

Asai Ryōi, *Racconti del mondo fluttuante* (*Ukiyo monogatari* – 1662)

A Kyoto

Il mio 清水 の 舞台 から 飛び降りる

INDEX

ABSTRACT

Single-cell biology is a new discipline which aims to address and solve the problem of cellular heterogeneity. Single-cell omic, which allows the molecular investigation of different cell types in a high throughput manner, is driving the Precision Medicine approaches.

Single B cell isolation strategies, the starting points of the single-cell omics, have become essential research procedures for efficiently sampling the natural repertoire of immunized animals and humans (*Tiller et al*, 2008). The goal of the first study is to demonstrate the feasibility of a novel approach to rapidly generate recombinant mAbs recovering rare antigen-specific plasma cells from complex samples derived from immunized mice. TLS Foundation, where this work has been carried out, has recently invested in Precision Medicine activities and, in particular, in the development of an alternative method to hybridomas technology to isolate rare antigen-specific B cells from blood of immunized or infected individuals. In **Study 1** we have set-up a FACS sorter-free method for a fast identification and isolation of antigen-specific plasma cells producing IgG with unique and desirable features and, moreover, we have obtained high yield TAP-PCR products. This could simplify the actual hybridomas technology procedure for the identification and molecular cloning of antigen-specific antibodies from single-B cells.

Single-cell biology is also used to address and solve problems related to tumour heterogeneity. Cancer is one of the research areas that has greatly benefited from single-cell analysis. The complexity of immune responses to cancer has hampered the development of novel therapeutical approaches with the exception of monoclonal antibody based-therapies that target specific immunomodulators. In the last 10 years PD-1 blockade monoclonal therapy has indeed revolutionized cancer treatments but a substantial population of patients is still unresponsive. To rescue unresponsive patients, the mechanism of unresponsiveness and phenotype must be elucidated. The second part of this work (**Study 2**) deals with the possibility to reveal one of the

mechanism responsible for T cells exhaustion in patients that are non-responsive to monoclonal anti-PD-1 therapy. We demonstrated that there is a correlation between the overexpression of TFX (Transcriptional Factor X, the real name of the factor has been hidden for confidentiality issues) and the onset of the characteristic features of exhaustion. Indeed the KO of this gene restores in T cells their functionality through a more active metabolism. Further in-depth study of the modulation of this transcription factor may elucidate the pathways and the genes responsible for the exhaustion phenotype in T cells.

STUDY 1: SINGLE-CELL RESOLUTION FOR PRECISION DIAGNOSTICS AND NEW THERAPIES

Introduction

Personalized Medicine

In the last few years the "*one-size fits all*" healthcare approach (*Lehrach*, 2015) has been questioned. The individual molecular landscape of the patient has been taken into account when looking at the effectiveness and safety of therapies. We know that patients do not respond to therapies and drugs in the same way (*Hafen et al*., 2014; *Lehrach*, 2015; *Roden*, 2015) for their different genomic and epigenomic profiles (*Leyens et al*., 2014).

Personalized Medicine is currently an exciting topic in medicine. The concept of Personalized Medicine was introduced for the first time on April 16th, 1999, in a short article appeared in The Wall Street Journal (*Langreth et al*., 1999). Personalized Medicine is a value-based, patient-centric paradigm that has the potential to deeply transform medical interventions by providing 'the right drug, with the right dose at the right time to the right patient' (*Sadée et al*., 2005), based on the genomic, epigenomic and proteomic profiles of an individual, whilst also remaining mindful of a patient's personal situation.

Thus, the main aims of Personalized Medicine are:

- to favour research and understanding a wide range of diseases;
- to identify the causes of different responses to drugs (pharmacogenomics) commonly used to treat different patients;
- to identify biological markers able to objectively and accurately describe signals of the risks of developing specific diseases.

According to the FDA, the aim of Personalized Medicine is to elevate benefits and reduce risks to patients by targeting prevention and treatment more effectively. It does not seek to establish novel medication for patients, but to stratify individuals into

subpopulations that vary in their response to a therapeutic agent for their specific disease. Increased utilisation of molecular stratification of patients, for example assessing for mutations that give rise to resistance to certain treatments, will provide medical professionals with clear evidence upon which to base treatment strategies for individual patients (*Mathur et al*., 2017). Furthermore, the power of Personalized Medicine lies not only in treatment, but in prevention.

In fact, the term "stratification" delineates the identification of a group of patients with similar biological characteristics and who could respond to a same drug in a similar way (*Laifenfeld et al*., 2012) and this would be possible via identification of biomarkers. With this development, there will no longer be a dependence on the adverse outcomes of trial and error prescribing methods (*Vogenberg et al*., Part1 and Part2 , 2010).

Biomarkers are biological indicators which could have a specific molecular, anatomic, physiologic, or biochemical character, which can be detected and evaluated accurately (*Biomarkers Definition Working Group*, 2001). They play a key role as indicators of an ordinary or a pathogenic biological process, having a specific physical characteristic or a biological changing produced.

Personalized Medicine is an innovative approach towards delivering improved healthcare and reducing overall healthcare costs. This would be achieved by implementing the digitalization of healthcare, by improving the healthcare IT system and by introducing innovative technologies, such as developing single-cell omics, which permit the investigation of different single-cells in a high throughput manner (*Hood et al*., 2003).

Single-cell omics

Probing cellular population diversity at single-cell resolution became possible only in recent years and it helped to answer biological questions with unprecedented resolution. The popularity of single-cell "omics" approaches, which allow researchers to dissect samples heterogeneity and cell-to-cell variation, continues to grow. Single-cell omics are becoming increasingly prevalent, thanks to the continuous and rapid

technological improvements, and contribute to the discovery of new and rare cell types and to the deciphering of disease pathogenesis and outcome.

Animal tissues are heterogeneous, encompassing numerous types of cells with unique functions, features and stages of differentiation. So far, the study and the understanding of homeostatic or pathologic mechanisms progressed by studying cell population in bulk but, in this way, the analysis revealed only the average features of the population and could hide the cell-to-cell variability present in all tissues which have direct and significant consequences on the cell function (*Altschuler and Wu*, 2010; *Strzelecka et al*., 2018), but also the importance of rare populations. A deep understanding of cellular variability and the impact of this variability in tissue function will allow us to understand how changes in cellular dynamics can influence the entire organism and even lead to cancer, diabetes, metabolic disorders and accelerated ageing (*Cheung et al*., 2018; *Ecker et al*., 2018; *Enge et al*., 2017; *Hurria et al*., 2016). In parallel, isolation and characterization of rare cell populations may uravel different sensitivity to therapies but also identify novel accurate biomarkers.

Recent advantages in methodology and cost effectiveness of high-throughput 'omic' technologies have enabled their application to the study of single cells, allowing a complete and unbiased analysis of the content of individual cells.

Individual –omic, as well as the integrated profiles of multiple -omes, such as the genome, the epigenome, the transcriptome, the proteome, the metabolome, the antibodyome, and other omics information, are expected to be valuable for health monitoring, preventative measures, and for the application of the Personalized Medicine paradigm (*Chen et al*., 2013).

Diverse approaches for studying different "layers" of single-cells have been developed (Fig.1):

- ***Single-cell genomics***: this technology could be used to resolve the variation between individual cells at the genomic level, including the analysis of single-nucleotide variants (SNVs) and subchromosomal copy-number variants (CNVs), but also somatic mutations and insertions or microdeletions. Several amplification methods have been developed for single-cells DNA sequencing

(*Gawad et al*., 2016; *Wang and Song*, 2017) allowing researchers to reconstruct cell lineages and to study genetic alterations of rare cell types, such as cancer stem cells (CSCs). Indeed, cancer biology is one of the research areas that greatly benefited from the application of single-cell DNA sequencing;

- ***Single-cell epigenomics***: the identification of epigenetic events at the single-cell level is particularly informative during development where key epigenetic signatures correlate to active or inactive transcriptional states (*Clark et al*., 2016);

- ***Single-cell transcriptomics***: single-cell RNA sequencing (scRNA-seq) technologies have also advanced. These technologies rely on the conversion of RNA into complementary DNA, which is then amplified to obtain large enough quantities for sequencing. Studying the transcriptome of individual cells is a useful tool since it allows an unbiased determination of the cell state, representing a step forward from the use of cell surface markers, wherein cells that homogeneously express such markers can differ substantially in their transcriptome, state and function (*Altschuler and Wu*, 2010). A wide adoption of scRNA-seq approaches have shifted the application of this method from descriptive analyses of cell heterogeneity towards the understanding of disease mechanisms, to the discovery of new biomarkers to be used in research (*Strzelecka et al*., 2018);

- ***Single-cell proteomics***: Proteome analysis at the single-cell level could provide essential information on the actual state and function of a cell. However, analysing the protein content of a single cell is still challenging, even if approaches based on FACS, single-cell mass spectrometry, liquid chromatography and tandem mass-spectrometry have been successfully applied (*Strzelecka et al*., 2018);

- ***Single-cell multiomics***: this discipline integrates of data from diverse single omics platforms, providing muti-faceted insight into the interrelation of these omics "layers". Such parallel analysis of the genome and transcriptome is appealing as it allows to link the genotype of a cell to its phenotype.

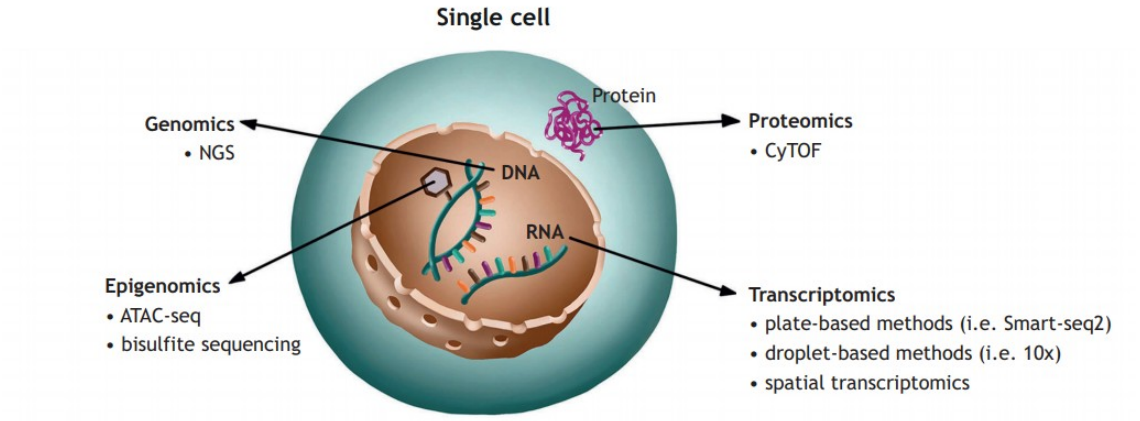

Fig. 1. *Schematic representation of single-cell omic technologies. Combined information about the transcriptome, genome, proteome and epigenome of a single cell, obtained with constantly evolving technologies, will drive the progress of personalised medicine and generation of improved targeted therapies.*

As single-cell multi-omics technology becomes progressively high throughput, computational resources and time needed for processing the raw data will be an important aspect. Raw files for each omic type must be separately processed, aligned, filtered and quality-controlled in a manner that accounts for complications inherent in single-cell measurements, such as low signal-to-noise ratio, technical amplification artifacts and technical variation (*Bock et al*., 2016). Each omics layer of processed data is then assigned back to the single cell and co-analyzed with both mathematical and statistical models to reveal patterns of regulation. Pipelines and new algorithms that treamline and shorten the computational time needed for a data processing will be essential for increasingly complex, multi-dimensional experiments (*Hu et al*., 2018). The harmonization and standardization of single-cell technologies will lead to unprecedented discoveries and translational applications from bench to clinic (*Shalek and Benson*, 2017; *Strzelecka et al.*, 2018; *Wang and Song*, 2017).

Single-cell genomic and epigenomic techniques have become necessary for early disease detection, accurate diagnosis and prognosis, monitoring disease progression in

tissues, paving the way for personalized treatment and next-generation health care (*Kamies and Martinez-Jimenez*, 2020).

Recovery of single cells

At present, the isolation and separation of rare single cells is still a technically challenging task. Main challenges are the yield and quality or, in other words, the integrity and purity of the cells as well as the throughput and the sensitivity of single cell isolation methods (*Gross et al*., 2015). Another challenge with rare cells is the enrichment procedures that are necessary when the target cells have a frequency below one out of one million contaminants.

Then, isolating multiple types of molecules from a single cell is the starting point for single-cell omics measurement.

The first step is to collect a single cell randomly from a heterogeneous population. The standard protocol is based on the disaggregation of complex biological matrices into a single intact and viable cell by mechanical or enzymatic dissociation and, in a second step, to capture single cells from the dissociated cell suspension.

Several approaches can be used and rely on different working principles, mainly physical and biological properties, including size, density, cellular charge, and specific expression of cellular markers, including serial dilution, robotic micromanipulation, flow-assisted cell sorting (FACS) and microfluidic platform (*Wang and Navin,* 2015). The outcome of this first collection step is critical and many limitations persist, despite the rapid development of new techniques. One of them is the variations induced by sample processing (*van den Brink et al*., 2017). Currently new protocols that minimise dissociation-induced gene and protein expression changes are being developed (*Lambrechts et al*., 2018). Moreover, generation of single-cell suspensions that are representative of the initial cell population of interest, including the spatial contextualisation, is still challenging.

Technologies for single-cell separation can be briefly classified according to their:

- ***Level of automation***, distinguishing manual methods from automated devices for cell separation;

- ***Ability to isolate specific/individual cells***, distinguishing statistical methods from a targeting specific rare populations one;
- ***Compatibility with certain future application requirements***, distinguishing technologies mainly applied for production of monoclonal cell cultures (derived from single cells) from technologies preferably used for single-cell genome/proteome analysis (*Gross et al*., 2015).

In general, the method to be applied strongly depends on the nature and origin of the sample and the processing or analysis to be performed on the cells once being isolated. The most widespread technologies used for the handling of single-cells are (Fig.2):

- ***Limiting Dilution***: Due to the statistical distribution of cells in a suspension, the number of cells in a highly diluted sample can be as low as one per aliquot, when the suspension is split into small volumes (aliquots). Such seeding of cells in low concentration is indeed simple to carry out with standard pipetting tools, but it is not very efficient since the probability of achieving a single-cell in an aliquot is of statistical nature and the technique is subjected to manual errors. The probability to obtain a certain number of cells per aliquot (i.e., 0, 1, 2, etc.) is described by Poisson's distribution (*Staszewski*, 1984). In order to confirm the presence of one single cell per well, an additional control step (e.g., by microscopy) is required (*Gross et al.*, 2015). The advantages of serial dilution include the simplicity and manual operator's immediacy of moving single cells from the cell suspension to individual reaction chambers. This helps limit the degradation of more volatile molecules such as RNA or protein and may reduce the possibility of non-physiologic changes in chromatin accessibility and conformation (*Wang and Navin*, 2015; *Svensson et al*., 2017), but it results time/effort consuming.

- ***Flow cytometry***: FACS systems employ laser excitation to exctract information by fluorescent staining. Indeed, cell suspensions are pressure driven through a flow cell and then the cell stream rapidly passes by a laser which gives signal,

which, on their turn, are converted into cells' respective physical, chemical, or optical properties often enhanced by synthetic markers such as fluorescent dyes. This approach results more expensive for this reason. Apart from size analysis and counting, the bypassing cells can also be sorted. After the analysis, the cell stream is forced through a small nozzle (typically 60–100 μm orifice diameter) and, applying ultrasound vibrations, it is broken in droplets, some of which carry cells. Using electrically charged plates, these droplets can be guided to a collector vessel. FACS technology is nowadays an accepted, worldwide standard in analysis and sorting of cell populations (*Underwood et al*., 1988; *Herzenberg et al*., 2002. Nevertheless, for certain applications, FACS systems are still limited: cells must be in suspension, so tissues need to be dissociated resulting in loss of cellular functions and cell-cell interactions as well as tissue architecture (*Jahan et al*., 2012); Subpopulations with similar marker expression are difficult to differentiate and overlap of emission spectra between fluorochromes may lead to an increasing noise level and difficulty for a good separation of sub populations; Further, FACS sorting may have non-negligible effects on cell viability.

- ***Laser capture microdissection (LCM):*** it is an advanced technique to isolate individual cells or cell compartments from mostly solid tissue samples which are fixed in formalin, embedded in paraffin, or cryo-fixed (*Emmert-Buck et al*., 1996; *Espina et al.,* 2007; *Esposito*, 2007). Using a microscope, the target cells are identified on a tissue section. The operator marks the section to be cut off on the display by drawing a line around it. Along this trajectory the laser cuts the tissue and the isolated cell (or compartment) is extracted. Analysis of solid tissue is of great interest when investigating heterogeneous tissue sections regarding their cellular structure as well as physiological and pathological processes (*Fink et al*., 2006). In oncology, the correlation of molecular information obtained from single-cells with their location in the tissues has become an important research field. In combination with immune histological staining, LCM is a powerful tool for solid sample analysis at the single-cell level

(*Nakamura et al*., 2007). However, for full exploitation of this technology, the spatial mapping of single-cell in the tissue is required. Moreover proceeding with the extraction, single-cell integrity might be compromised (*Liu*, 2010) but also some contaminants as adjacent cells could be transferred together.

- ***Manual Cell Picking***: it consists in micromanipulators which, combined with a microscope and micro-pipettes, to pick cells manually form suspensions in dish or well-plate. Micropipettes are made of ultrathin glass capillaries coupled to an aspiration and dispensation unit. Via microscope observation the operator selects a specific cell, moves the micro-pipette in close proximity and aspirates the cell by applying suction to the micropipette. The aspirated liquid volume, including the selected cell, can be transferred to a collection vessel, where it is released by dispensation. Similar to LCM systems, the targeted isolation of a specific cell under microscope vision is one of the key benefits of this technology. However, the manual process limits the throughtput and it should always be coupled with an additional microscope to confirm that the single-cell has been successfully transferred (*Gross et al*., 2015).

- ***Microfluidics*** (*Lecault*, 2012): several microfluidic devides have been proposed for single-cell analysis and all of them have been created following one of the following microfluidic principles to extract single cells:
    - Droplet-in-oil-based isolation (*Brouzes et al*., 2009) which uses channels filled with oil to hold separated aqueous droplets (similar to an emulsion). Within these droplets, single cells can be contained and thus be isolated according to Poisson's distribution;
    - Pneumatic membrane valving (*Gomez-Sjoberg et al*., 2007) uses pressurized air, digitally managed from an operator, to open and close a membrane which controls a microfluidic channel;
    - Hydrodynamic cell traps (*Di Carlo et al*., 2006) where a microfluidic channel allows only one cell to enter the "trap".

Microfluidic systems can be operated with very low volumes regarding cell sample as well as reagents, which is advantageous for rare cell applications.

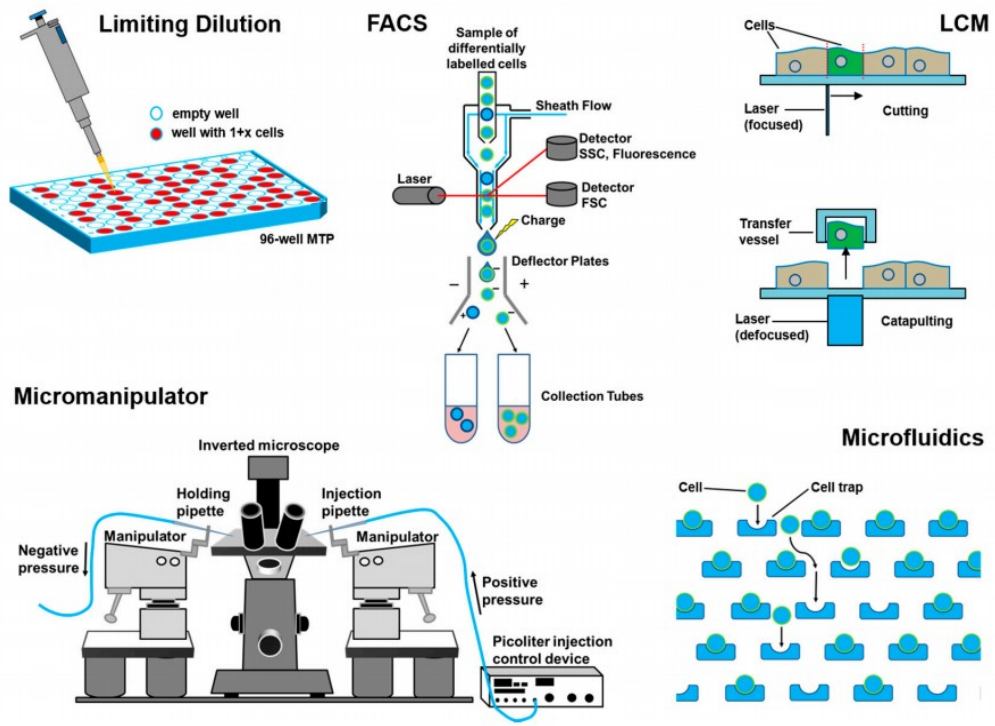

Fig. 2 *Schematic overview of single-cell separation technologies;*

Furthermore, approaches to miniaturize flow cytometers by use of microfluidic technologies have been proposed (*Zhang et al*., 2014). One of the goals of this field of research is to combine the advantages of each technology to create new more performing technological solutions.

In the last decade, Menarini Silicon Biosystems has developed an image-based cell-sorting technology, named DEPArray™, which synergistically combines microelectronics and microfluidics in an highly automated platform, enabling a simple and reliable way of isolating pure, single, viable rare cells from the heterogeneous sample, with unprecedent purity for molecular analysis (*Gambari et al*., 2003; *Polzer et al*., 2014; *Manaresi et al*., 2003). It is based on the ability of a non-uniform electric field to exert forces on neutral, polarizable particles, such as cells, that are suspended

in a liquid. This electrokinetic principle, called dielectrophoresis (DEP), can be used to trap cells in stable levitation in DEP cages by creating an electric field above a subset of electrodes in an array that is in counter phase with the electric field of adjacent electrodes. When a DEP cage is moved by a change in the electric field pattern, the trapped cells move with it (Fig.3).

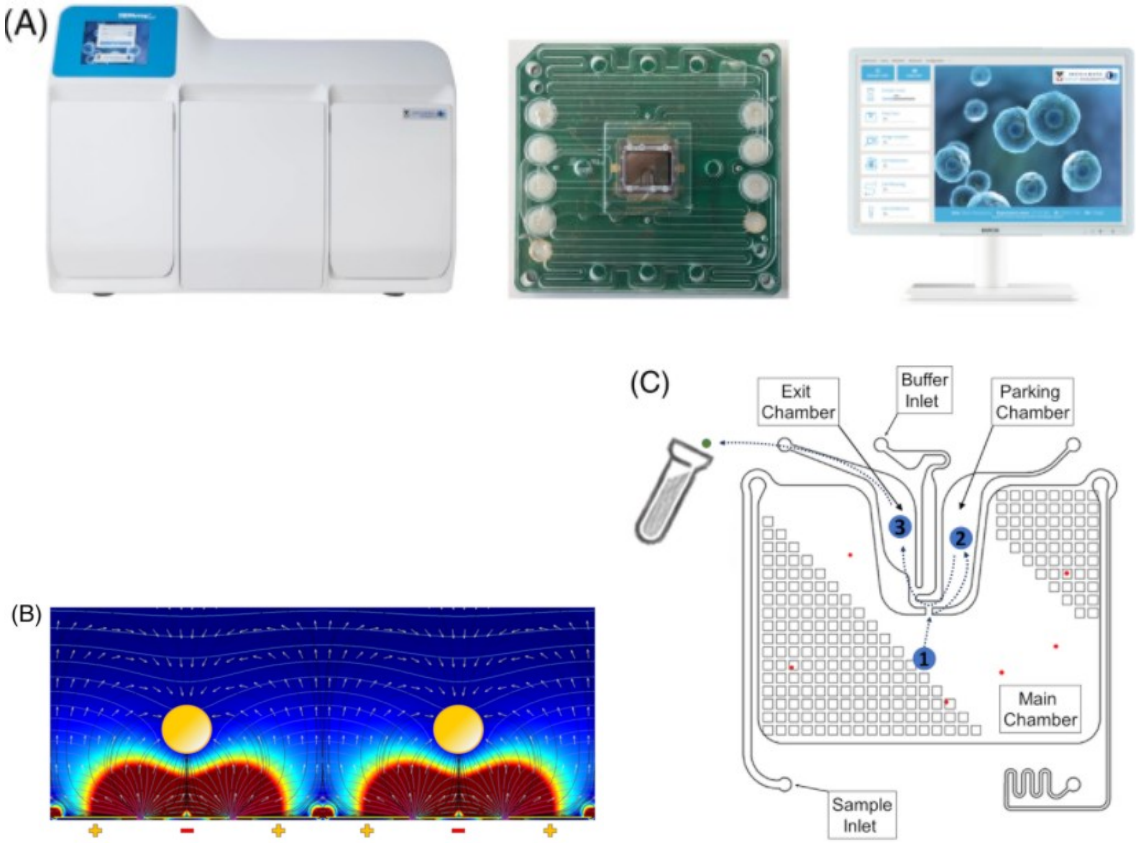

Fig.3 *Main components of DEPArray™ NxT system: the benchtop instrument (left), the cartridge (middle) that combines microfluidics and microelectronics, and the CellBrowser™ software (right) to elaborate fluorescence and bright field images for automatic or operator-assisted cell selection (a); Schematic representation of dielectrophoresis (b); Schematic representation of DEPArray™ chip (**c**).*

The ability to manipulate individual cells is combined in the DEPArray™ with high quality image-based cell selection and it allows the user to identify and recover specific individual cells of interest from complex, heterogenous samples. Indeed, in the instrument, the illumination is provided by a stabilized LED lamp, which combines high efficiency excitation and emission filters, providing the possibility to get images in up

to five fluorescent channels. Moreover, the fluorescent microscope allows acquiring high-resolution images for each individual cell in the sample thus enabling a high-definition analysis of in-cage events, detecting the specific expression markers. Bright field filter visualization coupled to fluorescence signals allows an accurate selection based on the combination of physical and biological parameters, including cell size, shape, circularity, and fluorescence intensity. Then, the elaboration of high-resolution images minimize the possibility to select inappropriate events, such as debris and doublets (Fig.4).

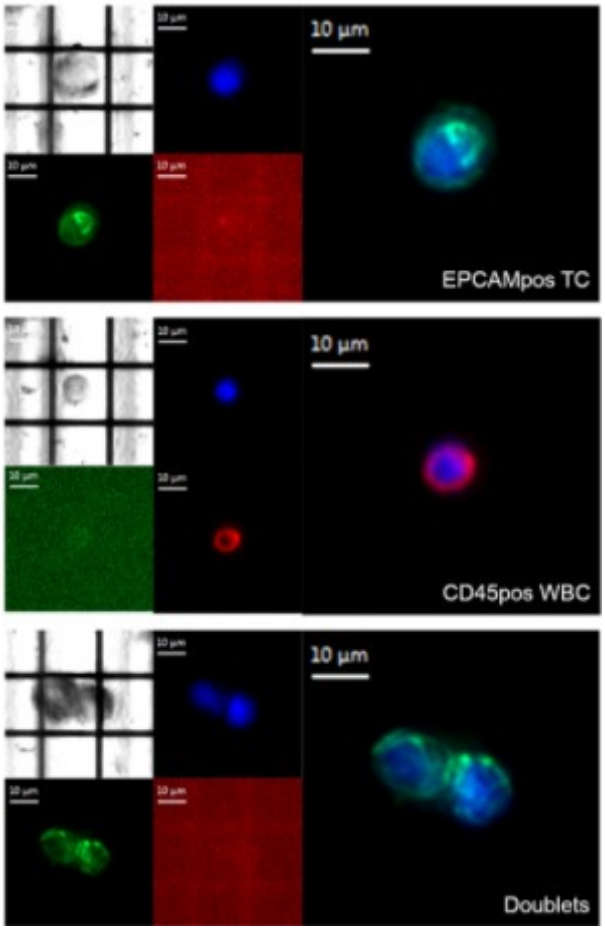

Fig.4 *Images of individual trapped cells, identified by high-resolution optical system, which gives a real-time acquisition and multichannel analysis of cell population during the chip scan.*

Once identified, each target cell can be isolated from the bulk population, automatically, moving the selected DEP cages and eluting cells in various supports, through an accurate microfluidic control.

The DEPArray™ technology is a promising technology which finds broad application from translational research—to identify biomarkers of response and resistance—toward routine clinical application (*Di Trapani et al*., 2018).

Biomarkers and monoclonal antibodies: powerful weapon for Personalized Medicine

For the development and rapid adoption of Personalized Medicine it is vital that pharmaceutical companies invest in these new technologies and show willingness to work collaboratively with research teams. Identification of more accurate biomarkers are fundamental to pave the way to a pro-active approach to Personalized Medicine. Biomarkers have a key role in identifying patients' sub-groups, but also, in a more specific and microscopic-vision, they can be a potent tool for identifying and isolating rare populations from homogenous suspensions and identify rare populations. It is impossible to implement with this last mentioned approach during a bulk analysis.

In the workshop "*Stratification biomarkers in Personalized Medicine*" held in Brussels on June 2010 (*European Commission, DG Research*) biomarkers have been described as biological indicators which could have a specific molecular, anatomic, physiologic, or biochemical characteristic, which can be detected and evaluated accurately (*ec.europa.eu/research/health/pdf/biomarkers-for-patient-stratification_en.pdf*). From this point of view, a biomarker can be used for different purposes:

- ***Diagnostic biomarker***: to detect a specific disease as early as possible;
- ***Susceptibility/risk biomarker***: used to assess the risk of developing a disease;
- ***Prognostic biomarker***: to monitor the evolution of a disease (indolent or aggressive) but can also be predictive. These biomarkers provide further understanding of disease mechanisms, not necessarily linked to drug treatment;
- ***Predictive biomarker***: used to value the response and the toxicity to a given treatment. In this case the markers are able to predict the evolution of a disease.

Biomarkers are used in order to stratify dissimilar patient groups and thus have an important role in the development of personalized, preventive or therapeutic strategies.

Genomics, transcriptomics and proteomics have largely contributed to the identification and the development of biomarkers. Understanding the patient's genetic make-up is essential for providing the best possible care approach for many disorders. Gene therapy is coming "back to center stage" (*Naldini*, 2015) in fact, recent clinical trials have shown its significant therapeutic benefits and a brilliant safety record. However, the genomic approach has some technological limitations, such as the occurrence in same cases of false negative results that could be misleading. For this reason, a multiplex approach integrating various fields such as proteomics, phenotype studies, imaging and functional in vivo studies should be privileged (*ec.europa.eu/research/health/pdf/biomarkers-for-patient-stratification_en.pdf*). The identification of biomarkers remains a key element in the research of both common and rare diseases (*Trusheim et al*., 2011). The related process is quite complex and comprises of four steps:

- Discovery;
- Development;
- Validation;
- Application.

Once biomarkers have been identified, monoclonal antibodies (mAbs), acting as "molecular probes" able to selectively recognize and bind a specific marker, are a fundamental tool to exploit this technology for both research and clinic.

Since the first generation of monoclonal antibodies in 1975, the antibody industry has grown exponentially. Even if this industry has largely focused its efforts on the development of mAbs for therapeutic and diagnostic purposes, it is important to point out that the antibody discovery field fuels the growing demand of these novel diagnostics and therapeutics (*Mike Fan*, 2018).

Past market data (2012–2017) indicated a doubling of the mAbs market, a trend that is anticipated to continue to 2022 when mAbs sales are expected to reach US$130–200 billions driven by a healthy pipeline and increasing roles for biosimilars and emerging economies (Fig. 5b). Following a decade of stagnation (2002–2012) with an average of 1.6 new mAbs approved per year between 2002 and 2012, recently the regulatory bodies in the USA and the EU have streamlined approvals, resulting in 35 mAbs entering the market since 2013 and an additional ~350 are currently in clinical trials (*Reichert*, 2012) (Fig.5a). To counteract the 'biosimilars effect', pharmaceutical companies are attempting to identify new disease targets for existing mAbs (drug repositioning) and the development of new technologies that facilitate faster drug discovery and shorter time-to-clinic processes, including single-cell printing and cloning, high-throughput screening, and selection of the best clones and culture in miniaturized bioreactor systems for improved scalability (*Grilo et al.*, 2018).

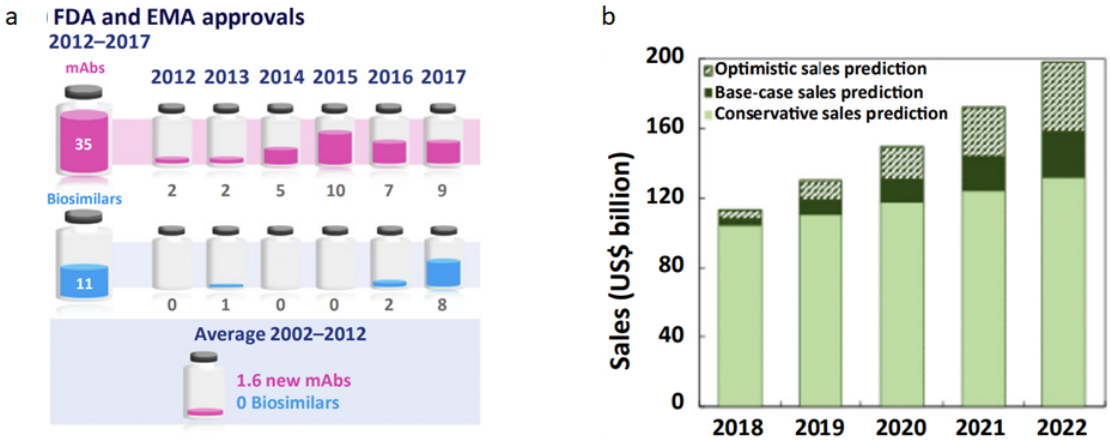

Fig. 5 *Schematic representation of FDA and EMA approuved mAbs and Biosimilars between 2012 and 2017 (a); Schematic representation of mAb sales prevision from 2018 to 2022 (b).*

Since *Köhler* and *Milstein* first described a method for the generation of mAbs via their hybridoma technology in 1975 (*Köhler and Milstein*, 1975), monoclonal antibodies have become both essential research reagents and highly successful therapeutic molecules. The rapid production of monoclonal antibodies isolated from an immunized animal is an essential starting step to develop therapeutic and diagnostic agents and to support vaccine studies.

Although the traditional hybridoma method has revolutionised the use of monoclonal antibodies (*Aman et al*., 1984; *Kozbor et al*., 1982; *Redmond et al.,* 1986; *Stahli et al*., 1980; *Steinitz et al*., 1977; *Striebich et al*., 1990), the technology is relatively inefficient due to genomic instability (loss of chromosomes and onset of mutations) and low mAb expression in the resulting cell lines. Moreover, its reliance on fusion of a B cell to a suitable myeloma partner, means that only a very small percentage of splenocytes from an immunized animal are immortalized (5×10^{-6} efficiency with conventional PEG fusion) (*Yu et al*., 2008). As a result, the vast majority of B cells are not sampled, and it is possible that rare antibodies, with desirable properties, will not be identified and recovered. Hybridoma screening is also mostly restricted to rodent immunizations, limiting the potential diversity, and time consuming (Fig.6).

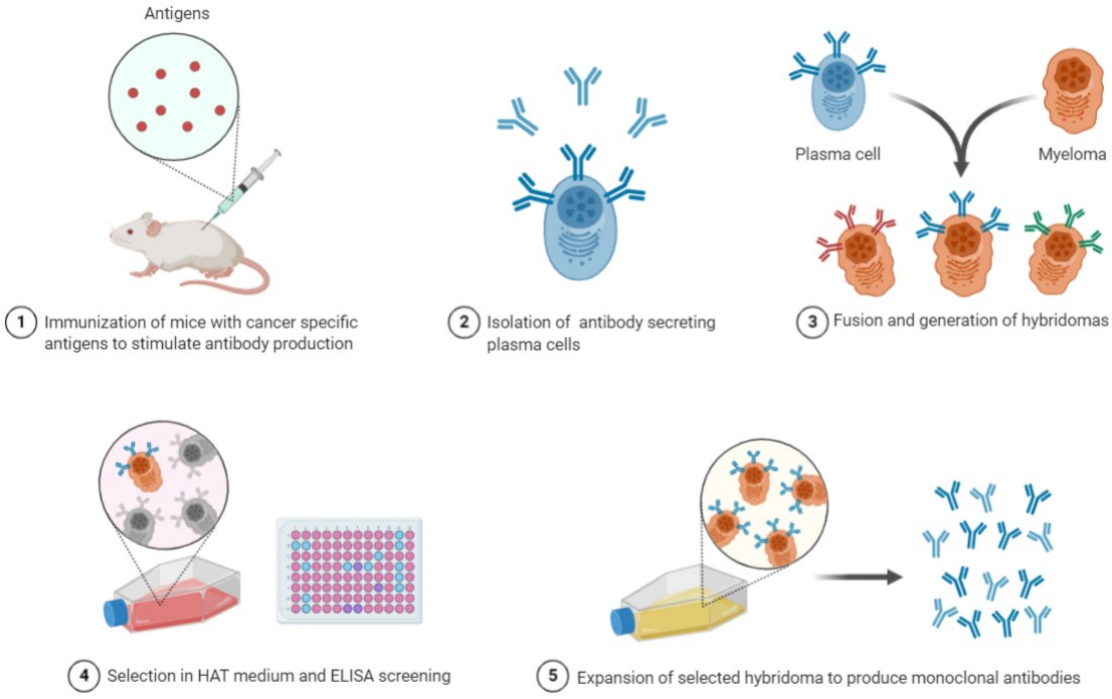

Fig. 6 *Schematic representation of the traditional hybridoma protocol to obtain immortalized cells producing mAbs.*

To solve these limitations, display methodologies have been developed, such as phage, yeast, ribosomal or mammalian display platforms (*Beerli et al*., 2010*; Lim et al.,* 2014; *Saggy et al*., 2012; *Strohl,* 2014). PCR amplified variable heavy- (VH) and light- (VL)

regions from an immunized organism are randomly paired within a library that can be successively screened for antigen binding. Finally, the VH-VL region pairs binding with higher affinity are subcloned into mammalian expression plasmids for large-scale production (Fig.7).

However, the random combination of antibody variable region genes results often in the loss of natural cognate heavy and light chain pairings that are evolved and selected in vivo during an immune response, resulting in reduced specific diversity (*Meijer et al*., 2006; *Smith et al*., 2009). Moreover, as a result of this random pairing, antibodies from naïve antibody libraries typically require further engineering steps in vitro in order to increase affinity and stability prior to progression as a therapeutic molecule.

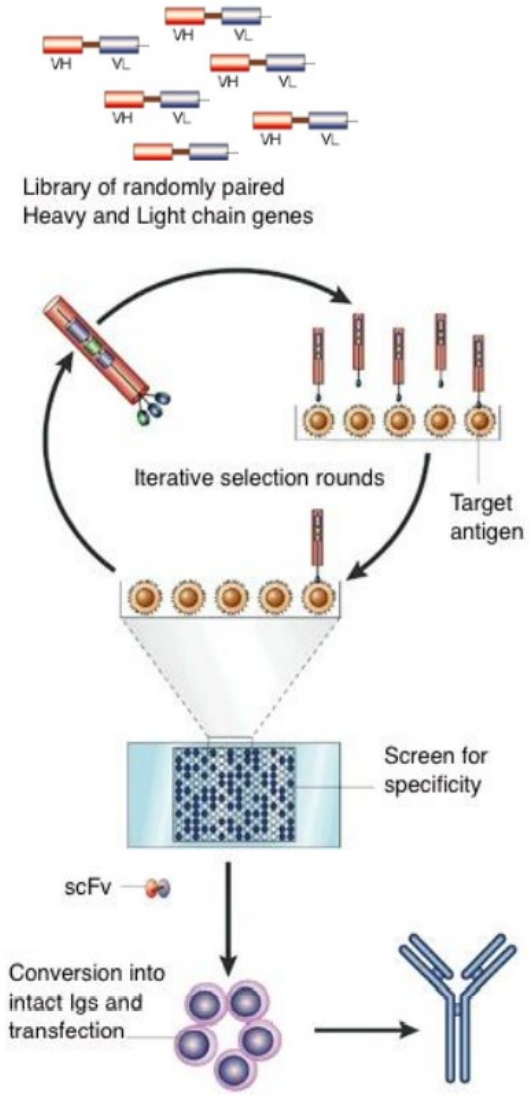

Fig.7 *Schematic representation of display methodologies.*

To deal with these problems associated with both hybridoma/immortalized cell lines and combinatorial display platforms, new techniques have been developed to isolate and clone variable region of cDNA from antigen-specific single B cells into antibody expression vectors (*Scheid et al*., 2009; *Smith et al*., 2009).

In recent years, there has been an emergence of a number of single-B cell technologies that allow the direct sampling of the immune repertoire (*Tiller*, 2011). Antigen-specific memory B cells expressing surface IgG have been utilized extensively as a source of monoclonal antibodies. For example flow cytometry, but also B cell panning were used to sort single, antigen-labelled B cells (*Di Niro et al*., 2017; *Dohmen et al*., 2005; *Townsend et al*., 2001; *Scheid et al*., 2009; *Kodituwakku et al*., 2003; *Lagerkvist et al*., 1995; *Lightwood et al*., 2006). Alternatively, memory B cell culturing and screening followed by micromanipulation of single antigen-specific B cells (*Lightwood et al*., 2013) or single-cell memory B cell cultures (*Kwakkenbos et al.*, 2010) have also been successfully employed as methods for monoclonal antibody generation.

The terminally-differentiated plasma cell subset of B cells also represent an excellent source of high quality antibodies (Fairfax et al., 2008; Radbruch et al., 2006; *Reddy et al*., 2009; *Shapiro-Shelef et al*., 2005; *Slifka et al*., 1998; *Slifka et al.,* 1998; *Smith et al*., 1997; *Tarlinton et al*., 1997*; Tarlinton et al*., 2000; *Manz et al.,* 1997; *Manz et al*., 2005; *Benner et al*., 1981). Plasma cells represent <1% lymphoid cells, but are responsible for the production of the vast majority of circulating IgG (*Shapiro-Shelef et al*., 2005; *Manz et al.,* 2005). Therefore, following screening of an immune serum for a particular target, it is an attractive option to “go fishing” for the plasma cells that are directly making the antibodies against the antigen of interest.

To exploit the high secretory capacity of plasma cells, a number of techniques have been developed that allow for the identification and isolation of antigen-specific cells. *Manz et al*. (1995), and more recently *Carroll and Al-Rubeai* (2005), described the use of a cell-surface affinity matrix to capture secreted immunoglobulin and allow for phenotypic screening via flow cytometry. *Babcook et al*.(1996) described a hemolytic plaque assay that allowed the identification of plasma cells producing antibody against

a target protein attached to sheep red blood cells. The use of microengraved array chips, designed to harbor and screen single plasma cells or activated B cells, has also been described (*Jin et al*., 2009; *Jin et al.*, 2011; *Love et al*., 2006; *Ogguniyi et al*., 2009; *Ozawa et al*., 2012; *Park et al*., 2011; *Yoshimoto et al*., 2013). Anyway, the number of antibodies capable of being cloned and expressed using this method is limited by the methods for single cell isolation which currently rely on manual micromanipulation and are therefore time/effort consuming and low throughput.

Plasma cells also benefit from an increased level of immunoglobulin mRNA compared with memory B cells (*Shapiro-Shelef et al*., 2005; *Coronella et al*., 2000; *Chen-Bettecken et al.*, 1987), thereby facilitating the recovery of variable-region genes from single isolated cells.

Since the heavy- (HC) and light- (LC) chains are already paired, there is no need to screen large libraries to identify correctly paired mAbs and avoid the inefficient hybridoma fusion step, thereby enabling efficient mining of the immune B cell population. This approach can facilitate the discovery of rare antibodies that may possess unique highly desirable properties as well as the generation of large and diverse panels of antibodies. The preservation of the natural heavy and light chain pairings during cloning of antibody genes favours the generation of recombinant antibodies with high affinity, specificity and stability.

Only a single cloning and expression step and a single round of screening are required to select the highest affinity mAbs whose recombinant production will be then accomplished by establishing high-producing stable cell lines.

The goal of the first study is to demonstrate the feasibility of a novel approach to recover unique and single plasma cells and, then, to rapidly generate recombinant mAbs through TAP-PCR protocol. This platform contains a single high-throughput cloning step followed by rapid generation of a continuous source of recombinant mAbs.

Materials and Methods

Cell cultures

- Expi293™ (Life Technologies – catalog #A14527) were cultivated in 25mL of Expi293 medium (Gibco - Life Technologies – catalog #A1435101) in sterile PC Flasks, Vented, Plain Bottom, 125mL (Fisher Scientific) at 37°C in a 8% CO_2 environment at 125rpm in the Benchtop CO_2 incubator with built in shaker Brunswick™ S41i (Eppendorf) incubator. Deepwell plate 96/2mL white border (Eppendorf) were also used in the same conditions but at 1000rpm with Eppendorf Mixmate Shaker (Eppendorf).

- Ramos (ATCC – catalog #CRL-1596), TF-1 (ATCC – catalog #CRL-2003), NIH-3T3 (ATCC – catalog #CRL-1658) and Flp-In™-3T3 Cell Line (Thermo Fisher Scientific – catalog #R76107) cell lines were cultured in RPMI1640™ or D-MEM™ medium (Corning – catalog #10-040-CV and #10-017-CV, respectively) with 10% (v/v) heat inactivated fetal bovine serum (FBS – Gibco – Life Technologies), 1% (v/v) penicillin-streptomycin mixed solution (Gibco - Life Technologies – catalog #15140122), 2mM (v/v) glutamine (Gibco - Life Technologies – catalog #35050038) and 1% (v/v) Sodium Pyruvate (NaP - Gibco - Life Technologies – catalog #11360070).

Cell lines were free of mycoplasma contamination. Cell cultures were maintained in cell culture dishes or 6-12-24-96-384 wells sterile plates for cell culture (Corning) and at 37°C in a 5% CO_2 and humified environment in the GalaxyS incubator (RS Biotec). For the TF-1 cell line, 2-5ng/mL of Human Granulocyte Macrophage Colony Stimulating Factor (Human GM-CSF – Sigma Aldrich – catalog #H5666) was added to the medium.

Plasmid Design

The pEF5/FRT/V5-DEST™ Gateway™ (Invitrogen - Thermo Fisher – catalog #V602020) vector, containing the DNA sequence of the full length of the protein TLS1 (3XFLAG-TLS1full-PEF5-F), and the pcDNA™ 3.4 TOPO® vector (Invitrogen - Thermo Fisher – catalog #A14697), containing the DNA sequence of the same protein without the transmembrane domain but fused together with a HIS-tag domain and the

sequence of the heavy chain of IgG1 (TLS1-L-ECD-HIS and TLS1-L-ECD-hiGg1E1-F, respectively), but also the plasma cell #3 heavy and light variable regions (PB3_mIgG12 and PB3_mIgK), were obtained from GeneArt Gene Synthesis (Thermo Fisher Scientific). pGLuc, pCDM8-GFP plasmids were already available in house. Each plasmid was resuspended in 50µL of TE buffer (10mM Tris pH8, 1mM EDTA – Sigma Aldrich) to reach a final concentration of 100 ng/µL.

Heat shock bacterial transformation and plasmid extraction, precipitation and quantification

All plasmids, at a final concentration of 10ng/µL, were amplified in *Escherichia coli* DH5α or Mach1 $T1^R$ competent cells (Life Technologies – Invitrogen – catalog #18265-017 and #C869601, respectively), following manufacturer's instructions. Briefly, an aliquot of 50µL of competent cells for each transformation was thawed on ice into a 1.5mL microcentrifuge tube. Each plasmid was diluted 1:10 in TE buffer and then 1µL was added to the cells and mixed gently. Tubes were incubated on ice for 30 minutes and then heat-shocked for 20 seconds in a 42°C heating block module (Eppendorf). Tubes were placed again on ice for 2 minutes. Afterwards, 950µL of pre-warmed sterilized LB medium (Miller LB broth - Sigma Aldrich – catalog #L3522) were added to each tube and they were incubated at 37°C for 1 hour at 225 rpm, using Minitron Incubator Shaker (Infors HT) . Then 100µL and 900µL from each transformation were spreaded on pre-warmed selective plates for bacterial cultures (Fisher Scientific) previously prepared with Lennox LB broth with agar (Sigma Aldrich – catalog #L2897) and 100µg/mL Ampicillin (Ampicillin Sodium Salt - Shelton Scientific – catalog #171254). Plates were incubated at 37°C O/N. The following day a single colony was spotted and added to 25mL of LB medium and 100µg/mL Ampicillin in Glass Flasks (Schott Duran) and incubated at 37°C, O/N at 225rpm. 50% of the culture, recovered the next day, was used to create a working seed with the addition of 10% glycerol (Glycerol for molecular biology, >99% - Sigma Aldrich – catalog #G5516) and kept at -80°C, while the other part was submitted to the plasmid extraction using QIAprep Spin Miniprep Kit (Qiagen – catalog #27104), following manufacturer's instructions. To

quantify, plasmids were eluted in 40µL of TE buffer pH 8 and then the absorbances at 260 and 280nm were misured with Nanovue (GE Healthcare). Only plasmid preparations with A_{260}/A_{280} ratios between 1.75 and 2.00 were used. If DNA was too much diluted, DNA was extracted by ethanol precipitation. Briefly, 0.1 volumes 3M Sodium acetate, SigmaUltra, minimum 99% (Sigma Aldrich – catalog #S2889) and 3 volumes ice cold 100% Ethanol (Sigma Aldrich – catalog #51976) were added to each sample and then we incubated at -20°C O/N. The following day samples were centrifuged at 13000rpm at 4°C for 30 minutes through Microcentrifuge 5415-R (Eppendorf), the recovered pellet washed twice with 0.5mL ice cold 75% ethanol and spinned again at 4°C for 10 minutes each time. Next, ethanol was removed and we spinned quickly to remove any trace of it. In the end samples were air dried and resuspended in 20µL of UltraPure Distilled Water DNAse/RNAse free (Invitrogen – catalog #10977049). The absorbance at 260 and 280nm were measured again.

Transfection and supernatant recovery

The plasmids TLS1-L-ECD-HIS, TLS1-L-ECD-hiGg1E1-F, PB3_mIgG12 and PB3_mIgK were transiently transfected into Expi293 cells using ExpiFectamine 293 Transfection Kit (Gibco - Life Technologies – catalog #A14524) in sterile PC Flasks, Vented, Plain Bottom, 125mL (Fisher Scientific) as per manufacturers' instructions.

Plasmids PB3_mIgK and PB3_mIgG12 were transiently cotransfected with a proportion of 70% and 30%, respectively, but optimization of the protocol has been made: the number of cells was reduced from 7.5 x 10^7 to 2x10^7, the quantity of the transfected DNA from 30µg to 26µg (70% Vh + 30% Vl) and, in proportion, also the quantities of Expi medium, OptiMEM I 1x + Glutamax–I (Gibco - Life Technologies – catalog #31985062), Expifectamine and Enhancers to use were modified. The recombinant mAb's transfection was performed in quadruplicate for a total of 10 times. The flasks were incubated for 6 days at 37°C in a 8% CO_2 environment at 125rpm in the Brunswick™ S41i incubator. Two recoveries of the supernatants were made after 48h and 6 days from the addition of enhancers. Supernatants were harvested by centrifugation through Juan MR23-I centrifuge (Thermo Electron) at

1800rpm for 15 minutes, filtered with 0.22µm syringe filters (Fisher Scientific) and 5mL syringe (PIC indolor) and kept at +4°C for further characterization, while pellets were resuspended with fresh medium and placed in incubation again.

The fragments obtained through TAP-PCR were transiently transfected maintaining the proportion of 70% and 30%, for Vl and Vh respectively, but scaling down the protocol from 125mL flasks to Deepwell plate 96/2mL white border (Eppendorf – catalog #DWP962000W2-EP), following manufacturers' instructions. Optimization of the protocol has been made: the number of cells was reduced from 2x10^6 to 4.5x10^5, the quantity of DNA to transfect from 0.7µg to 0.4µg (70% Vl + 30% Vh) and, consequently, we have modified also the quantity of Expifectamine, OptiMEM I 1x and Enhancers used in proportion. Plates were incubated for 48h at 37°C in a 8% CO_2 environment at 1000rpm with Eppendorf Mixmate Shaker (Eppendorf). Supernatants were then harvested by centrifugation through Microcentrifuge 5415-R (Eppendorf) at 1800rpm for 5 minutes after 24h and 48h after the addition of enhancers.

FACS staining

To assess the efficacy of the supernatants of the miniaturized and the scaled-up to flasks transfections, to value mice's sera antibody titer, but also to identify the positive plasma cells to sort and of the final product mAb α-TLS1, the flow cytometry analysis was carried out. FACS analysis was executed coating Assay Round-bottom 96 well plates (Corning) with 10µL of surnatants/well and then adding 10.000 cells/well. Each sample was analyzed with two different cell lines : Flp-In-3T3 as negative control, as it did not express the antigen on the membrane, and the stable clone called 'F4', which was transfected to stably express the antigen on the surface. mAb α-TLS1 was also tested on TF-1 cell line and it was used at 2.3µg/mL. Plates were incubated for 1 hour at 4°C. Then 100µL of 1XPBS were added to each well, centrifuged at 1200 rpm for 5 minutes, supernatants were recovered and replaced with 10µL of 1:1000 anti-mouse IgG APC-conjugated (Life Technology). The secondary antibody was also used as negative control. Plates were incubated for 1 hour at 4°C and then washed again with

100µL of 1XPBS. At the end, cells were resuspended in 20µL of 1XPBS and analyzed at the cytofluorimeter BD FACS Canto II (Beckton Dickintson).

Moreover a serial dilution of α-TLS1 from 10µg/mL to 0.0003µg/mL in 1XPBS was tested to have a dose-response data. Once the mAb was limiting diluted by hand, the protocol used was the same as reported before. The dose-response was tested on F4 and TF-1 cell lines.

FACSCanto was used also to analyse the GFP positivity on TAP-PCR constructs to assess the best promoter, poly-adenilation and leader sequences.

Results were analyzed using the FlowJo software (FLOWJO, LLC, Ashland, OR, USA).

TLS1 stable clone (F4) creation

1.2 x 10^6 Flp-In™-3T3 (Thermo Fisher Scientific) were seeded into p100 tissue culture dishes (Corning) and allowed to adhere overnight. The next day, 1.5mL of OptiMEM I 1X (Gibco - Life Technologies) containing 50µL Lipofectamine LTX Plus (Gibco - Life Technologies – catalog #15338100) was then combined with the DNA mixture, which contained in one hand 10µg Recombinase plasmid (available in house – pOG44) and pEF5-FRT-GFP plasmid, as control, and in the other hand the Recombinase plasmid with 10µg 3XFLAG-TLS1full-pEF5-F plasmid, previously purified. Complexes then were added drop-wise to the cells. After 24 hours of incubation, the transfection medium was replaced with fresh growth medium supplemented with Hygromycin B (300µg/mL – Thermo Scientific – catalog #10687010). Every two days of selection, the medium was replaced and the selection was monitored with the Leica DMI 3000 B Fluorescence Microscope (Leica), indirectly comparing the GFP emission with the expression of the antigen of our interest on the membrane. After 12–14 days of selection, well-isolated, drug-resistant colonies were removed from the plates using Cloning Rings (Sigma Aldrich) and plated in new 24-well plates to selectively expand only the clones of our interest. We waited until clones reached the confluence and then we tested their positivity in the expression of TLS1 with a FACS staining analysis through α-Flag-tag M2 antibody (1:50 - Sigma Aldrich – catalog #F1804) as primary antibody and Goat Anti-mouse IgG DyLight 633 Conjugated (1:1000 – Invitrogen) as secondary antibody. Only

the clones that were staining positive were kept, expanded and kept frozen in -80°C until their use.

Purification of IgG-tagged protein

The IgG-tagged protein was purified from the supernatants using HiTrap™ Protein G HP 1mL columns (GE Healthcare – catalog #17-0402-01) using a peristaltic pump P1 (Pharmacia), following the instructions reported in *Rial DV, Ceccarelli EA 'Protein Expression and Purification' (2002)*. Briefly, the pump tubing must be filled with buffer A (50mM Tris-HCl , 150mM NaCl) and then connected with the column, drop-to-drop to avoid introducing air into the column. Once the column was conditioned with 10mL of buffer A at 1mL/min, the sample was applied by pumping it onto the column and recovering the flow-through. The column was washed with 4mL of buffer B (50mM Tris-HCl, 150mM NaCl, 25x PMF and 5mM ATP) for 3 times. A 4th wash was made with buffer A, followed by elution with 2.5mL of a suitable solution (0.1M Glycine-HCl pH 2.7) and buffered with 200µL of 1M Tris-HCl, pH 9. In order to regenerate the column and prevent cross contamination, each run included a strip of the protein G column using 20mL of buffer A followed by 20mL of 20% EtOH.

α-TLS1 mAb was also purified from the supernatants using HiTrap™ Protein G HP 1mL columns (GE Healthcare), following the same protocol reported before, but substituing buffer A with 20mL of binding buffer (20mM Sodium Phosphate, pH 7) to condition the column and to do 3 washes after the application of the sample.
The good quality of purifications was then confirmed through SDS-PAGE analysis.

Ides/IdeZ cleavage

IdeZ Protease, Lyophilized (Promega – Catalog #V834A) specifically cleaves IgG molecules below the hinge region to yield F(ab)2 and Fc fragments. After having reconstituted the protease with 100µl of deionized water to make a 50units/µl solution, the antibody fragmentation was reached adding 1 unit of IdeZ Protease per

1µg of IgG to be digested. Samples were incubated at 37°C for 30–60 minutes in the heating block module (Eppendorf). The cleavage was then confirmed through SDS-PAGE analysis, as described below.

Lightning-Link APC/R-PE Conjugation

Once the IgG-tagged protein was obtained, part of the main fraction was labeled with two fluorochromes (R-PE and APC) with Lightning-Link Conjugation Kit (Innova Biosciences) following manufacturer's instructions.

Mice's immunization

10 Female BALB/c mice (Charles River) were maintened in specific germ-free conditions in the animal facility in the TLSF (Toscana Life Sciences Foundation) building n°36, inside the GSK campus (Siena). Once 4 weeks old, they were immunized intra-peritoneally every 14 days with a total volume of 100µL 1XPBS containing 20µgr of the purified protein TLS1-L-ECD-hiGg1E1-F, 1µL of 200mM Dithiothreitol (DTT – Invitrogen – catalog #P2325) and Incomplete Freund's Adjuvant and Complete Freund's Adjuvant (IFA and CFA, catalog **#**F5506 **and** #F5881 respectively - Sigma Aldrich) per mouse for 5 injections . CFA was used only for the first dose and IFA for the subsequent boosts. Blood for sera analysis was recovered after the 3rd and the 5th immunization to evaluate the antibody titer through ELISA test and FACS staining analysis. At the end of the study, the mice were anesthetized with IsoFlo (Zoetis – catalog #50019100), terminal bleeds were taken and then sacrificed with cervical dislocation to recover also the spleens and bone marrows, that were cryopreserved until their use.

Purification of HIS-tagged protein

Proteins were purified from the supernatants using Ni-Seph resin 2.5mL (GE Healthcare – catalog #17-5268-01), previously prepared with 3 washes with dH_2O and then conditioned with 5mL, 10mL and10mL of 1XPBS. Then the sample was applied

and recovering the flow-through by gravity. The column was washed with 5mL of washing buffer (20mM Sodium Phosphate pH 7.4, 0.5M NaCl, 10mM Imidazole) for 5 times. We proceeded with 5 elutions with 2mL of elution buffer (20mM Sodium Phosphate pH 7.4, 0.5M NaCl, 500mM Imidazole). Aliquots were stored at -80°C and used for ELISA tests. The good quality of the purification was then confirmed through SDS-PAGE analysis.

Protein quantification

To quantify the proteins and the eluted antibody , we measured the A_{280} absorbance with Spectramax M2 (Molecular Devices) through the help of a black quartz cuvette (STARNA Scientific). After having set the reference (Elution buffer and Tris pH9 or 1XPBS), only for the antibodies's main elutions were evaluated and divided for the molar extinction coefficient of 1.35. To confirm the quantification obtained, we evaluated the eluted fractions also with Pierce BCA Protein and Bradford Assay Kits (Thermo Scientific – catalog #23225 and #23236, respectively), following manufacturer's instructions. Samples were valuated into 3 different dilutions (1:1, 1:5 and 1:10). To confirm quantification of the concentrated mAb, we created a standard curve with IgG mAb, as control, and we compared known concentrations of the control mAb with the measured concentrations of the new antibody through SDS-PAGE analysis, reported below.

Buffer exchange

The main purified fractions were buffer exchanged using Slide-A-Lyzer MINI Dialysis Devices 3.5 or 20K MWCO (Thermo Scientific – catalog #88405) in 1XPBS at 4°C for 3-4 hours at 10-15 rpm through Orbit 300 refrigerated shaker (LABNET). Then, 1XPBS was substituted with fresh one and the dialysis step proceeded O/N at 4°C at 10-15 rpm. The samples then were recovered the next day in LoBind tubes (Eppendorf – catalog #Z666505).

Volume reduction and concentration

For the antibodies, the sample was then concentrated through Pierce™ Protein Concentrator PES, 30K MWCO (Thermo Fisher – catalog #88531), previously conditioned with 3mL of 1XPBS, at 4000rpm for 5 minutes and then at 3000rpm for 1-2 minutes reducing the volume to reach the requested concentration of 1mg/mL.

SDS-PAGE and Westen Blot

To verify the correct outcome of the purifications, each fraction was analyzed with SDS-PAGE and Western Blot. Briefly, 30µL of each fraction was added to 10µL of NuPAGE™ LDS Sample Buffer (4X) (Invitrogen – catalog #NP0007), the resulting solution was mixed and then boiled at 95 °C in the heating block module (Eppendorf) for 10 min. Subsequently, 12µL were loaded onto NuPAGE 4-12% Bis-Tris pre-cast Gel (Invitrogen – catalog #NP0326BOX) as well as 5µL of SeeBlue™ Plus2 Pre-stained Protein Standard (Invitrogen - catalog #LC5925). At the same time, the reduced sample was prepared adding 4µL of Bolt™ Sample Reducing Agent (Invitrogen – catalog #B0009). 50mL of 20x NuPAGE™ MOPS SDS Running Buffer (Invitrogen – catalog #NP0001) were added to 950mL of deionized water to prepare 1x SDS Running Buffer and it was added to the XCell SureLock™ Mini-Cell (Invitrogen – catalog #EI0001) to proceed with the run at 150 V for 1h through 200M Dual Power (Invitrogen). At the end of the run, the gel was stained using SimplyBlue™ SafeStain (Invitrogen – catalog #LC6060) at RT for 1h at 10-15 rpm. Then, the staining solution was removed and the gel was rinsed with deionized water until it became clear again. Images of the gels were obtained by ImageQuant LAS4000 (GE Healthcare).

Alternatively, the gels were subjected to Western Blot analysis using iBlot™ Transfer Stacks with PVDF membranes (Invitrogen – catalog #IB24002) through the iBlot™ Gel transfer Device (Invitrogen) following manufacturer's instructions. At the end of the transfer, the immunoassay was performed on the PVDF membrane, made ready with an incubation of 1 hour with Skin Milk Powder (Fulka – catalog #70166) to block the free sites left on the membrane to avoid non-specific binding of the antibody on them.

We proceeded with the incubation for one hour with primary antibodies directed against the protein of interest at 4°C under agitation and, then, with the secondary antibodies Goat Anti-Mouse IgG (H-L)-HRP Conjugated (Bio-Rad Laboratories – catalog #1706516), diluted at 1:5·000/10·000.

At the end of the incubation, three TBS-T (50 mM Tris-Cl, pH 7.6; 150 mM NaCl; Tween 0.1%) washes were performed. The detection of the bands was obtained using the ECL reagent (Enhanced ChemioLuminescence – Invitrogen – catalog #WP20005) for 2-5 minutes and images were taken by ImageQuant LAS4000 (GE Healthcare). Even if the Western Blot analysis is performed, gels were in any case recovered and subjected to Coomassie blue staining.

To confirm quantification of the concentrated mAb, we created a standard curve with IgG mAb, as control, and we compared known concentrations of the control mAb with the measured concentrations of the new antibody. The standard curve was created by limiting dilution 1:2 of the control antibody from a concentration of 1mg/mL to 31µg/mL, taking 10µL and diluting in 10µL of dH_2O. Then we added 8µL of dH_2O and 6µL of 4x-NuPAGE LDS Sample Buffer. For the new antibody preparation, 10µL were taken and added to 8µL of dH_2O and 6µL of 4x-NuPAGE LDS Sample Buffer. At the same time, the reduced sample was prepared replacing 8µL of dH_2O with 2.4µL of 10x Bolt™ Sample Reducing Agent and 5.6µL of dH_2O. We proceeded with the SDS-PAGE and Western Blot analysis as described before.

Western Blot analysis was done also on NIH-3T3, F4 and TF-1 cell lines's lysates obtained with RIPA Buffer (Sigma Aldrich – catalog #R0278), following manufacturer's instructions. Lysates were quantified by Pierce™ BCA Protein Assay Kit. 20µg of NIH-3T3 and F4, and 200µg of TF1 cell lysates were loaded on NuPAGE 4-12% Bis-Tris pre-cast Gel and transferred then to iBlot™ Transfer Stacks with PVDF membrane, as described before. The α-TLS1, the α-FLAG-tag (M2 – Sigma Aldrich – catalog #F4049) and the α-βActin (Sigma Aldrich – catalog #A5441) antibodies were used at 10µg/mL as primary antibodies. For all was used the 2nd Goat Anti-mouse IgG(H+L) HRP-conjugated diluted at 1:5000.

ELISA test

Antibody titres in mice sera and levels in Expi293 supernatants were assessed via ELISA. Briefly, the purified TLS1-L-ECD-HIS **or** TLS1-L-ECD-hiGg1E1-F were used to coat ELISA assay plates 96well Flat Bottom, Black (Corning) at 10 µg/mL in 50µL 1XPBS/well, O/N at 4°C. The following day plates were washed 3 times with 1XPBS and then blocked with 5% BSA (Bovine Serum Albumine – Fisher Scientific) in 1XPBS 200µL/well for 2 hours at 37°C. Afterwards, washes with 1XPBS were repeated (200µL) and then sera or supernatants were applied (50µL/well) to the plates at various dilutions along with a purified mouse IgG standard for 1 hour at RT. Following washing with 0.05% Tween-20 (Sigma Aldrich) in 1XPBS, Anti-mouse IgG Fc specific HRP-conjugated antibody (Sigma Aldrich – catalog #A0168) was added at a 1:2500 dilution in PBS-BGT (0.5% BSA, 2.5% FBS, 0.05% Tween-20 – 50µL/well) for 1 hour at RT. Plates were developed with 50µL/well of 3, 3', 5, 5'-Tetramethylbenzidine Substrate Solution (TMB – Sigma – catalog #N301) for 30 minutes at RT and then the reaction was stopped with 1M HCl (50µL/well – Siigma Aldrich). Plates then were read at 492nm with Spectramax M2 (Molecular Devices).

Antigen-specific plasma cells identification

Cryopreserved bone marrow samples, derived from immunized mice, as previously described, were thawed and crushed pipetting several times up and down into a petri dish to resuspend all the cell suspension contained in them. Cells were then washed twice with 1XPBS by centrifugation at 1200rpm for 5 minutes. The enrichment of cells of interest was performed using the $CD138^+$ Plasma Cell Isolation Kit, an LD and two MS Columns, a MidiMACS™ and a MiniMACS™ Separators (Miltenyii Biotec – catalog #130-092-530), following the manufacturer's instructions. Briefly, cells were fluorescently stained with CD45R (B220)-APC, CD19-FITC, and CD138-PE. Cell debris and dead cells were excluded from the analysis based on scatter signals and propidium iodide fluorescence by flow cytometry analysis. Enrichment of the sample was around 40%.

As first attempt, isolated in bulk cells were inserted into the DEPArray™ cartridge to be used in the DEPArray™ technology (Menarini Silicon Biosystems). The following monoclonal antibodies (mAbs) were used to detect and to sort single plasma cells: Rat Anti-Mouse CD3 (17A2), Rat Anti-Mouse CD4 (GK1.5), Rat Anti-Mouse CD8 (53-6.7), Rat Anti-Mouse Ly6C/Ly6G (RB6-8C5 - RUO), Rat Anti-Mouse F4/80-Like receptor (6F-12), Rat Anti-Mouse IgM (R6-60.2), Rat Anti-Mouse IgD (11-26c.2a) and Rat Anti-Mouse CD19 (6D5) from BDPharmingen; and Anti mouse CD335 (29A1.4) from Invitrogen. Image-based selection allowed us to identify and isolate of cells of interest and to plate them in multiplate PCR plates 96 well clear (Biorad), following manufacturer's instructions.

As second attempt, we proceeded to seed them by hand in 384 wells-plate (Corning) and then in Terasaki plates (available in house) with a distribution of 0.3 cells per well, with the addition of RPMI1640™ (Corning). After 24h of incubation at 37°C with 5% CO_2, the supernatant of each well was tested for the capability to bind to the target antigen. FACS analysis was executed through BD FACS Canto II (Beckton Dickintson), coating U bottom 96 well plates with 10µL of surnatants/well and following the same protocol as reported before for the staining.

Cells, which supernatant resulted positive, were identified, washed with 1XPBS and moved to 96-well PCR-plate containing 4µl of Lysis buffer (Table n.1), in sterile conditions, frozen and stored at -80°C until Reverse Transcription-PCR was performed.

Table n.1

Lysis Buffer	**96X**	**Final conc.**
• **UltraPure™ DNase/RNase-Free Distilled Water (Invitrogen – catalog #10977035):**	310 µL	
• **10X sterile PBS**	20 µL	
• **DL-DTT 100mM:**	40 µL	(18.3ng/µL)
• **RNasin Plus RNase inhibitor 40U/µL (Promega – catalog #N2611):**	30 µL	(40U/µL)
Volume to add per well	4µL	

RT and TAP-PCR

cDNA from single or in bulk cells was prepared using Superscript III reverse transcriptase (Invitrogen – catalog #18080085) primed with Random Hexamers (Invitrogen – catalog #N8080127) as described in *Lotta von Boehmer 'Sequencing and cloning of antigen-specific antibodies from mouse memory B cells' Nature protocols (2016)*. Ep Duafilter T.I.P.S. PCR clean and sterile were used (Eppendorf – catalog #0030 078 500 , #0030 078 535, #0030 078 551 and #0030 078 578).

Briefly, samples were thawed on ice for 5 min and then centrifuged at 400*g* for 30 s at 4 °C through Juan MR23-I centrifuge (Thermo Electron). In a DNA/RNA-free hood, RT mix I was prepared, as described below in Table n.2, in sterile conditions :

Table n.2

RT-PCR Mix I	**1X**	**Final conc.**
• **UltraPure™ DNase/RNase-Free Distilled Water (Invitrogen – catalog #10977035):**	5.87µL	
• **IGEPAL 10% (Sigma Aldrich – catalog #18896-50mL)**	0.5µL	
• **Random Hexamers 300ng/µL (Invitrogen – catalog #N8080127):**	1.5µL	(18.3ng/µL)
• **RNasin Plus RNase inhibitor 40U/µL (Promega – catalog #N2611):**	0.16µL	(0.8U/µL)
Volume to add per well	7µL	

Outside the hood, on a clean surface, 7µl of RT mix I were added to each sample in a circular motion along the edges and then they were centrifugated at 400*g* for 1 min at 4°C. Samples were Incubated for 5 min at 65 °C in the preheated thermocycler (MyCycler thermocycler – Biorad). Samples then were placed on ice for 1–5 min. During this time, in a DNA/RNA-free hood, RT mix II was prepared under sterile conditions (Table n.3):

Table n.3

RT-PCR Mix II	**1X**	**Final conc.**
• **UltraPure™ DNase/RNase-Free Distilled Water (Invitrogen – catalog #10977035):**	2.44µL	
• **5x First Strand Buffer (Invitrogen – catalog #18080051):**	3.4µL	(2.3x)
• **DL-DTT 100mM (Invitrogen - catalog #P2325):**	1.15µL	(14.3mM)
• **dNTP 25mM (Thermo Scientific – catalog #R1121):**	0.6µL	(1.8mM)
• **RNasin Plus RNase inhibitor 40U/µL (Promega – catalog #N2611):**	0.11µL	(0.6U/µL)
• **SuperScript III RT 200U/µL (Invitrogen – catalog #18080085):**	0.3µL	(7.1U/µL)
Volume to add per well	7µL	

Outside the hood, on a clean surface, 7µl of RT mix I were added to each sample in a circular motion along the edges and then they were centrifugated at 400*g* for 1 min at 4 °C. Samples were Incubated following the program reported:

42°C, 10 min

25°C, 10 min

. 50°C, 60 min

94°C, 5 min

4°C , ∞

Samples were removed from the thermocycler and dilute cDNA was diluted by adding 10µl of UltraPure™ DNase/RNase-Free Distilled Water. Samples were stored at -20°C until their use.

Subsequently 3 rounds of antibody-specific PCR, using KOD Hot Start DNA Polymerase (EMD Millipore - Sigma – catalog **#**71086**)** or JumpStart AccuTaq LA DNA Polymerase (Sigma Aldrich – catalog #D1313), following manufacturer's instructions, and gene specific primers (Eurofins Genomics), were performed to amplify heavy and light chain variable region genes and generate two separate linear transcriptionally-active-PCR (TAP) products, one encoding the heavy- and the other one the light-chains (Fig. 1).

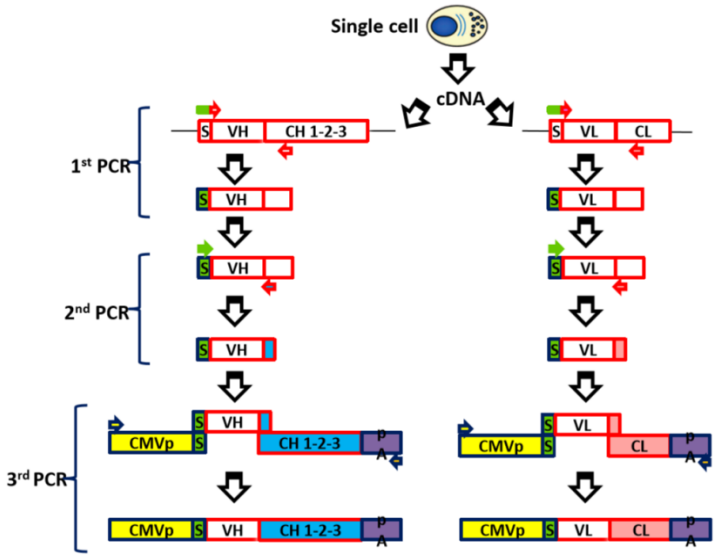

Fig.1 *Schematic representation Transcriptionally Active PCR (TAP) fragment construction*.

In each amplification step, primers were resuspended at 100pmol/µL with DNAse/RNAse free water and then 1µL of the 1:10 dilution was added to the PCR mix (Table n.4). Every PCR product was verified by 1% Agarose (Sigma Aldrich) gel electrophoresis in 1X Electrophoresis buffer (50X = 242g Tris-free-base, 18.61g Disodium EDTA, 57.1 mL Glacial Acetic Acid, dH_2O to 1L and then diluted to 1X) with 1Kb Plus DNA Ladder (Invitrogen – catalog #10787018) and used as a DNA template for the subsequent second PCR step. Multiplate PCR plates 96 well clear (Biorad) or DNAse/RNAse free PCR tubes 0.2mL (Eppendorf) were used.

Table n.4

PCR MIX 1x	**KOD**	**JumpStart**
• **UltraPure™ DNase/RNase-Free Distilled Water (Invitrogen – catalog #10977035):**	16.5µL	12.75 µL
• **10x Buffer PCR:**	2.5µL	2.5 µL
• **dNTPs 2mM each (Invitrogen – catalog #R72501):**	2.5µL	6.25 µL
• **$MgSO_4$ 25mM:**	1µL	-
• **Polymerase:**	0.3µL	0.5 µL
• **Addition of Taq polymerase (Invitrogen – catalog #10342020):**	0.2 µL	
Volume to add per well	23µL	22 µL

We followed the method described below:

- For the primary PCR:

		Sequence
Vl	IL2lea-Mk-F	F- AGTCTTGCACTTGTCACGAATTCGGAYATTGTGMTSACMCARWCTMCA
	kc-R	R- GGATACAGTTGGTGCAGCATC
Vh	GAU-lea-MH1-F	F- CTGCATCGCTGTGGCCGAGGCCSARGTNMAGCTGSAGSAGTC
	mIgGcoU-R	R- TCATTTACCMGGRGWSYGRG

Then, 4µL of the cDNA obtained through the RT step were added. The reaction program used for the first PCR step was the following:

94°C, 3 min		
94°C, 30 sec		
45 °C, 30 sec	X 50 cycles	
72°C, 2 min		
72°C, 10 min		
4°C, ∞		

- For the secondary PCR:

		Sequence
Vl	GAUlea-Mk-F	F- CTGCATCGCTGTGGCCGAGGCCGAYATTGTGMTSACMCARWCTMCA
	kc-R	R- GGATACAGTTGGTGCAGCATC
Vh	GAU-lea-MH1-F	F- CTGCATCGCTGTGGCCGAGGCCSARGTNMAGCTGSAGSAGTC
	IgG1-R	R- ATAGACAGATGGGGGTGTCGTTTTGGC

Then, 1µL of 1:10 of the first amplification of Vl and 1µL direct from the first amplification of Vh were added in the PCR mix, respectively. The reaction program used for the second PCR step of Vh was the same protocol described for the first amplification, while for the second amplification of Vl was the following:

95°C, 5 min		
95°C, 30 sec		
55 °C, 30 sec	X 30 cycles	
72°C, 3 min		

72°C, 10 min

4°C, ∞

- To obtain the promoter fragment and the polyA constant region the primers mentioned below were used:

		Sequence
Prom	CMV-F	F- GTTGACATTGATTATTGACTAG
	GAU-Lea-R	R- GGCCTCGGCCACAGCGATGCAG
pA Vl	mIgkco-F	F- GGGCTGATGCTGCACCAAC
	GAU-BGH-R	R- GATGCAATTTCCTCATTTTATTAG
pA Vh	mIgGcoU-F	F- GCYAMAACRACASCCCCATC
	GAU-BGH-R	R- GATGCAATTTCCTCATTTTATTAG

As template, two plasmids were used which contained the heavy and light variable regions of the m-Ab produced by an hybridoma (15K), previously used to test the feasibility of the method. These were diluted 1:100 and then 1µL of the solution was added to the PCR mix. The reaction program used was the following:

95°C, 5 min

. 95°C, 30 sec
55 °C, 30 sec
72°C, 3 min
} X 30 cycles

72°C, 10 min

4°C, ∞

- Finally, to obtain the two complete linear transcriptionally-active PCR (TAP) products were used:

		Sequence
Vl and Vh	CMV-F GAU-BGH-R	F- GTTGACATTGATTATTGACTAG R- GATGCAATTTCCTCATTTTATTAG

Primers were combined with promoter, 2nd amplification of the variable heavy and light regions and pA k-region, previously obtained. Primers and templates were all diluted 1:10 and 1µL of each was added to the PCR mix. The reaction program for the final PCR step were :

.

95°C, 5 min		
95°C, 30 sec	}	X 30 cycles
55 °C, 30 sec		
72°C, 3 min		
72°C, 10 min		
4°C, ∞		

To quantify, complete TAP-PCR Vh and Vl fragments were quantified evaluating the absorbances at 260 and 280nm with Nanovue (GE Healthcare).

Sequencing

To sequence the TAP-PCR products, we used the LightRun barcode service (Eurofins), following manufacturer's instructions. Briefly, 5µL of 20-80 ng/µL purified PCR fragments were added to 5µL of 5pmol/µL of primer in 1.5mL LoBind tubes (Eppendorf). The primers used were: GAU-lea-Mk-F and GAU-lea-MH1-F as primer

forward for Vl and Vh respectively, while kc-R as primer reverse for both Vl and Vh. Then, the samples were delivered to the GATC Collection Point at Le Scotte Hospital in Siena. The following day we obtained the results by email and we analysed them through VECTOR NTI software (Thermo Fisher Scientific).

Peptide mass fingerprint (PMF)

In order to get information on the primary aminoacidic sequence, an aliquot of the recombinant antigen and the antibody were reduced, alkylated, digested with Trypsin Gold, Mass Spectrometry Grade (Promega – catalog #V5280) and analysed by UHPLC Ultimate 3000 coupled with Q-Exactive mass spectrometer (Thermofisher Scientific). 10µl of the resulting peptide mixtures were injected on a column Acquity UPLC Waters CSH C18 130Å (Waters - 1 mm X 100 mm, 1.7µm – catalog #186005297). The column oven was maintained at 50°C, the analysis was carried out using a gradient elution (phase A: 0.1% Formic Acid – Sigma Aldrich- in DDwater; phase B: 0.1% Formic Acid in Acetonitrile – Sigma Aldrich). The flow rate was maintained at 0.1 mL/min. The mass spectra were acquired using a "data dependent scan", able to get both the full mass spectra in high resolution and to "isolate and fragment" the ten ion with highest intensity present in the mass spectrum. The raw data obtained were analysed using the Biopharma Finder 2.1 software (ThermoFisher Scientific). The elaboration process consisted in the comparison between the peak list obtained "in silico" considering an expected aminoacid sequence of a certain protein/antibody, a particular enzyme and fixed or variable modification (carboamidomethylation, oxidation…) and the experimental data. The peptide mass fingerprint (PMF) was determined considering both the molecular weight (from the full mass) and the fragmentation (from the MS/MS mass spectra) of all the peptides detected in the LC-MS/MS analysis. The results obtained, expressed as sequence coverage (%). Briefly, the protein was represented by its aminoacidic sequence in FASTA format and a coloured frame in correspondence with each peptide experimentally identified was reported. The colour of the frame was related to the signal intensity (the red one was the most intense, the blue one the lowest one).

Results

Graphic experimental workflow

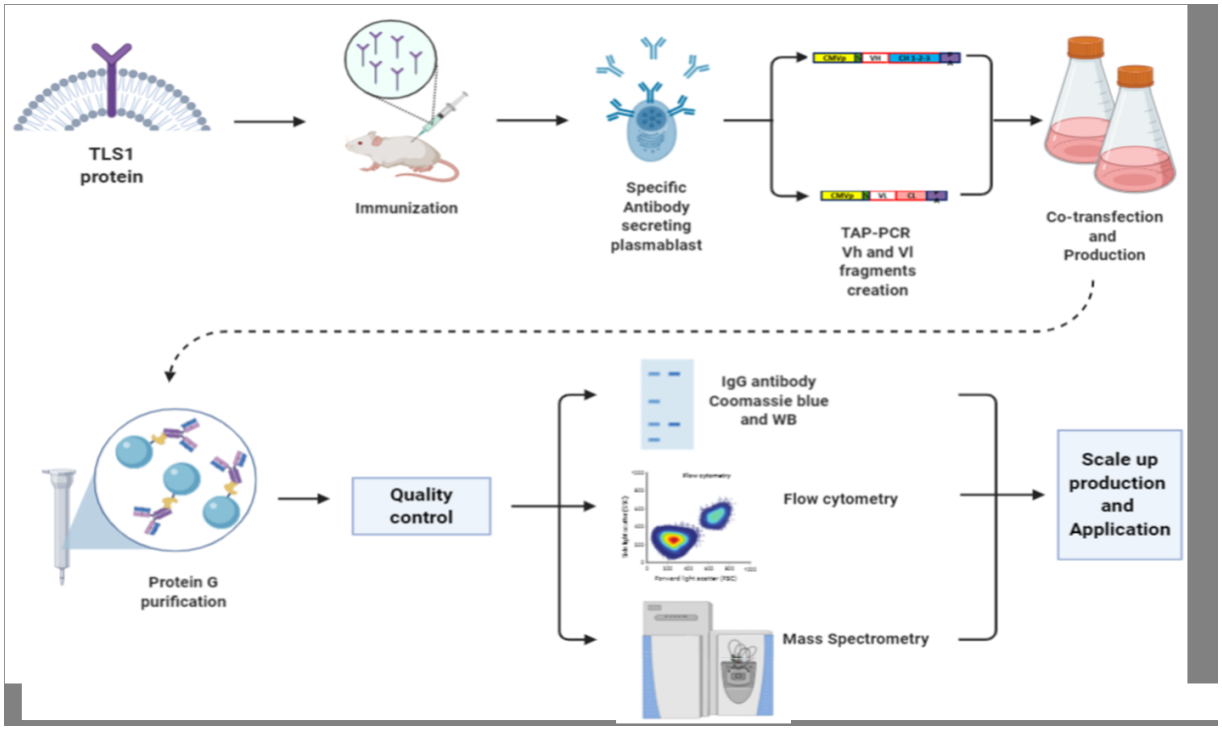

Plasmids design

Based on the TLS1 protein sequence, three plasmids have been designed and ordered to GeneArt Gene Synthesis allowing the expression of recombinant proteins. Plasmids are reported here below:

1. **TLS-L-ECD-hIgG1e1-F**
2. **TLS-L-ECD-HIS**
3. **3xFLAG-TLS1full-pEF5-F**

The first and the second plasmids were generated with the pcDNA™ 3.4 TOPO® vector backbone, containing the sequence only of the extracellular domain of the protein, allowing the secretion of these recombinant proteins in the culture supernatants. (1) encoded for TLS1 extracellular domain fused in frame to the sequence of the heavy

chain of IgG1 and it was used to have the production of the recombinant protein and to search for antigen-specific antibodies expressing cells. (2) encoded for TLS1 with a 6His-tag domain and it was used to verify the specificity of mice sera and single cells supernatants to recognize and to bind to the antigen.

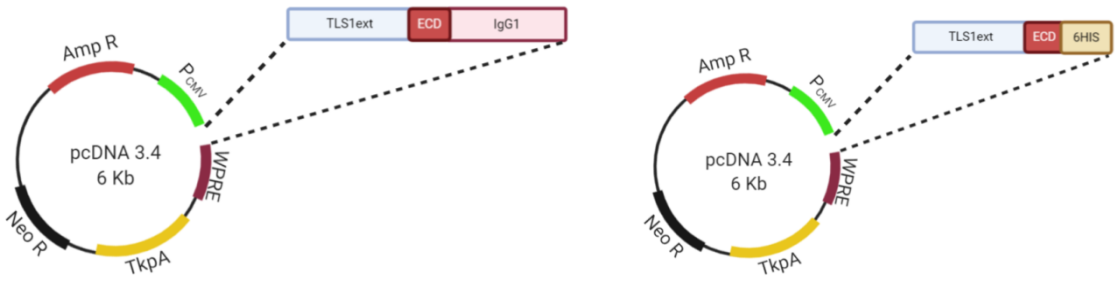

Fig.1 *Schematic representation of TLS-L-ECD-hIgG1e1-F and TLS-L-ECD-HIS.*

The third vector contained the DNA sequence of the full length of the TLS1 protein with the addition of a FLAG-tag in the pEF5/FRT/V5-DEST™ Gateway™ plasmid backbone. This plasmid has been constructed allowing expression of recombinant proteins in the cytoplasmatic membrane, allowing the creation of the stable expressing TLS1 clone.

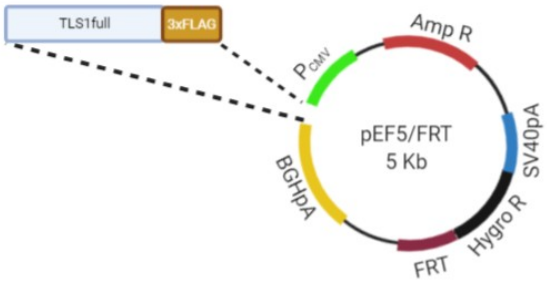

Fig.2 *Schematic representation of 3xFLAG-TLS1full-pEF5-F.*

Expression and purification of TLS-L-ECD-hIgG1e1-F

TLS-L-ECD-hIgG1e1-F was amplified in *Escherichia coli* (DH5α) grown in LB medium and purified. Subsequently, DNA was extracted by ethanol precipitation. The absorbance at 260 and 280nm was measured obtaining the following value:

- **TLS1-L-ECD-hIgG1e1-F** = 413 ng/µL A260/280 = 1.775

30µg of the purified plasmid were transiently transfected into Expi293 cells and the IgG-tagged protein was purified manually from the supernatants using HiTrap™ Protein G HP columns with the help of a peristaltic pump, following the instructions reported in 'Removal of DnaK contamination during fusion protein purification' *Rial DV, Ceccarelli EA. Protein Expression and Purification (2002)*. This protocol allowed us to purify the fusion protein by washing then it, which is bound to the purification resin, with Mg-ATP before elutions. The result is that DnaK contamination is dramatically reduced in the eluates. To verify the correct outcome of the purification results, each fraction was analyzed by SDS-PAGE and Comassie Blue staining. The IgG-tagged protein was found mostly in the second elution, as reported in Fig.3.

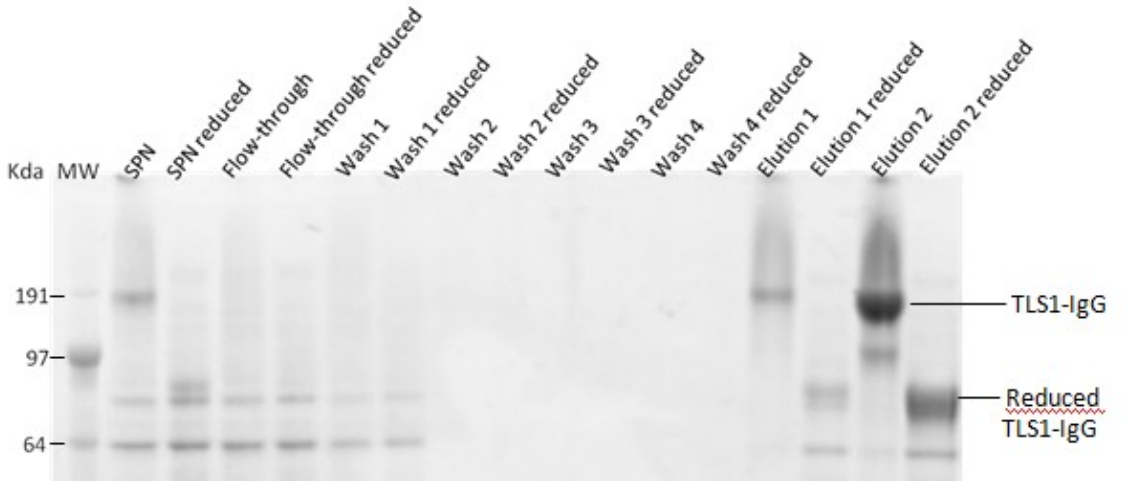

Fig.3 *SDS-PAGE analysis of the purified TLS1-IgG-tagged protein.*

After having verified the good quality and purity of the protein through the SDS-PAGE analysis, the purified fractions containing the protein of interest were buffer exchanged in 1XPBS. The eluted protein was quantified measuring the absorbance at 280nm and dividing the obtained values for the antibodies's molar extinction coefficient of 1.35, as it presents the IgG fraction :

- **Elution 1** = 0.31 mg/mL A260/280 = 1
- **Elution 2** = 2.09 mg/mL A260/280 = 0.857

To confirm these values the eluted fractions were evaluated also with Pierce BCA Protein Assay Kit, obtaining the following results:

- **Elution 1** = 0.44 mg/mL
- **Elution 2** = 2.36 mg/mL

The elution 2 was used to prepare the boost for the immunizations and kept at -80°C until its use.

The remaining part of the protein was then subjected to the IdeS/IdeZ specific cleavage: this protease specifically cleaves IgG molecules below the hinge region to yield F(ab')2 and Fc in antibodies but it can be used also in fusion recombinant proteins, so we could remove the IgG component and kept only the the TLS1 one in the next steps (Fig.4). After the cut, the protein was purified, buffer exchanged and checked through SDS-PAGE again.

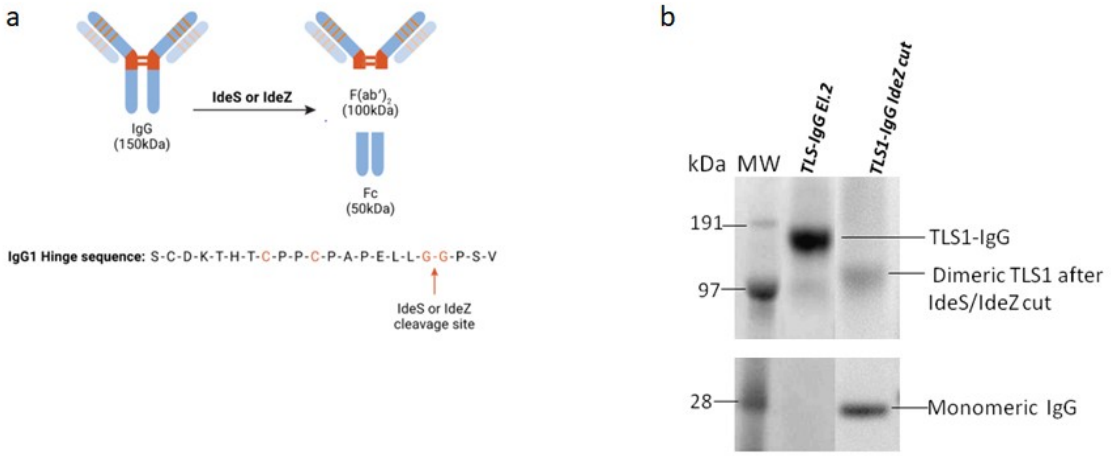

Fig.4 *Schematic representation of antibodies's IdeS or IdeZ cleavage (a); SDS-PAGE analysis of the purified TLS1 protein after the removal of IgG (b).*

We proceeded with the labeling the protein with two fluorochromes: R-PE and APC through Lightning-Link Antibody labeling kits, so then they were tested for the

capability to selectively identify antigen-specific cells expressing antibodies on their surface in complex splenic mixtures in the consequent steps.

Expression and purification of TLS-L-ECD-HIS

TLS-L-ECD-HIS was amplified in *Escherichia coli* (DH5α) grown in LB medium and purified. Subsequently, DNA was extracted by ethanol precipitation. The absorbance at 260 and 280nm was measured obtaining the following value:

- **TLS1-L-ECD-HIS** = 484.5 ng/µL A260/280 = 1.778

30µg of the purified plasmid were transiently transfected into Expi293 cells and the HIS -tagged protein was purified from the supernatant manually using Ni-Sepharose resin. To verify the correct outcome of the purification results, each fraction was analyzed by SDS-PAGE and Comassie Blue staining. The HIS-tagged protein was found mostly in the first elution, as reported in Fig.5.

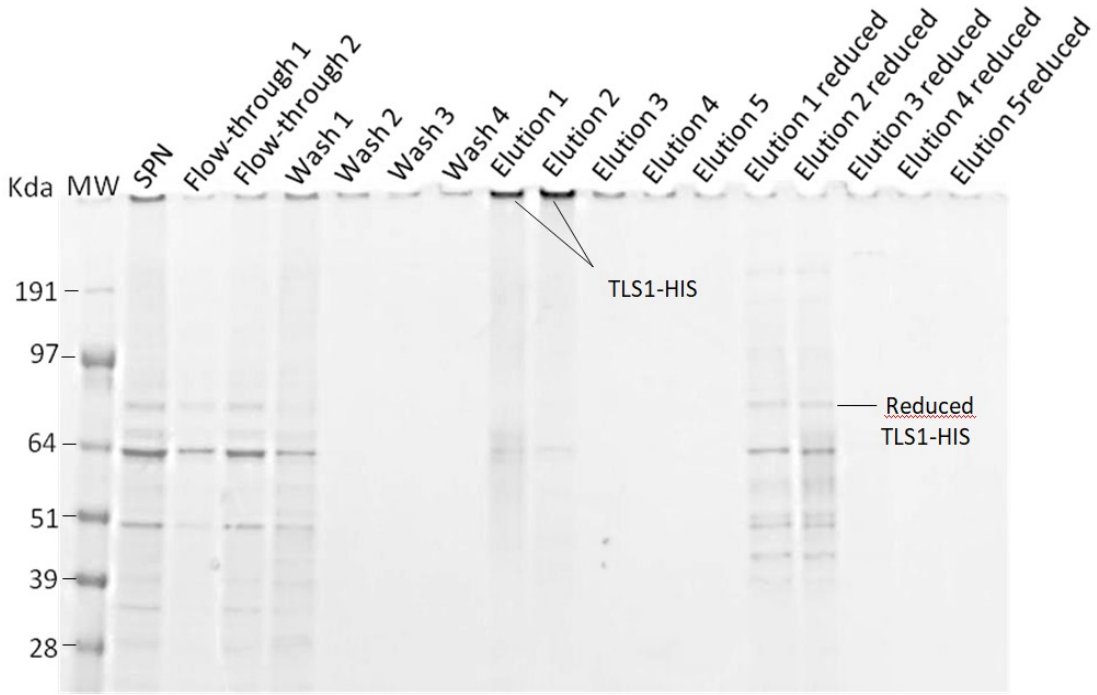

Fig.5 *SDS-PAGE analysis of the purified TLS1-HIS-tagged protein.*

After having verified the good quality and purity of the protein through the SDS-PAGE analysis, the purified fractions containing the protein of interest were buffer exchanged in 1XPBS. The eluted protein was quantified measuring the absorbance at 280nm and with Pierce BCA Protein Assay Kit, obtaining the following results:

- **Elution 1** = 1.94 mg/mL (A_{280})
- **Elution 1** = 2.36 mg/mL (BCA)

The elution 1 was aliquoted and kept at -80°C until its use.

Expression of 3xFLAG-TLS1full-pEF5-F and creation of the stable clone F4

To generate the stable TLS1 expressing cell clone, the Flp-In™ System was used. This system allows integration and expression of genes of interest in mammalian cells at a specific genomic location. It involves the Flp recombinase expressed by the pOG44 plasmid and Flp Recombination Target (FRT - *O'Gorman et al*., 1991) site to facilitate the integration of the gene of interest, introduced through an expression vector, into the genome of mammalian cells.

Our expression vector was 3xFLAG-TLS1full-pEF5-F, which contained our gene of interest. It was amplified in *Escherichia coli* (DH5α) grown in LB medium and purified. Subsequently, DNA was extracted by ethanol precipitation. The absorbance at 260 and 280nm was measured obtaining the following value:

- **3xFLAG-T2full-pEF5-F** = 366 ng/µL A260/280 = 1.768

Once purified, 3xFLAG-TLS1full-pEF5-F vector and the pOG44 plasmid were cotransfected into the Flp-In™-3T3 host cell line. Upon cotransfection, the Flp recombinase, expressed from pOG44, mediated a homologous recombination event between the FRT sites (integrated into the genome and on 3xFLAG-TLS1full-pEF5-F) such that the pEF5/FRT construct was inserted into the genome at the integrated FRT site. Insertion of pEF5/FRT into the genome at the FRT site brought the SV40 promoter and the ATG initiation codon (from pFRT/lacZeo, previously introducted into the cell

line system) into proximity and framed with the hygromycin resistance gene. Thus, stable Flp-In™-3T3 expression cell line was selected for hygromycin resistance and the expression of the recombinant TLS1 (Fig.6).

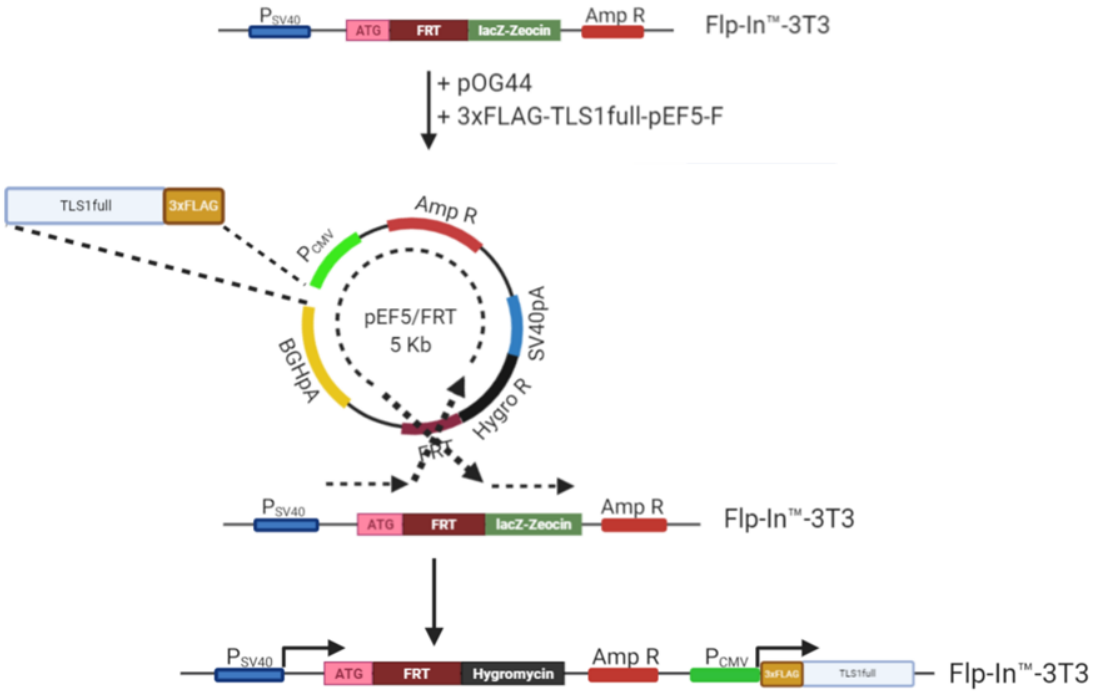

Fig.6 *Schematic representation of the FRT recombination between Flp-In-3T3 genome and 3xFLAG-TLS1full-pEF5-F which leads to the generation of the stable clone F4.*

The same concept was followed with the pEF5-FRT-GFP vector, through which the selection was monitored by the fluorescence microscope, indirectly comparing the GFP emission with the expression of the antigen of our interest on the membrane (Fig.7).

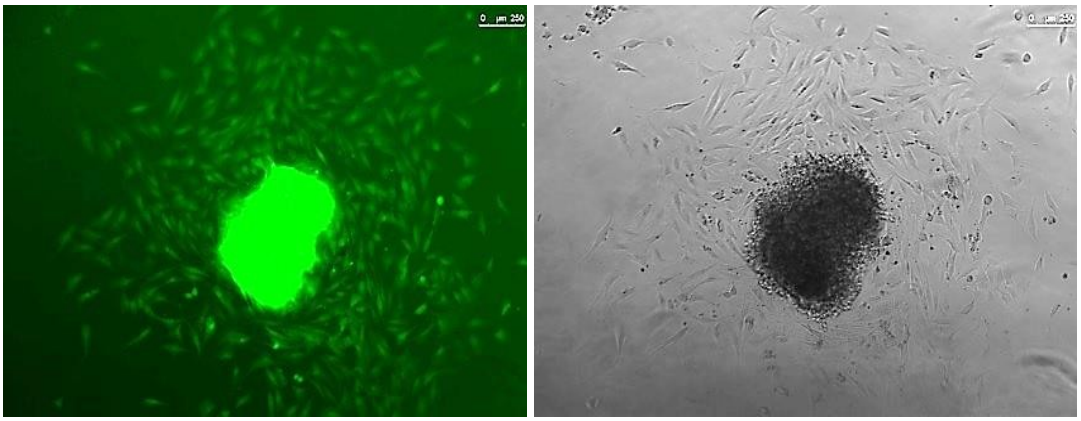

Fig.7 *Brightfield and GFP-fluorescence images taken by Fluorescence microscope of a single resistant clone.*

Single, well-isolated, drug-resistant colonies were expanded and then their positivity for TLS1 expression on their surface was tested by FACS analysis through α-Flag mAb as primary antibody (Fig.8). The isolated clones emitted a higher APC-fluorescence on F4 (Fig.8b) than on the control wild-type NIH-3T3 cells (Fig.8a), thus there was the recognition of TLS1. Only the positively stained clones were selected, expanded and stored at -80°C until their use.

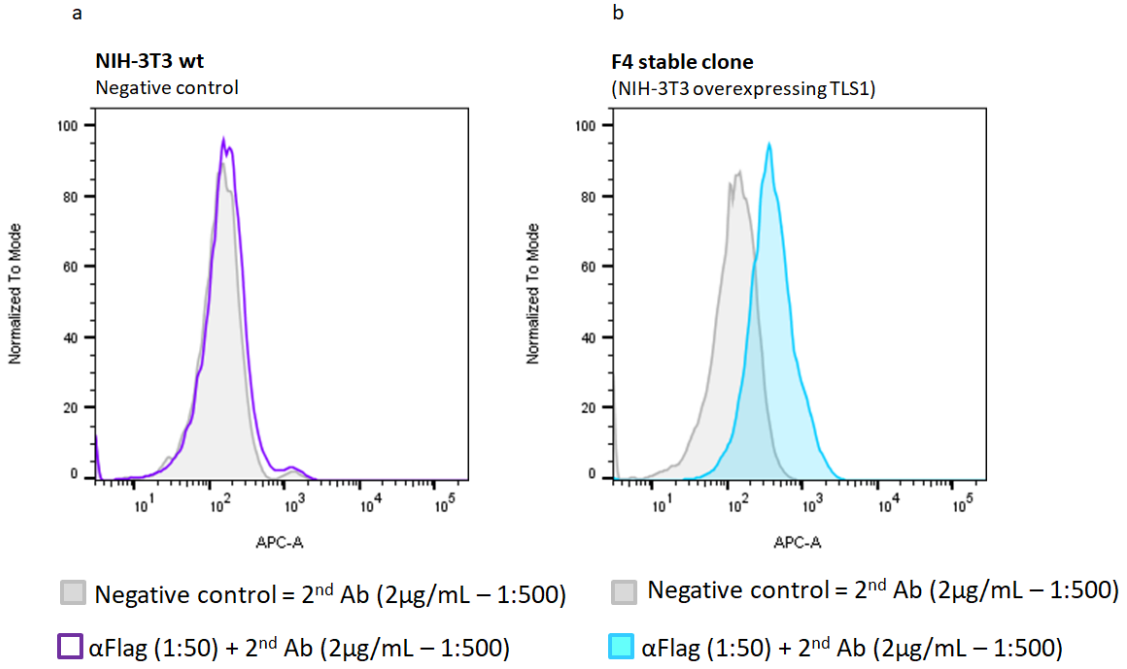

Fig.8 *Histograms representing **c**ell surface staining on NIH-3T3 wt (a) and F4 stable clone (b). FlowJo software was used for the analysis: gating strategy was done only on alive and single cells.*

Balb/c Mice immunization

10 Female Balb/c mice (4 weeks old) were treated every 14 days with 20µg of TLS1 protein, previously purified, for 5 times, as reported in the diagram reported below (Fig.9).

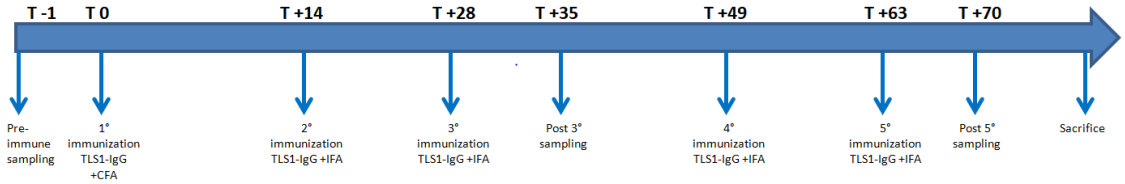

Fig.9 *Time line of the samplings and the immunizations done on Balb/c mice.*

After the 3rd and 5th immunizations, antibody titer in mice sera was verified for each mouse through ELISA test, using both the purified TLS1-L-ECD-HIS and TLS-L-ECD-hIgG1e1-F for the coating of the ELISA plate and the pre-immune sampling as negative control. Results demonstrated that a good immunization was reached in every experimental animal, giving high absorbance values even at the highest dilutions. These data were then confirmed by flow cytometry analysis (Fig. 10b) where mice's sera in pool recognized TLS1 expressed on the surface of F4 stable clone, while no binding was visible on NIH-3T3 wt cell line. At the end of the 5th immunization, bone marrows and spleens from immunized and non-immunized animals (as controls) were recovered.

a

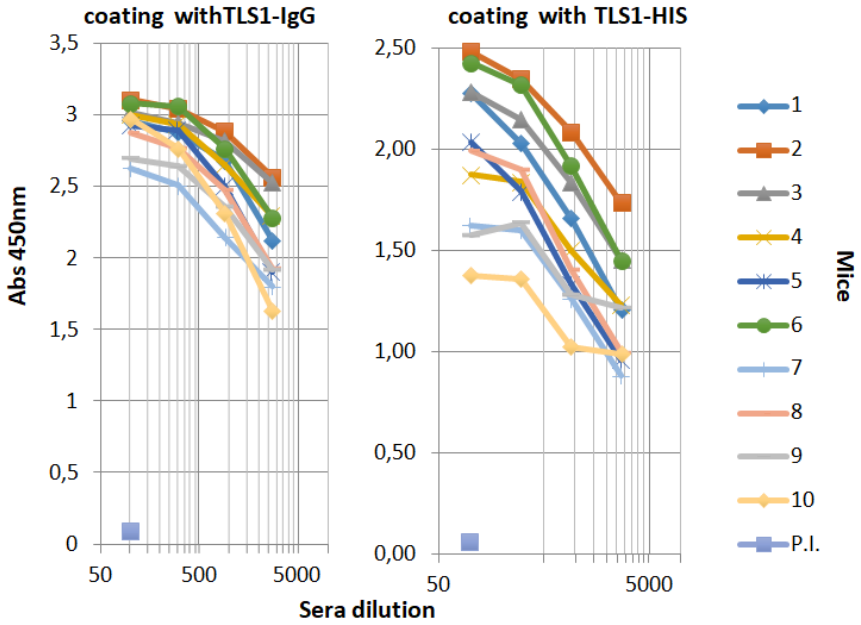

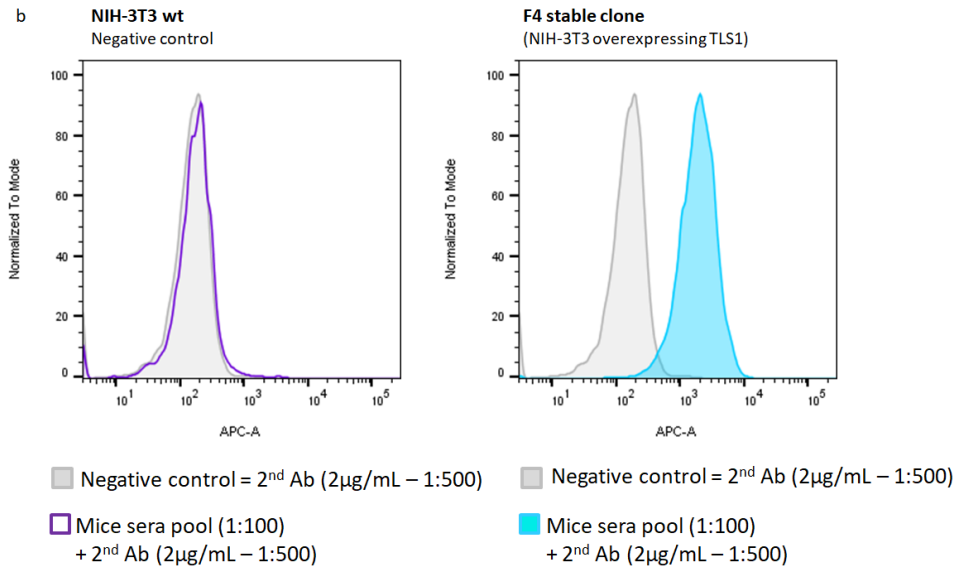

Fig.10 *ELISA test (a) and FACSCanto analysis (b) after 5 immunizations for the evaluation of the antibody titer of each immunized mouse. FlowJo software was used for the analysis: gating strategy was done only on alive and single cells.*

TLS1 antigen-specific plasma cells identification

The bone marrow is the major niche that supports the stable survival of long-lived plasma cells and these cells are responsible for secreting the vast majority of IgG present in serum (*Slifka et al.*, 1998; *Slifka et al.*, 1998; *Manz et al.*, 2005; *McMillan et al.*, 1972.). Thus, analyzing mice sera samples which contained antibodies with desirable characteristics, bone marrows were the origin of these interesting molecules released directly from the plasma cells repertoire rather than in other sub-groups of antibodies secreting cells like B cells. This enabled us to focus on individual animals that were producing higher levels of interesting functional antibodies. Cryopreserved bone marrow samples were thawed and crushed to obtain the cell suspension. Plasma cells enrichment was performed using the $CD138^+$ Plasma Cell Isolation Kit, as in mice CD138 is expressed on pre-B and immature B lymphocytes. Then usually it is lost when B cells emigrate into the periphery, it is absent on circulating and peripheral B cells but it is re-expressed upon B cell differentiation into plasmablasts and plasma cells. The isolation of mouse plasma cells was performed in a two-step procedure. First, non-plasma cells were indirectly magnetically labeled and were subsequently depleted by

separation over a MACS® Column. In the second step, plasma cells were directly labeled with CD138 MicroBeads and isolated by positive selection from the pre-enriched cell fraction.

The enriched sample was then ready to be loaded onto the DEPArray™ instrument: DEPArray™ technology is based on the ability of a non-uniform electric field to exert forces on neutral, polarizable particles, such as cells, that are suspended in a liquid. This electrokinetic principle, called dielectrophoresis (DEP), can be used to trap cells in DEP "cages" by creating an electric field above a subset of electrodes in an array that is in counter phase with the electric field of adjacent electrodes. When a DEP cage is moved by a change in the electric field pattern, the trapped cell moves with it.

The ability to manipulate individual cells using DEPArray™ technology, combined with high quality image-based cell selection, allowed us to identify and recover specific individual cells of interest from complex, heterogeneous samples. Target cells were sought as DAPI- , CD19+, CD138+ and both TLS1-APC+ and -R-PE+. The use of two fluorochromes helped us to discriminate between true and false positives, being positive only the events emitting two positive signals.

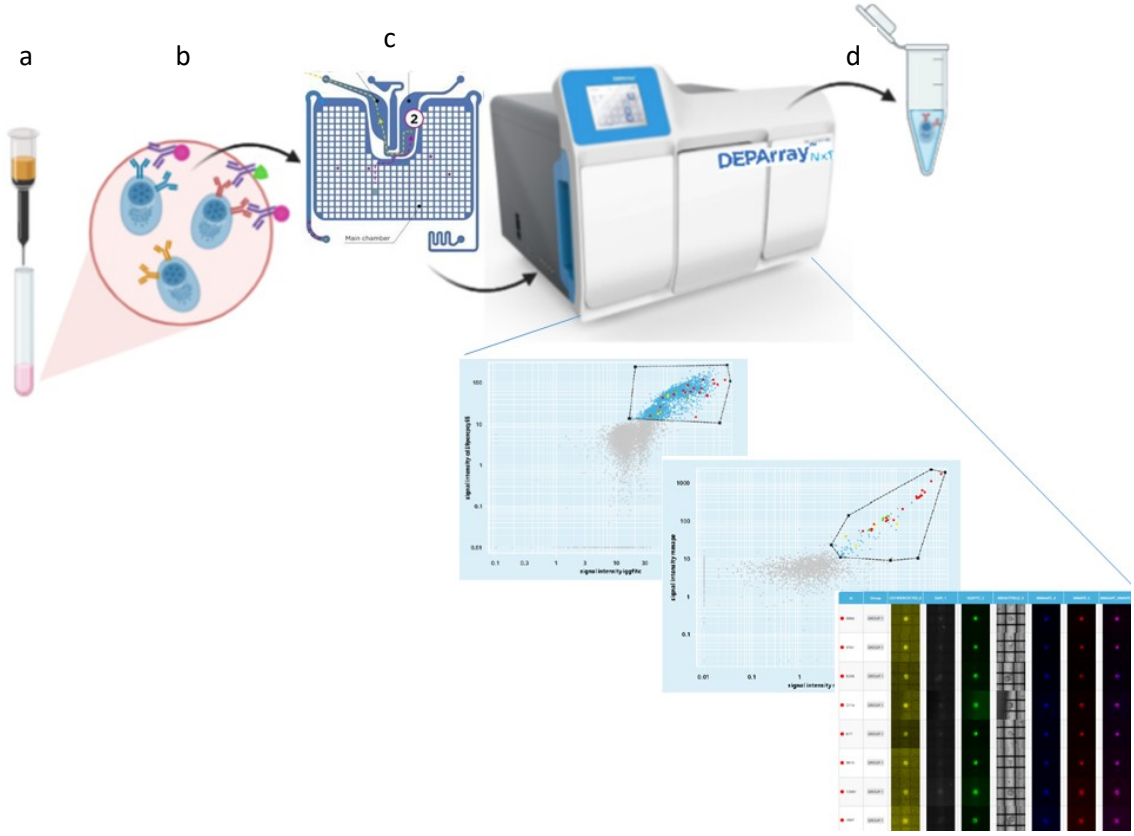

Fig.11 *Workflow from the enriched sample to the recover of pure single cells through the DEPArray™ technology; Cell suspension from murine bone marrows was enriched for plasma cells through CD138+ Plasma Cell Isolation Kit (a); Plasma cells were then labelled (b) and loaded into DEPArray™ cartridge (c) and only antigen specific plasma cells were recovered with DEPArray™ technology into 96 well plate (d), ready to proceed with the next steps.*

This first attempt let us to sort in average 30 target cells at single-cell per well, per immunized mouse, while no target cells were found in control animals.

Even if the quality of the sorting given by the use of the DEPArray™ was extremely accurate, due to the possibility of selecting each single cell through images and being sure of where exactly each chosen cell was positioned inside the multi well plate, we ran into some downsides:

- Time consuming to run the instrument;
- Low amount of sortable cells;
- High suspension volume in which cells were sorted;

- Need to test, before head, the capacity of cells to produce antibodies which could bind to the antigen.

For these reasons, in our case the DEPArray™ instrument wasn't able to give us back what we needed and so we decided to modify the protocol to use and to proceed differently. After the enrichment of plasma cells with the magnetic kit, we proceeded to seed cells manually limiting diluting in 384 wells-plate and then in Terasaki plates. Terasaki plates are small size microassay plates which allowed us to miniaturize the system: a single cell per well was forced to produce antibodies which were concentrated in a minimum volume of medium added per well. Thus, only after 24 hours of incubation, it was possible to test the supernatant of each cell against the wt cell line (NIH-3T3) and the stable clone (F4) for their ability to bind the target antigen. Cells, which supernatant resulted positive, were identified and moved to 96-well PCR-plate containing 4µl of lysis buffer to continue with the Reverse Transcription-PCR step (Fig.12 a-d). In this way, it was possible to identify upstream cells which produced antigen specific antibodies, unlike the previous protocol where all cells were recovered, lysed and subjected to PCR amplifications indisciminately to their capability to produce antigen specific antibodies. Two plasma cells (#3 and #4) were identified as positive, as it is observable from the FACSCanto staining results (Fig 12e).

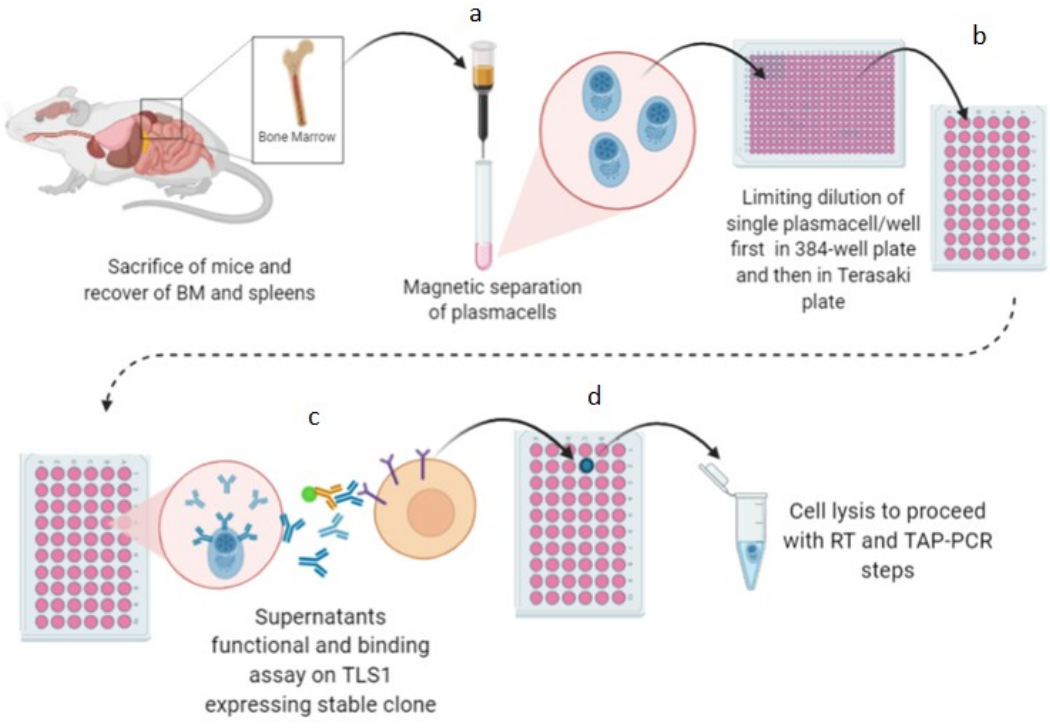

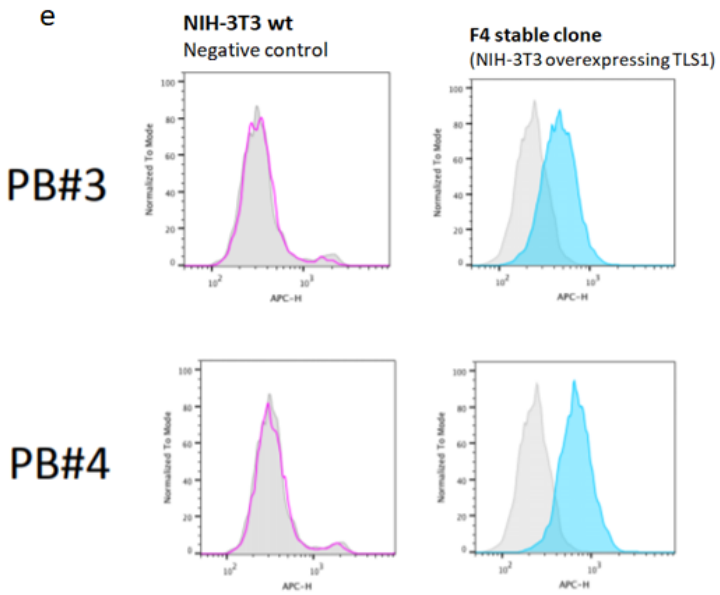

Fig.12 *Schematic representation of the sorter-free method to isolate single plasma cells. Cell suspension from murine bone marrows was enriched for plasma cells through CD138$^+$ Plasma Cell Isolation Kit (a); Plasma cells were then limiting diluted in 384-well plate and afterwards to Terasaki plates (b); Supernatants of single plasma cells were tested for the capacity to bind to TLS1 antigen expressed by the stable clone F4 through FACSCanto (c); Only positive cells were recovered and submitted to cell lysis, RT-PCR and TAP-PCR steps (d); Histograms representing FACSCanto staining analysis of single plasma cells's supernatants on wt NIH-3T3 and F4. Cell surface staining demonstrated that the isolated clones were able to produce antibodies which could recognize TLS1 expressed on F4 surface, emitting a higher APC-fluorescence than the control. FlowJo software was used for the analysis: gating strategy was done only on alive and single cells (e).*

Optimization of Expi293 transfection with pCDM8-GFP plasmid in 96 Deepwell plates

Before to proceed with TAP-PCR step, the optimization of the transfection in Expi293 cells with 96 Deepwell plates was done. Manufacturers already proposed a protocol so we wanted to replicate the indications suggested or to optimize them in our conditions for our objective.

Firstly, we wanted to identify the right number of cells to use per well: we established a curve from 1x10^5 to 2.8x10^6 cells per well to seed and they were transfected with

pCDM8-GFP plasmid, so we could recognize the highest number of transfectable cells through their GFP emission at FACSCanto. After 24 hours from the transfection, cells were analysed and the best condition to use was between 3x10^5 and 4x10^5 cells, as it is possible to see from the Fig.13. These amounts of cells not only had the highest GFP emission but also the lowest percentage of death cells.

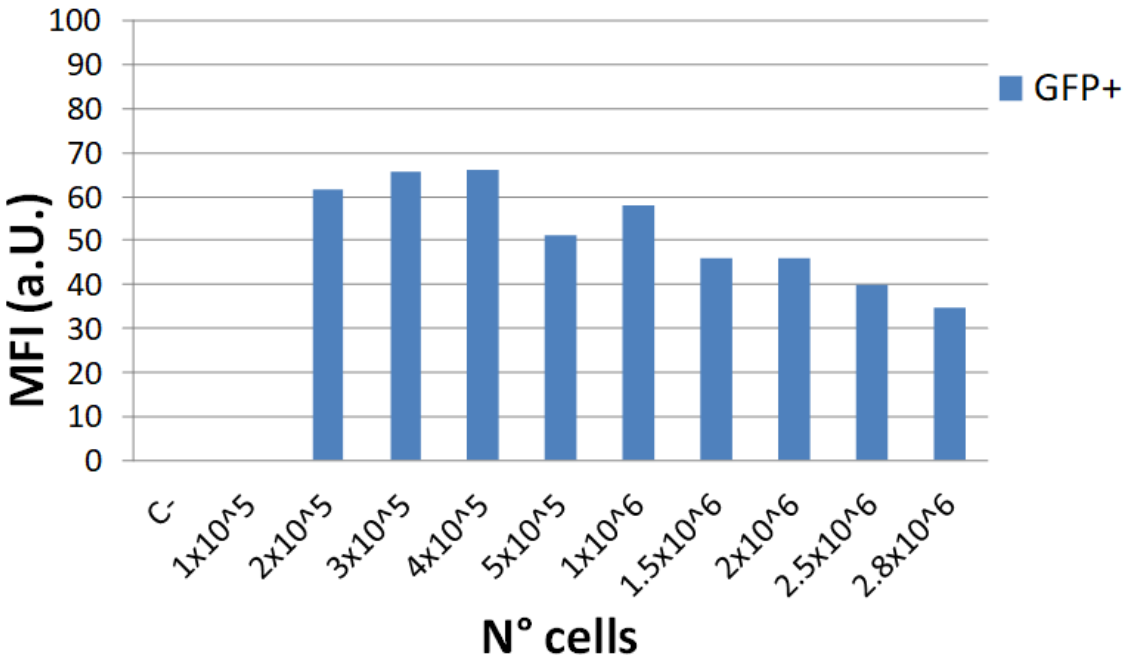

Fig.13 *Histograms representing the MFI of GFP of transfected cells. Cells were seeded in different numbers per well and their positivity was analysed through FlowJ software: gating strategy was done only on alive and single cells.*

Once identified the right number of cells to use, we wanted also to verify the right amount of DNA to use. Keeping fixed the number of cells to seed, a second curve was created from 100 to 800ng of pCDM8-GFP, demonstrating that 0.4µg was the best amount (Fig.14).

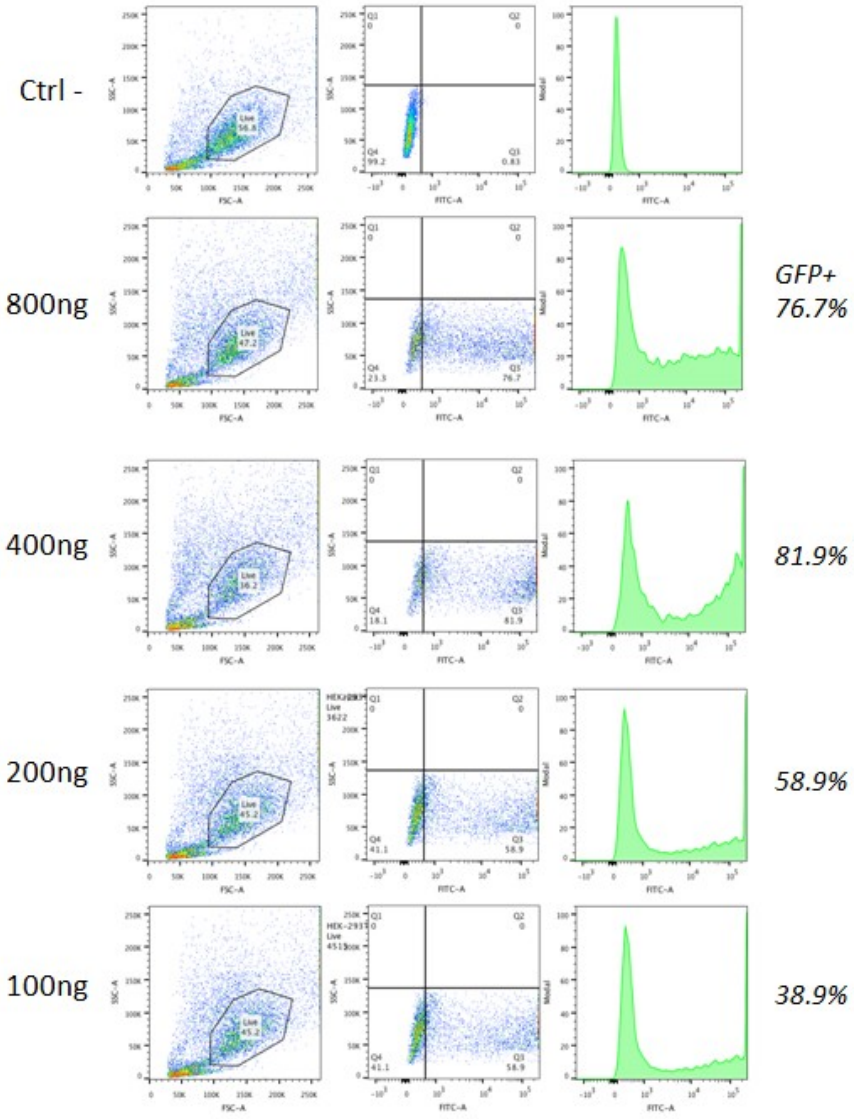

Fig.14 *FACSCanto dotplots and histograms reporting the percentages of GFP positivity of transfected cells. FlowJo software was used for the analysis: gating strategy was done only on alive and single cells.*

Assessing best promoter, poly-adenilation and leader sequences to create TAP-PCR products

Three sequencial rounds of antibody-specific PCR amplifications were performed to amplify heavy and light chain variable region genes and generate two separate linear transcriptionally-active-PCR (TAP) products, one encoding the heavy- and the other one the light-chain. These encompass, in addition of the amplified variable region, a

constant region fragment (including a poly-A signal sequence), a strong promoter region and a leader-sequence, so they could be used directly in a mammalian cell transfection to generate recombinant antibody without the need to perform a purification step. To identify the best constant region fragment and strongest promoter to add, we evaluated the efficiency of various combinations of these in the expression of the reporter gene GFP in Expi293 through FACS analysis. The strongest promoters and pA sequences were chosen (CMVprom, hEF1/HTLVprom, SV40prom, CMV-SCP3prom, CMV-SCP3Dprom, BGHpA and earlySV40pA, respectively) and they were combined with the GFP sequence through the TAP-PCR protocol, creating 10 different constructs to test (Fig.15a-b).

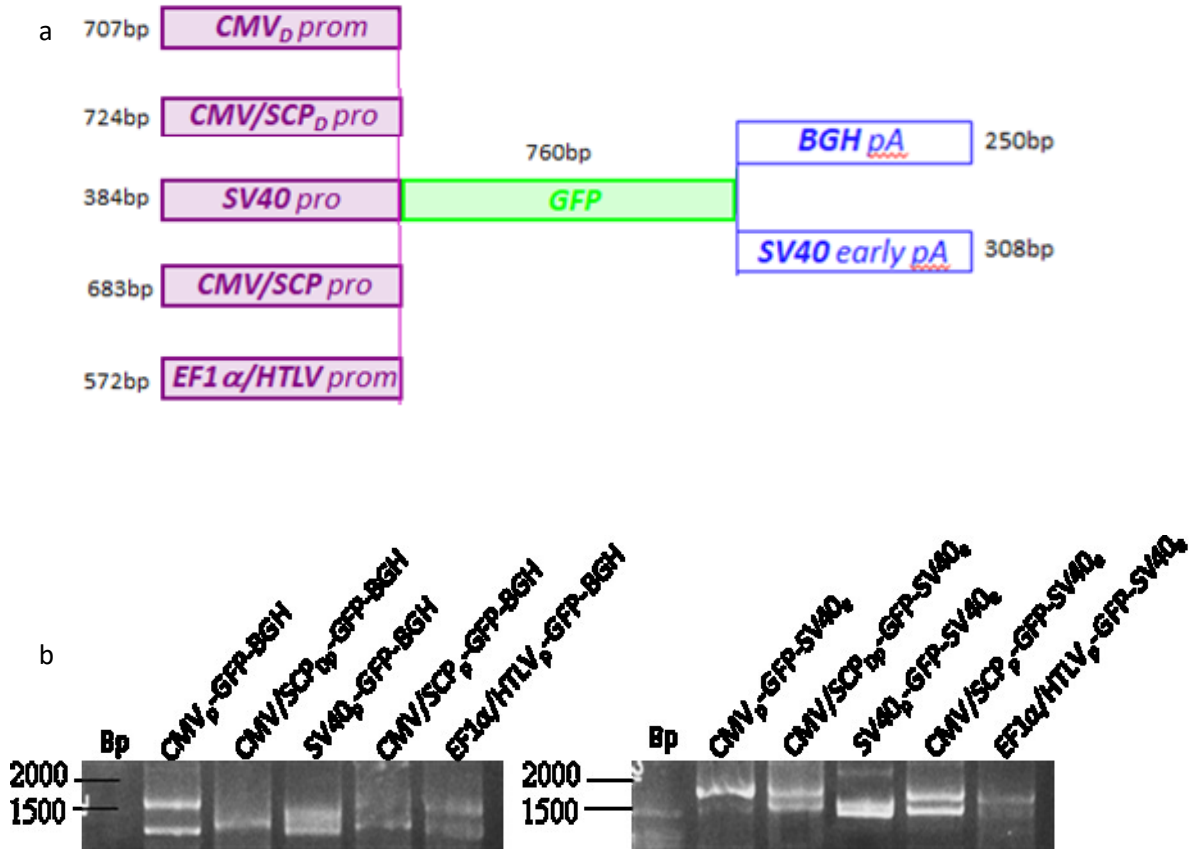

Fig.15 *Schematic representation of the creation of 10 different constructs through TAP-PCR protocol to identify the best promoter and poly-adenilation sequences (a); PCR results of the complete products (b).*

Once obtained, 400ng of each construct were transfected in 4x10^5 cells and the GFP emission was analysed after 48h through FACSCanto, demonstrating that the

citomegalovirus (CMV_p) promoter fragment and the BGH-polyA constant region sequence was the best combination, as it is visible from the percentages of GFP positivity reported below (Fig. 16).

Construct	Transfected DNA (400ng)	PCR product	% positive (GFP)
Negative control	-	-	0
CMVp-GFP-BGHpA	Plasmid Ctrl+	-	81,9
CMVp-GFP-BGHpA	TAP	assembled PCR	64.0
CMVp-GFP-SV40EpA	TAP	assembled PCR	52.0
CMV-SCP3p-GFP-BGHpA	TAP	assembled PCR	61.5
CMV-SCP3p-GFP-SV40EpA	TAP	assembled PCR	47.8
CMV-SCP3Dp-GFP-BGHpA	TAP	assembled PCR	35.3
CMV-SCP3Dp-GFP-SV40EpA	TAP	assembled PCR	39.0
hEF1/HTLVp-GFP-BGHpA	TAP	assembled PCR	33.5
hEF1/HTLVp-GFP-SV40EpA	TAP	assembled PCR	19.5
SV40p-GFP-BGHpA	TAP	assembled PCR	0
SV40p-GFP-SV40EpA	TAP	assembled PCR	0

Fig.16 *Schematic representation of the results obtained through FACSCanto of the Expi293 transfected with 10 different TAP-PCR construct. Transfection was done in triplicate and GFP emission analysis was done with FlowJo software (gating strategy was done only on alive and single cells).*

Once defined which are the promoter and poly-adenilation sequences to use, there was the need to define the best leader sequence to introduce in our fragments: the GFP region was substituted with the heavy and light chain variable region genes of a internal positive control, an hybridoma named 15K, to have proof of the feasibility of the method, and Gaussia- or IL2- leader sequences were added (Fig.17a and b).

Heavy and light chain TAP fragments were transiently co-transfected into Expi293 cells, in parallel to the transfection of the same constructs inserted in pGLuc vectors, obtained through the classical cloning method using ampicillin resistant Mach1 $T1^R$ cells. After 24h and 48h we harvested aliquots of the supernatants to assess IgG expression levels through Western Blot analysis and the reactivity against the target

antigen via ELISA test (Fig. 17d and c). ELISA test was performed using the purified TLS1-L-ECD-HIS for the coating of the ELISA plate, mice sera as positive control and dH_2O as negative control and it showed comparable results between the innovative TAP and the classic plasmid methods; in particular, constructs containing the Gaussia-leader sequence had an expression level of the antibody nearly to the plasmids's one (used as positive controls) and that the recognition of the target antigen occurs only when the two constructs are co-transfected. Western Blot results showed that there was the expression of the antibodies at the MW expected (~ 150Kda) in all four samples, but in the constructs containing Gaussia-leader sequence there was an higher expression than the others empassing the IL2-leader sequence (Fig. 17d). For this reason, in the next steps only the Gaussia-leader sequence was kept.

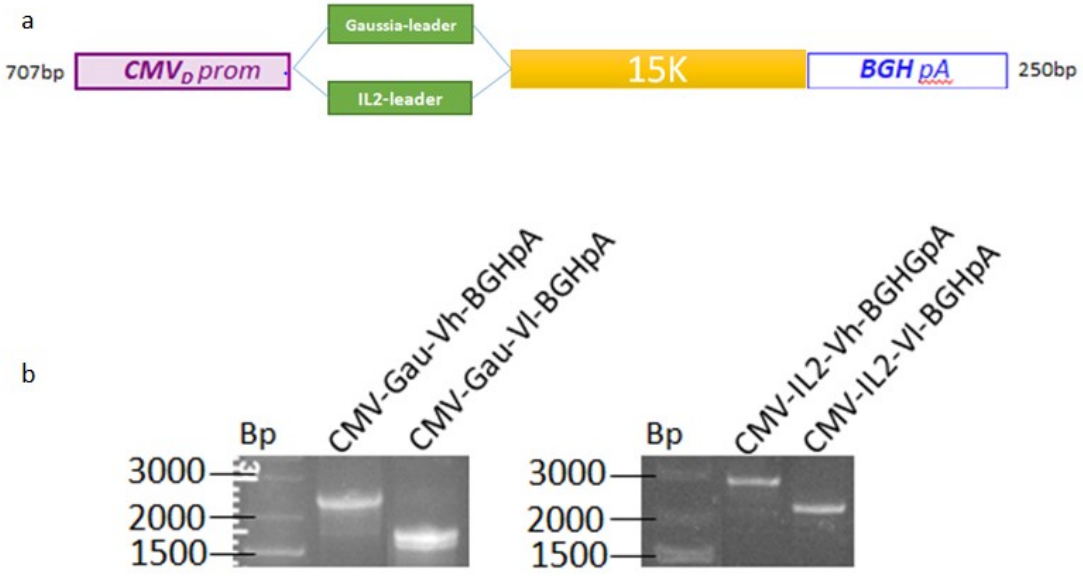

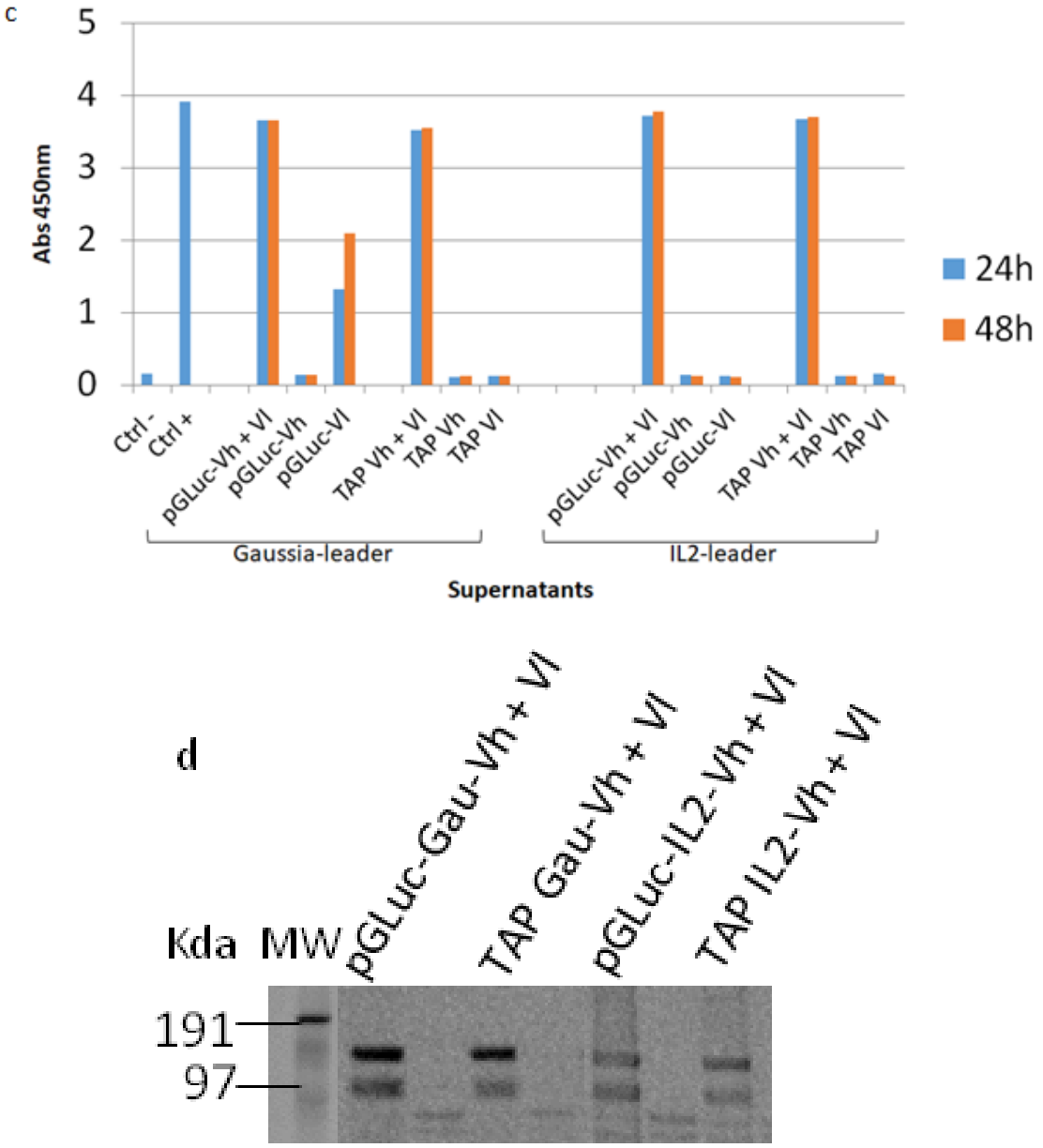

Fig.17 *Schematic representation of the creation of TAP-PCR constructs containing the best promoter and polyA sequences identified previously, two different leader-sequences alternatively (Gaussia-leader and IL2-leader, respectively) and the Vh and Vl of hybridoma 15K, taken as positive control (a); PCR results of the complete products (b); Elisa test results where the supernatants of Expi293 cells transfected with both TAP antibody's variable heavy and light chains had the same ability to recognize the antigen as the classic pGLuc plasmids. There wasn't significant difference between Gaussia-leader and IL2-leader empassing constructs (c); Western Blot result of supernatants harvested after 48h of culture. The PVDF membrane was tested with Goat Anti-Mouse IgG (H+L)-HRP Conjugated. The band relative to the Antibody appeared at 150kDa, as expected (d).*

Single plasma cell RT-PCR and TAP-PCR constructs creation

The recovered plasma cells were subjected to Reverse Transcription to obtain cDNA and subsequently 3 rounds of antibody-specific PCR were performed to amplify heavy and light chain variable region genes and generate two separate linear transcriptionally-active-PCR (TAP) products, one encoding the heavy- and the other one the light-chains.

Transcriptionally-active PCR (TAP) was a rapid method for generating recombinant antibody from amplified heavy and light chain variable region genes which can be immediately transiently transfected into mammalian cell lines, avoiding the need to clone genes into expression vectors or to purify fragments from the PCR reaction. Cognate pairs of variable region genes were amplified via 2 rounds of PCR. A primary PCR utilized gene-specific primers at both the 5′ and 3′ ends. The 5′ oligonucleotide set bound at the 5′ end of the framework 1 region of the mature variable region sequence, adding the Gaussia-leader sequence. The 3′ reverse primer set annealed to the CH1 or Cκ region. In the secondary PCR, a generic 5′ forward oligonucleotide that annealed to the leader-sequence at the 5′ end of the primary PCR product was used with a 3′ primer set that annealed in the J region, introducing for Vh the specific isotype. They also provided ~25 basepair overlap regions at the 5′ end with a human cytomegalovirus (HCMV) promoter fragment and at the 3′ end with a heavy or light chain constant region fragment containing a polyadenylation sequence. Then, in a tertiary PCR, variable region DNA, HCMV promoter fragment and constant region fragment were combined and amplified to produce two separate linear TAP products.

a

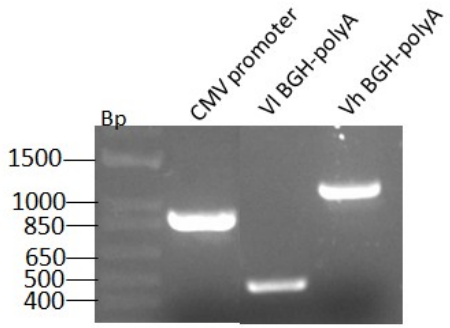

b

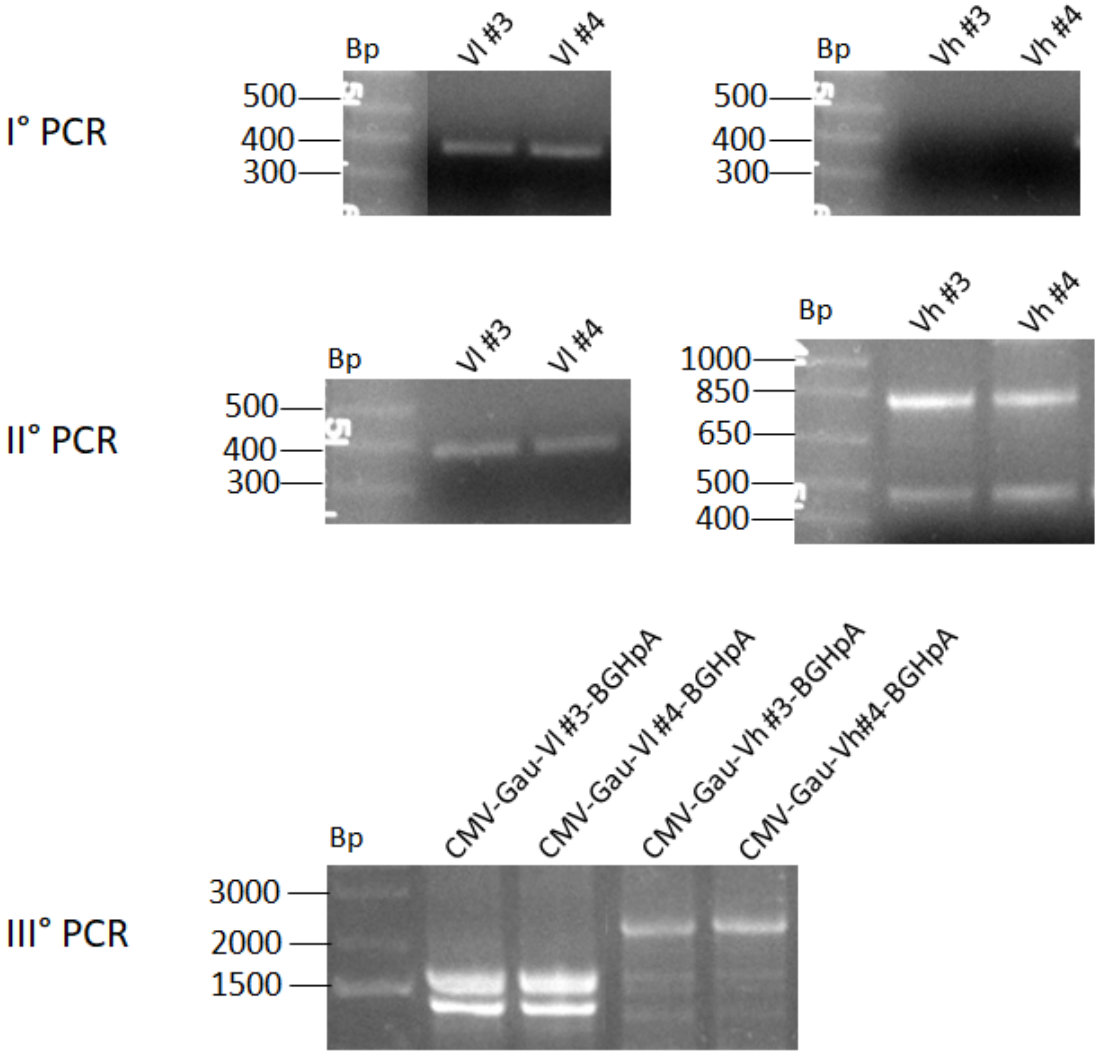

Fig.18 *PCR amplification results of the creation of the constant region fragment (including a poly-A signal sequence) and the strong promoter region (a); PCR amplification results of the three sequencial rounds of antibody-specific PCR steps and the creation of the complete Vh and Vl fragments (b).*

To quantify, the absorbance at 260 and 280nm was measured obtaining the following values:

- **CMV-Gau-Vl#3-BGHpA =** 830 ng/µL A260/280 = 1.804
- **CMV-Gau-Vl#4-BGHpA =** 858 ng/µL A260/280 = 1.807
- **CMV-Gau-Vh#3-BGHpA =** 843 ng/µL A260/280 = 1.787
- **CMV-Gau-Vh#4-BGHpA =** 854 ng/µL A260/280 = 1.794

Transfection into Expi293 cells in Deepwell plate and verification

Complete TAP-PCR Vl and Vh from both plasma cells #3 and #4 were transiently transfected into Expi293 cells using Deepwell plate 96/2mL, with a proportion of 70% and 30% , respectively, following the optimized protocol reported before. Supernatants were then harvested after 24 and after 48h to assess IgG expression levels via Western Blot (Fig. 19a) and reactivity against the target antigen via ELISA and FACS analysis (Fig.19b-c). Elisa test was performed using the purified TLS1-L-ECD-HIS for the coating of the ELISA plate, while FACS analysis was executed on the stable clone F4. In both analysis mice sera in pool were used as positive control and dH_2O as negative control.

Western Blot analysis showed that there was the expression of the antibodies at the MW expected for both plasma cells #3 and #4 and ELISA test demonstrated that there was a recognition of the target antigen only when both Vh and Vl were co-transfected. In particular, plasma cell #4 had higher absorbance result. FACSCanto staining analysis confirmed these data: the recognition of the target antigen occurred in the stable clone in both supernatants recoveries, giving a binding data very similar to the positive control one. Also from the results obtained from the cytofluorimetry analysis plasma cell #4 resulted the best one in comparison with plasma cell #3.

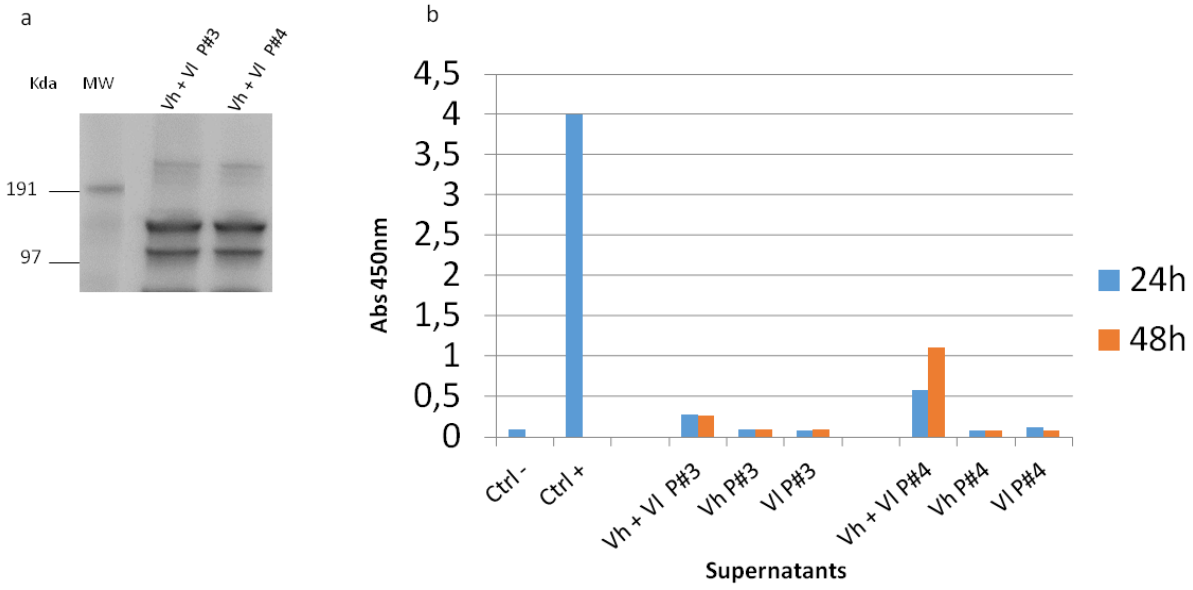

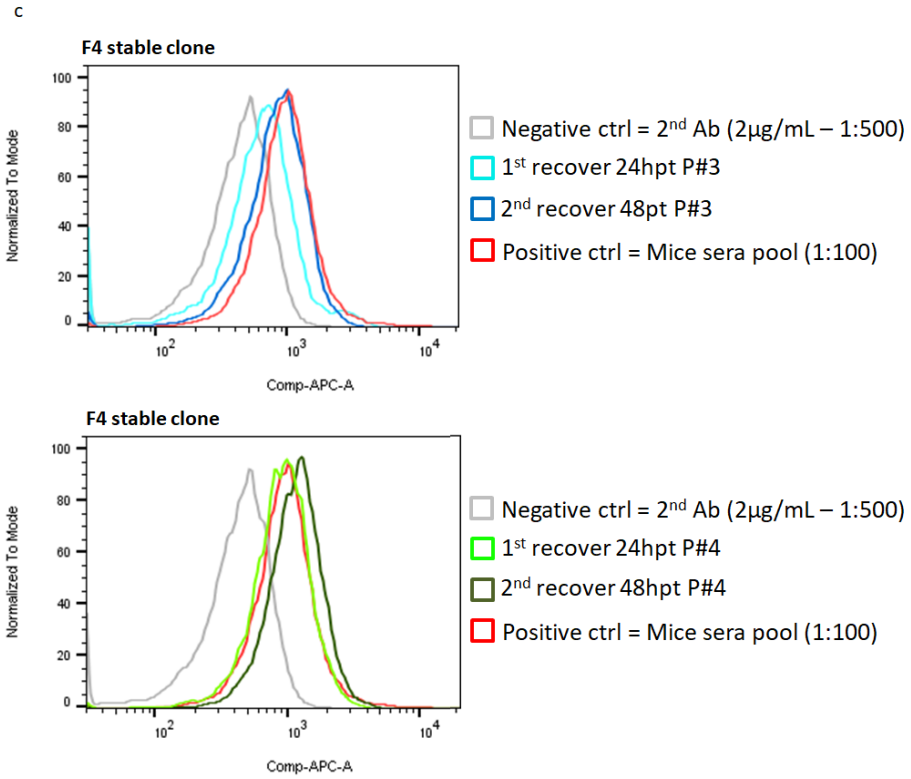

Fig.19 *Western Blot result of supernatants harvested after 48h of culture. The PVDF membrane was tested with Goat Anti-Mouse IgG (H+L)-HRP Conjugated. The band relative to the Antibody appeared at 150kDa, as expected (a); Elisa test results where the supernatants of Expi293 cells transfected with both TAP antibody's variable heavy and light chains had the capacity to recognize the target. (b); Previous results were confirmed via FACSCanto staining analysis. Data were analysed through FlowJo software: gating strategy was done only on alive and single cells (c).*

Sequencing of recombinant TAP-PCR Vh and Vl

Once the activity of the recombinant mAbs was established, the TAP-PCR products were sequenced, using the LightRun barcode service, following manufacturer's instructions. The primers used were: GAU-lea-Mk-F (CTGCATCGCTGTGGCCGAGGCCGAYATTGTGMTSACMCARWCTMCA) and GAU-lea-MH1-F (CTGCATCGCTGTGGCCGAGGCCSARGTNMAGCTGSAGSAGTC) as primer forward for Vl and Vh, respectively, while kc-R (GGATACAGTTGGTGCAGCATC) as primer reverse for both. Results were analysed through VECTOR NTI software (data not shown, for confidentiality) and they confirmed the perfect matching with the target epitope only

for recombinant Vh and Vl from plasma cell #3. This analysis allowed us also to confirm the IgG1 isotype of the Vh.

Cloning in plasmid, expression and purification of recombinant Vh and Vl

The recombinant heavy and light variable regions were inserted into the pCDNA3.4 plasmid backbone and the complete plasmids were obtained from GeneArt Gene Synthesis, named PB3_mIgG12 and PB3_mIgK, respectively. The introduction of the TAP-PCR constructs into the vector allowed us to have an higher reproducibility of the final results and to deal with the scaled-up production. Each plasmid was resuspended in 50µL of TE buffer to reach a final concentration of 100 ng/µL and used for heat shock transformation of *E coli* DH5α. Plasmid extraction was performed through the Qiagen MIDI spin prep as previously described. For quantification, plasmids were diluted in 40µL of TE buffer pH 8 and then the absorbances at 260 and 280nm were measured with Nanovue, obtaining the following results:

- **PB3_mIgG12** = 630 ng/µL A260/280 = 1.797
- **PB3_mIgK** = 557 ng/µL A260/280 = 1.797

Transfection into Expi293 cells in flasks and production of α-TLS1 mAb

Plasmids PB3_mIgG12 and PB3_mIgK were transiently cotransfected with a proportion of 70% and 30%, respectively, into Expi293 cells using 125mL flasks, following the optimized protocol reported before. Two recoveries of the supernatants were made after 48h and after 6 days from the enhancers addition and they were analyzed through FACS and Western Blot analysis (Fig.20). Both tests demonstrated that the antibody was present (expected MW was at 150KDa - Fig.20a) and that it was capable to link to the antigen expressed on the surface of F4 cell line, while no binding activity was found on NIH-3T3 wt cell line (Fig.20b) .

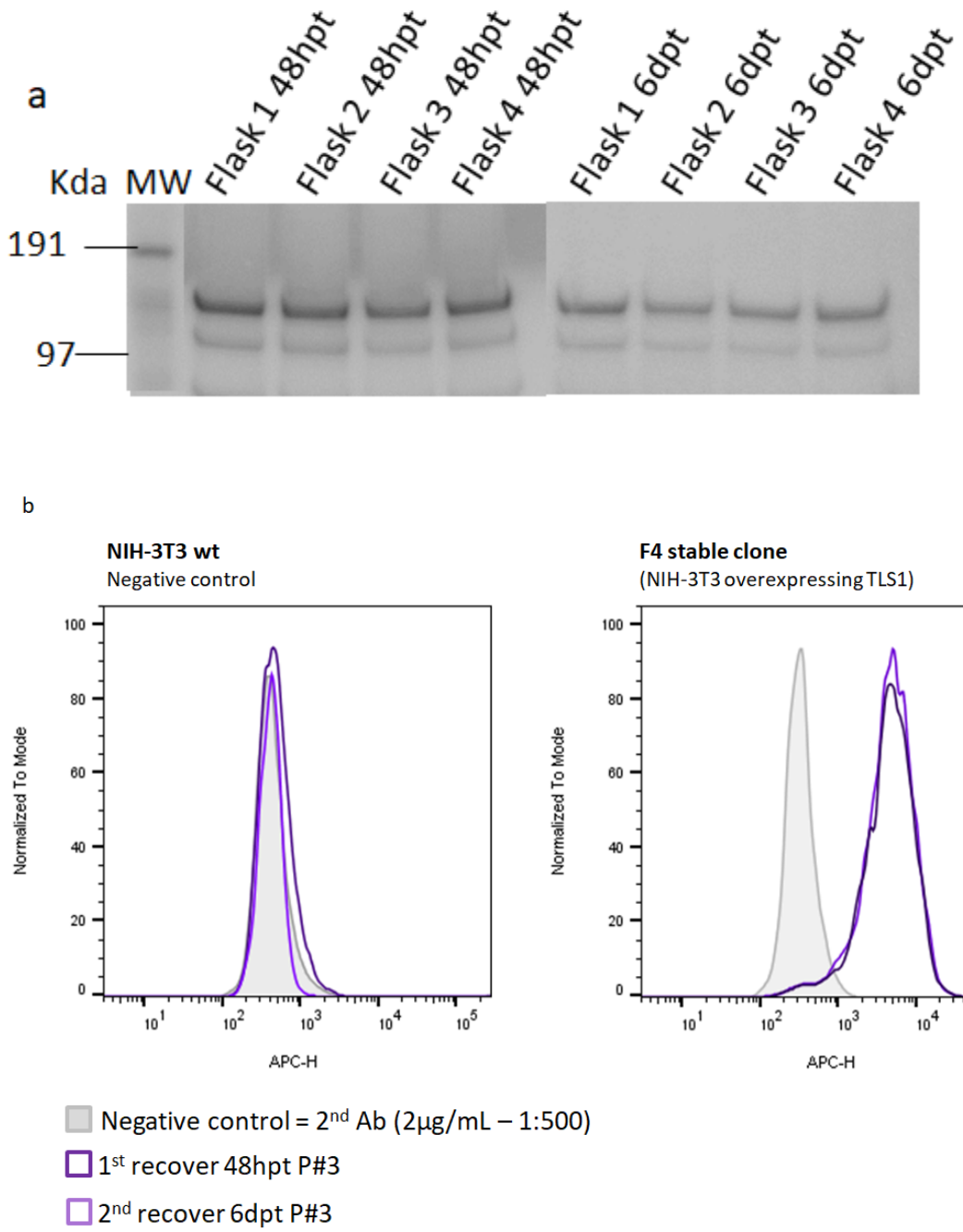

Fig.20 *Western Blot result of supernatants harvested 48h and 6 days. The PVDF membrane was tested with Goat Anti-Mouse IgG (H+L)-HRP Conjugated. The band relative to the Antibody appeared at 150kDa, as expected (a); Histograms representing FACSCanto staining analysis of supernatants on NIH-3T3 wt and F4. Cell surface staining demonstrated that the antibodies could recognize TLS1 expressed on F4 surface, emitting a higher APC-fluorescence than the control. FlowJo software was used for he analysis: gating strategy was done only on alive and single cells (b).*

Purification, concentration and quantification of α-TLS1 mAb

The recombinant mAb's transfection was performed in quadruplicate for a total of 10 times. α-TLS1 was purified from the supernatants using HiTrap™ Protein G HP 1mL columns using a peristaltic pump P1, following manufacturer's instructions. To verify the correct outcome of the purification results, each fraction was analyzed by SDS-PAGE stained with Comassie blue, and Western Blot. As it is possible to see in the Figure 21, in this purification the antibody was found mostly in the 1st and in the 2nd elution as the staining (Fig.21a) and the Western Blot (Fig. 21b) demonstrated.

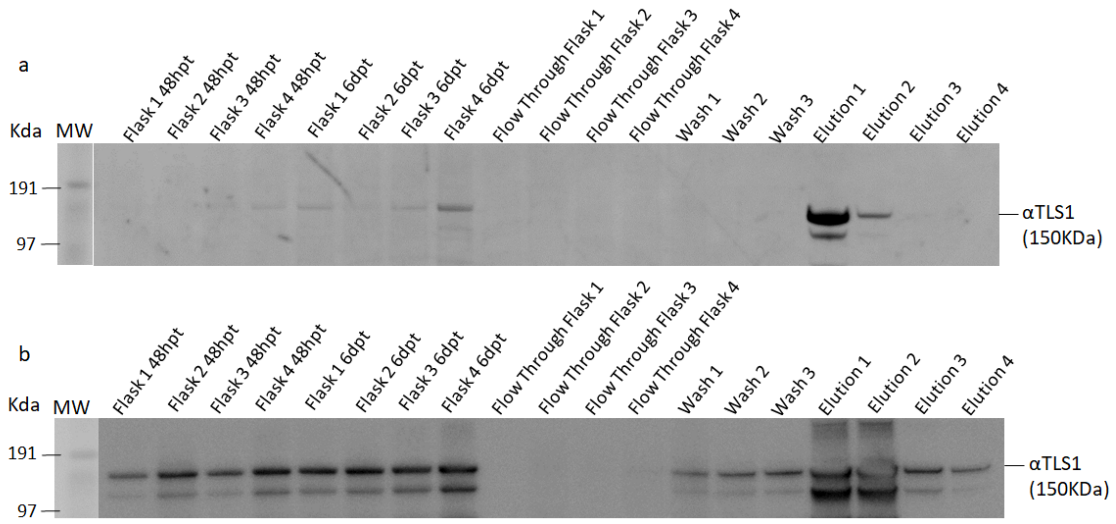

Fig.21 *SDS-PAGE (a) and Western Blot (b) analysis of purification n.8. The PVDF membrane was tested with Goat Anti-Mouse IgG (H+L)-HRP Conjugated. The band relative to the Antibody appeaeds at 150kDa, as expected.*

To quantify the eluted antibody, the elutions showing the most intense bands were quantified, dialyzed in 1XPBS and then quantified again the following day.

On average, about 100-150 µgr/mL of α-TLS1 were obtained from each purification.

The samples were individually concentrated through Pierce™ Protein Concentrator PES, 30K MWCO. Finally, the reading at A280 was repeated, obtaining on average **300 µgr/mL** for each purification. All these fractions, obtained from the 10 purifications executed, were collected to have a unique aliquot, concentrated and quantified: the

value of A280 obtained from the reading was of **1.442** corresponding to **1.06 mg/mL in a total volume of 1.5mL.**

To confirm quantification, we created a standard curve with a IgG m-Ab, available in house, and known concentrations of the control mAb were compared with the measured concentration of the new antibody through SDS-PAGE staining. The standard curve was created by limiting dilution 1:2 of the control antibody from a concentration of 1mg/mL to 31.2 µg/mL. As it is visible from Fig.22, the band relative to the recombinant α-TLS1 was very similar to the standard IgG m-Ab corresponding to 1000 µg/mL, validating the data of the A280 reading.

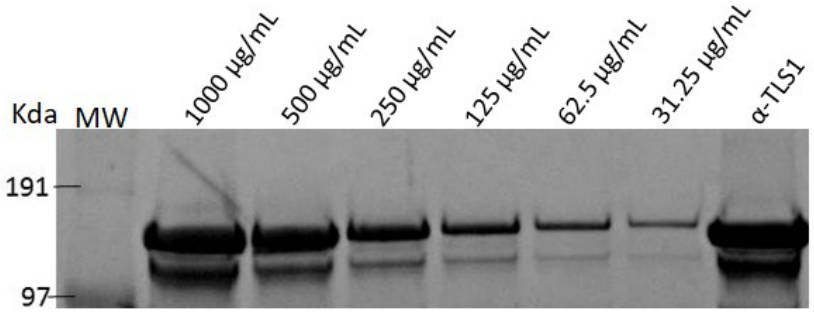

Fig.22 *SDS-PAGE analysis after Coomassie blue staining to compare and to verify the standard curve and the concentrated TLS1 mAb in its native form.*

Activity and specificity tests of α-TLS1 mAb

To assess antigen-binding efficiency of α-TLS1 mAb, the final product (1.06 mg/mL) was tested by flow cytometry using NIH-3T3 wt, F4 (NIH-3T3 stable clone overexpressing TLS1), TF-1 and Ramos cell lines. The α-TLS1 was used at 2.3µg/mL and the 2nd Anti-mouse IgG APC-conjugated at 2µg/mL. The secondary antibody was used also as negative control. mAb α-TLS1 stained positively F4, TF-1 and Ramos cells emitting a higher APC-fluorescence, while NIH-3T3 wild type cell line resulted negative (Fig.23a).

Different concentrations of α-TLS1 mAb ranging from 10µg/mL to 0.0003µg/mL were tested to have a dose-response curve data. Results demonstrated that α-TLS1 mAb stains down to nanomolar concentrations on both F4 and TF-1 cell lines (Fig. 23b).

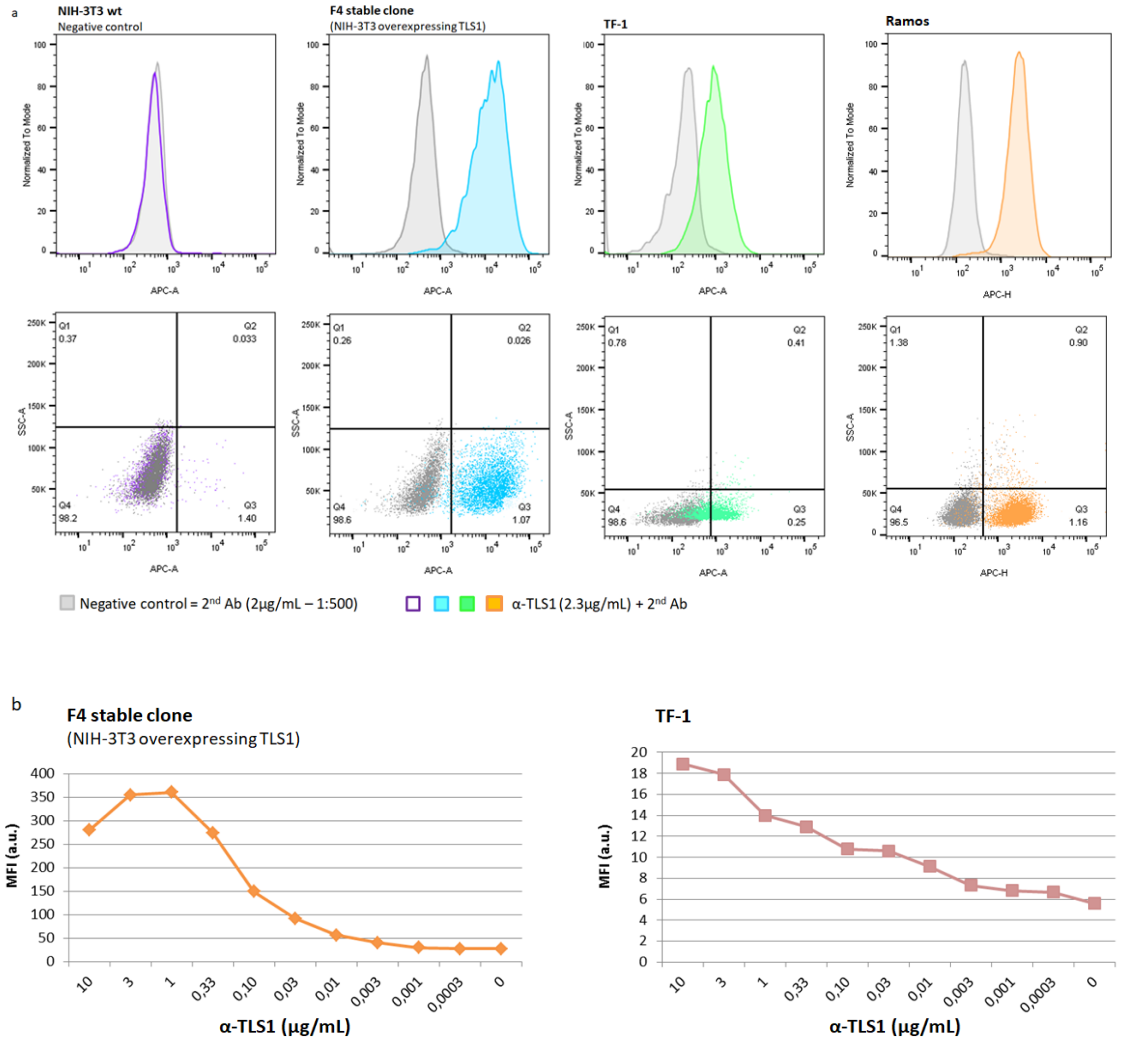

Fig.23 *Dot plots and histograms representing FACSCanto staining analysis of α-TLS1 on NIH-3T3 wt, F4 and TF-1 cell lines. Cell surface staining demonstrated that the antibody could recognize TLS1 expressed on F4, TF-1 and Ramos cell lines's surfaces. FlowJo software was used for the analysis: gating strategy was done only on alive and single cells (a); Dose-response graphs on F4 and TF-1 cell lines demonstrating that the antibody still worked at nanomolar concentrations (b).*

To confirm the specificity of the binding of the recombinant antibody, Western Blot analysis was carried out: 20µg of NIH-3T3 and F4, and 200µg of TF1 cell lysates were loaded on SDS-PAGE gel. On the left panel (Fig.24a), the α-TLS1 mAb was used at 10µg/mL. On the right panel (Fig.24b), since the F4 stable cell line was generated with the full length sequence of TLS1 fused with FLAG-tag, the α-FLAG-tag (M2) mAb was used at the same concentration as positive control. On the left panel, α-TLS1 mAb

stained a band around 65kDa only on TF1 and F4 cell lysates. At the same height on the right panel, the binding of α-FLAG-tag mAb confirmed the specificity of the binding on TLS1.

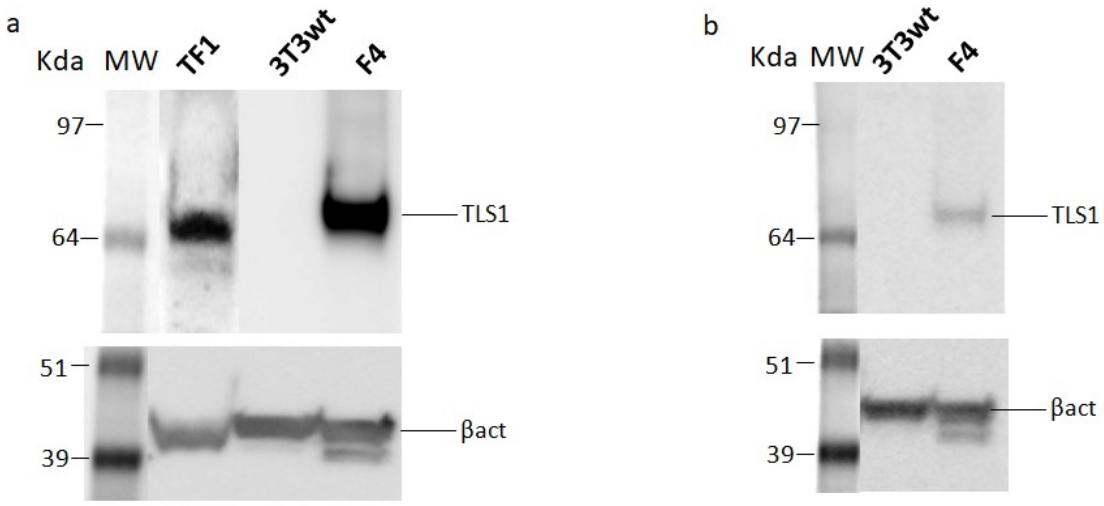

Fig. 24 *Western Blot results of cell lysates. The PVDF membrane was tested with α-TLS1 and α-FLAG-tag mAbs. The PVDF membrane was tested with Goat Anti-Mouse IgG (H+L)-HRP Conjugated. The band relative to the target antigen TLS1 appeared around 65-70Kda.*

To confirm the presence of TLS1 protein in the bands stained by α-TLS1 and α-Flag-tag mAbs, PMF (Peptide Mass Fingerprinting) through Mass Spectrometry analysis was performed. Gel slices around 65kDa (red box) were excided from the SDS-PAGE gel, discolored, reduced and alkylated prior to the trypsin digestion. The tryptic digest was analyzed by LC-HRMS-ESI-MS/MS and the data obtained were processed by Biopharma Finder which allows to compare a known amino acid sequence with the experimental data. The colored "blocks" indicated the identified amino acid sequence (Fig.25, the protein sequence has been hidden for confidentiality). All identified peptides showed a confidence score >98% and were identified by both molecular weight and MS/MS fragmentation.

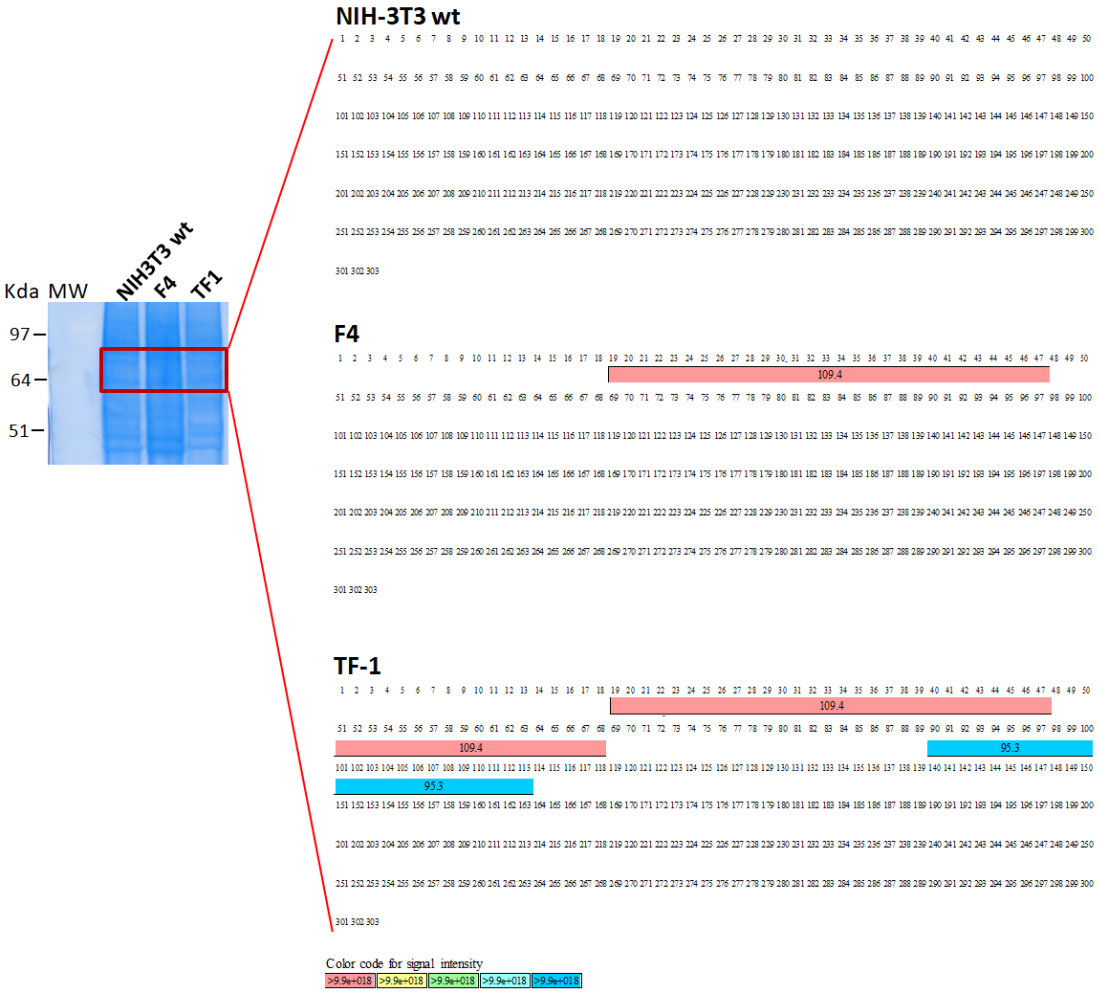

Fig. 25 *LC-HRMS-ESI-MS/MS results on gel slices containing NIH-3T3 wt, F4 and TF-1 cell lysates*

Final check on recombinant antibody sequence via PMF

In order to get confirmation on the primary amino acidic sequence, an aliquot of the antibody was analyzed via PMF, comparing the obtained data with the sequencing done previously (reported on page n. 72). The sequence coverage exceeded 80% for both Vh and Vl (Fig.26a), as it is possible to see also in the signal intensities of the frames (Fig. 26b), confirming that the antibody's sequence didn't mutate.

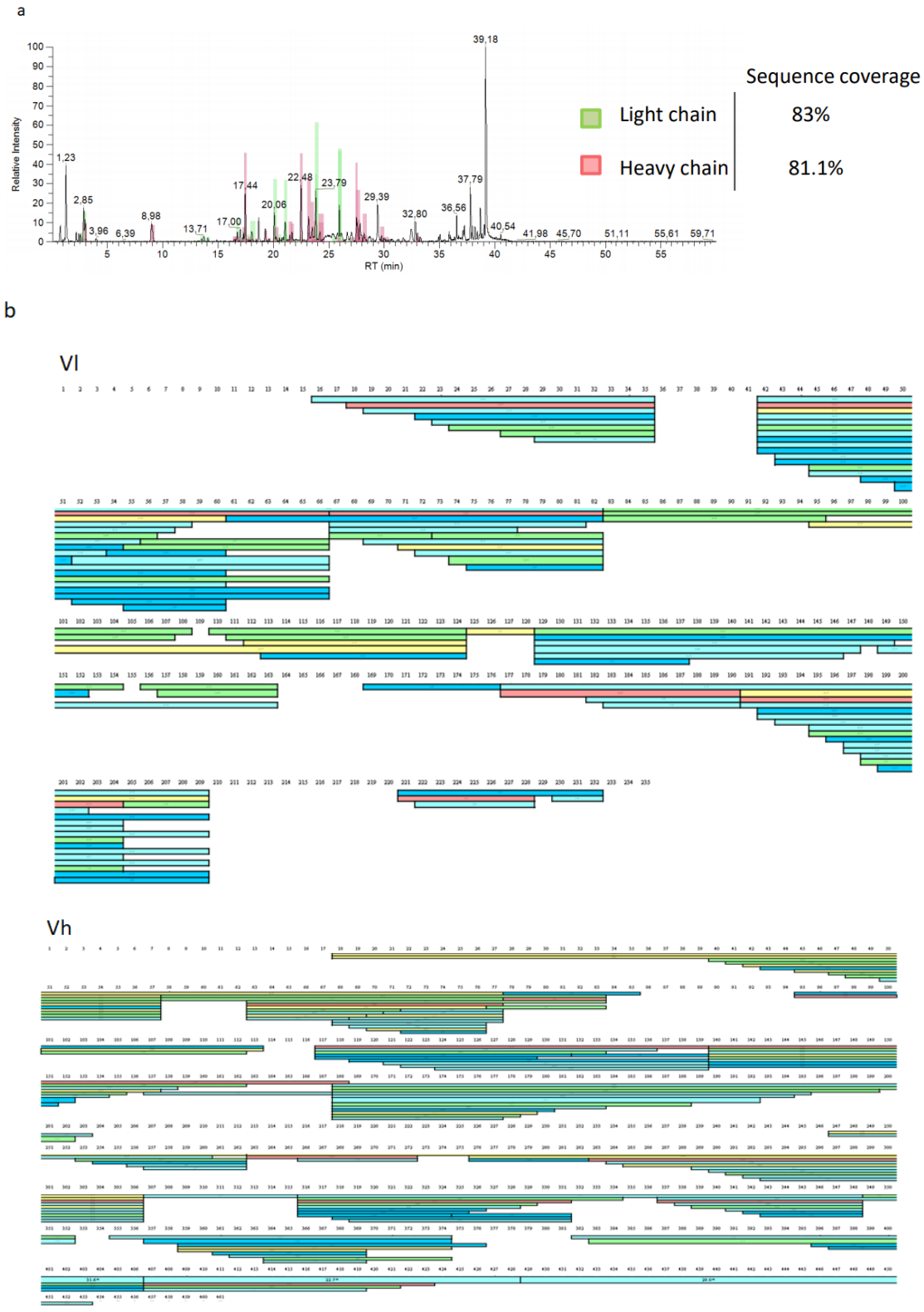

Fig. 26 PMF results on α-TLS1 m-Ab . Chromatogram (a) and frames (b) reported that the sequence coverage exceeded 80% for both Vh and Vl.

Discussion

Personalized Medicine is an advanced approach that integrates research disciplines and clinical practice to build up a knowledge base that can better guide individualized patient care. Single-cell omic, which allows the molecular investigation of different cell types in a high throughput manner, is driving this innovative approach.

Single B-cell screening and isolation strategies, the starting points of single-cell omics, have emerged as important technologies for efficiently sampling the natural antibody repertoire.

In Toscana Life Sciences (TLS) Foundation's laboratory a new platform FACS sorter-free has been set-up to identify and isolate antigen-specific plasma cells from heterogeneous and complex samples, able to produce IgG with unique and desirable binding characteristics. Moreover, we demonstrated that it is possible to obtain TAP-PCR products containing the variable light and heavy regions of antibodies which could be directly transfected in mammalian cell lines, utilized for determination of the antibody sequence variability, used for mAbs scale-up production and easily converted in more stable reagents (e.g. plasmids).

This could simplify the technical procedures for the identification of appropriate molecules that could be developed into therapeutic or research agents, but also this new technique reduces the time needed for the process of monoclonal antibody discovery relying to fast isolation, cloning and expression steps. Moreover, this fast approach overcome the problems associated both with hybridoma cell lines and phage display bypassing the multiple rounds of panning/screening and the subsequent sub cloning into mammalian expression vectors that are required by display techniques.

This new technique is also suitable for generating monoclonal antibodies only recognising conformational epitopes displayed on cell surface.

The future perspective is to establish a monoclonal antibodies production facility in TLS Foundation.

STUDY 2 – CD8$^+$ T CELLS EXHAUSTION: FIRST INSIGHTS FOR FUTURE SINGLE-CELL OMICS APPLICATION

Introduction

Cancer biology is one of the research areas that greatly benefited from the application of single-cell omics. Tumours are microenvironments consisting of heterogeneous population of cells including malignant, stromal and infiltrating immune cells (*Bussard et al.*, 2016) which make critical both accurate diagnosis and personalized treatments (*Qian et al*., 2017; *Sant et al*., 2017). In fact, tumour phenotyping at the bulk level does not provide sufficient information on the molecular profile of tumour cells and consequently the information for setting the most appropriate therapeutic approach. Conversely, with the application of single-cell technologies, a powerful tool for following the progression and expansion of individual clones (*Gawad et al*., 2016; *Navin et al*., 2011), researches can reconstruct cell lineage trees with high precision by detecting somatic mutations that have occurred in every DNA replication (*Frumkin et al*., 2005). This approach allows the identification of distinct molecular patterns involved in the disease progression and relapse, and the mechanism of tumour immune evasion. Identification of such changes will help to develop immunotherapy strategies, to develop new targeted therapies, to monitor cancer progression over time and also to predict drug sensitivity/resistance profile and patients could be switched to a different drug before resistance arises (*Lapin et al*., 2017; *Ramskold et al*., 2012; *Mitra et al*., 2016). Although classical histomorphologic evaluation of a malignant tumour is argued to be the most significant diagnostic, prognostic and predictive biomarker with the greatest impact on patient treatment (*Radpour and Forouharkhou*, 2018), in depth single-cell RNA sequencing in combination with protein profiling of pimary human tumours, has been proposed to be highly effective in discerning cell types and subtypes within tumour cells and for detection of distinct functional states of proliferation and activation (*Tirosh and Suvà*, 2019).

In this context, the PD-1/PD-L1 axis, and then the immune checkpoint cancer immunotherapy, was discovered. PD-L1, the ligand for PD-1, is highly expressed in several cancers and the role of PD-1 in cancer immune evasion is well established (*Wang et al*., 2016; *Gandini et al*., 2016; *Syn et al.,* 2017). Programmed Cell Death Protein 1 (PD-1) plays a vital role in inhibiting immune responses and promoting self-tolerance through modulating the activity of T-cells, activating apoptosis of antigen-specific T cells and inhibiting apoptosis of regulatory T cells. Programmed Cell Death Ligand 1 (PD-L1) is a trans-membrane protein that is considered to be a co-inhibitory factor of the immune response, it can combine with PD-1 to reduce the proliferation of PD-1 positive cells, inhibit their cytokine secretion and induce apoptosis. PD-L1 also plays an important role in various malignancies where it can attenuate the host immune response to tumour cells. Based on these findings, PD-1/PD-L1 axis is responsible for cancer immune escape and greatly affects the outcome of cancer therapy (*Han et al*., 2020).

Immunotherapy for cancer treatment has been recently developed with the aim of designing effective treatments to improve the specificity and strength of the immune system against malignant cells (*Salmaninejad et al*., 2019). James P. Allison and Tasuku Honjo won the 2018 Nobel Prize of Physiology or Medicine for discovering a cancer treatment by suppressing the negative immunomodulation. Their research on the immune checkpoints programmed cell death protein 1 (PD-1) and cytotoxic T-lymphocyte-associated protein 4 (CTLA-4), demonstrated that these proteins acted as a “brake” on immune functions, and the two scientists formulated the hypothesis that immune checkpoint inhibition may reactivate T cells and eliminate cancer cells more effectively (*Ljunggren et al*., 2018).

Monoclonal antibodies targeting PD-1 that boost the immune system are being developed for the treatment of cancer (*Syn et al*., 2017; *Weber et al*., 2010). Indeed, accumulating evidences demonstrate that the inhibition of the interaction between PD-1 and PD-L1 can re-activate and enhance T-cell responses against cancer cells and mediate preclinical antitumor activity. This is known as immune checkpoint blockade (Fig.1) (*Messenheimer et al.*, 2017).

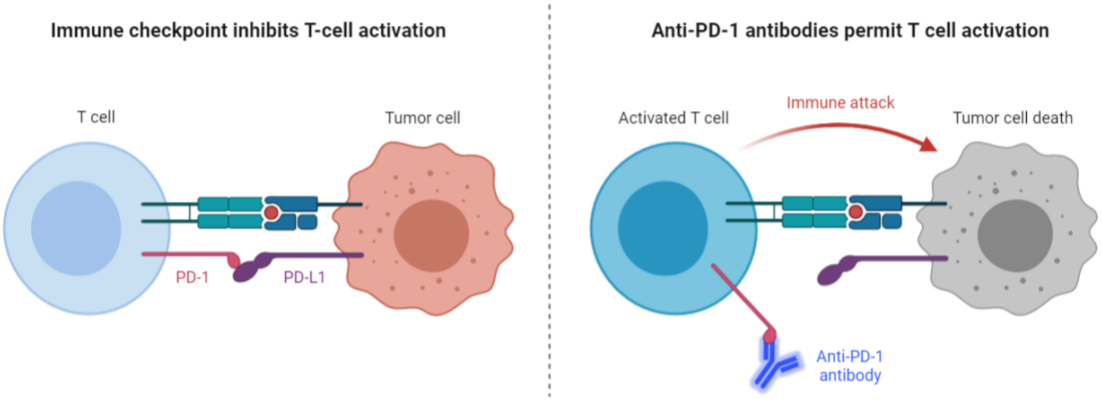

Fig. 1 *Schematic representation of Immune Checkpoint blockade mechanism.*

This new therapeutic approach has revolutionized cancer treatments for its efficacy, this treatment has sustained response even to terminal stage cancers and for major compliance, since patients experience, lesser adverse effects compared to the conventional cancer treatments (*Brahmer et al*., 2010; *Couzin-Frankel*, 2013; *Hodi et al*., 2010; *Mahoney et al*., 2015; *Topalian et al*., 2015). PD-1 signaling pathway suppression has shown that the clinical response of patients with different solid tumors and hematological malignancies mainly relies on T-cells effectively to penetrating the tumor (*Iwai et al*., 2017). In addition, targeting PD-L1 has been associated with a significant clinical response in a wide range of cancer patients (*Sacher et al*., 2016). The success of clinical trials for the PD-1/PD-L1 axis blockade led the FDA to approve antibodies for PD-1 (e.g. Nivolumab, Pembrolizumab) or PD-L1 (e.g. Atezolizumab, Avelumab, Durvalumab) for different types of human cancers including metastatic non-small cell lung carcinoma (NSCLC), squamous cell lung cancer, renal cell carcinoma, hodgkin's lymphoma, head and neck squamous cell carcinoma, and recently, for microsatellite instability-high (MSI-H) or mismatch repair deficient (dMMR) cancers that include many late-stage cancers (*Chowdhury et al*., 2018a).

Despite the impressive success rate of PD-1 blockade therapy, still a significant fraction of patients (~40%) shows unresponsiveness. In order to improve the success rate of cancer treatment, it is mandatory to elucidate the mechanism for unresponsiveness. To takle this issue, the future steps to take will be:

1. identify new biomarker(s) that predict the responsiveness/unresponsiveness;
2. develop improved strategy including the combination therapy.

Patients unresponsiveness could be the consequence of prolonged exposure to cognate antigens, as it happens in the upset of cancer, which often attenuates the effector capacity of T cells and limits their therapeutic potential (*Alfei et al*., 2019; *Wherry et al*., 2011; *Speiser et al*., 2014; *Schietinger et al*., 2014; *Gallimore et al*., 1998). This process, known as T cell exhaustion or dysfunction, is manifested by epigenetically enforced changes in gene regulation that reduce the expression of cytokines and effector molecules and upregulate the expression of inhibitory receptors, just like programmed cell-death 1 (PD-1) (*Barber et al*., 2006; *Chihara et al*., 2018; *Youngblood et al*., 2011; *Ghoneim et al*., 2017). This process, likely evolved to prevent excessive immune activation, remains a major stumbling block in the quest to develop more effective immunotherapies and vaccines. However, the underlying molecular mechanisms that induce and stabilize the phenotypic and functional features of exhausted T cells remain poorly understood (*Ghoneim et al*., 2017; *Pauken et al*., 2016; *Utzschneider et al*., 2013; *Philip et al*., 2017; *Wieland et al*., 2017). It is widely held that the process of exhaustion drives $CD8^+$ T cells into a transcriptionally distinct lineage (*McLane et al*., 2019) that encompasses 'precursor exhausted' and 'terminally exhausted' subsets within a unique differentiation spectrum (*Kallies et al*., 2019). Precursor exhausted $CD8^+$ T cells are throught to self-renew and if treated with immune checkpoint blockade antibodies, they are able to "wake up" and recover their functionality. However, precursor exhausted $CD8^+$ T cells can differentiate into terminally exhausted $CD8^+$ T cells, which display reduced effector functionality and inability to recover the active phenotype. There is no definitive marker that identifies exhausted $CD8^+$ T cells, yet.

Previous works (not mentionable, for confidentiality issues) reported, via RNA-seq analysis, an enrichment in the HMG-box genes in the exhausted phenotype encompassing TFX (Transcription Factor X, the real name of the factor has been hidden for confidentiality issues) which could have an important role in managing exhaustion phenotype; thus, studying its characteristics and its role in the transcription process, it

would be possible to find pathways wherein it is involved and regulates. This novel biomarkers could be a central candidate like PD-1/PD-L1, for the development of novel immune checkpoint agents.

Materials and Methods

Cell cultures

Jurkat (ATCC – catalog #TIB-152) and TK-1 (ATCC – catalog #CRL-2396), cell lines were cultured in RPMI1640™ medium (Corning – catalog #10-040-CV) with 10% (v/v) heat inactivated fetal bovine serum (FBS – Gibco – Life Technologies), 1% (v/v) penicillin-streptomycin mixed solution (Gibco - Life Technologies – catalog #15140122), 2mM (v/v) glutamine (Gibco - Life Technologies – catalog #35050038) and 1% (v/v) Sodium Pyruvate (NaP - Gibco - Life Technologies – catalog #11360070).

Cell lines were free of mycoplasma contamination. Cell cultures were maintained in cell culture dishes or 6-12-24-96-well sterile plates for cell culture (Corning) and at 37°C in a 5% CO_2 and humified environment.

Animals

C57BL/6 wt mouse (The Charles River Laboratories - Kanagawa, Japan) were maintained under specific pathogen-free conditions at the Institute of Laboratory Animals, Graduate School of Medicine, Kyoto University.

Murine CD8⁺ T cell isolation

To isolate naïve CD8+ T cells from B6 wild-type mice, the spleen and three LNs (axillary, brachial, and inguinal LNs) from both the right and left sides were harvested. The spleen was minced, treated with ACK lysis buffer (0.15 M NH_4Cl, 1.0 mM $KHCO_3$, 0.1 mM Na_2-EDTA Gibco – catalog #A1049201) for 2 min to lyse the erythrocytes, and mixed with pooled and minced LN cells. CD8+ T cells were then purified from total pooled lymphocytes using $CD8a^+$ T Cell Isolation Kit, mouse according to the manufacturer's instructions (Miltenyi Biotec, 130-104-075). $CD8a^+$ T cells were then stimulated with α-CD3 and CD28 mAb-coated dynabeads (Thermo Fisher Scientific, Gibco, Catalog #11452D).

Human PBMC isolation

To isolate human PBMC, blood samples from patients from Kyoto University Hospital (Kyoto University Hospital 54 Kawaharacho, Shogoin, Sakyo-ku Kyoto,606-8507, Japan) were used. Total PBMC were recovered using Ficoll-Paque Plus (Sigma Aldrich – catalog **#***GE17-1440-02).*

RNA isolation and RT-PCR

We isolated RNA from the experimental groups with the RNA isolation mini kit (Machinery Nagel Protocol – catalog #740955.50) and synthesized cDNA by reverse transcription through RevertraAce qPCR RT Master Mix and Kit (Toyobo – catalog #FSQ-101), following manufacturer's instructions.

PCR

KOD Fx Neo DNA Polymerase (Toyobo**)** or HiProof High Fidelity PCR Kit (BioRad – catalog #172-5331) and gene specific primers (Eurofins Genomics), were used following manufacturer's instructions (Table n.1).

Table n.1

PCR MIX 1x	**KOD**	**HF**
Promega Nuclease free Water (Fisher Scientific – catalog #PR-P1193):	6µL	32µL
Buffer PCR:	25µL (2X)	10µL (5X)
dNTPs 2,5mM each (Invitrogen – catalog #R72501):	10µL	2µL
Primer F :	1.5µL	2.5µL
Primer R :	1.5µL	2.5µL
Template :	5µL	0.5µL
Polymerase:	1µL	0.5µL
Volume to add per well	50µL	50µL

For each target gene were designed primers F and R primers (Eurofins Genomics), but also primers to carry out also the sequencing and the quantitative Real-Time PCR (qRT-PCR) steps, reported below. β-actin was used as control. In each amplification step the primers were resuspended at 10µmol/µL with DNAse/RNAse free water. Every PCR product was verified by 1% Agarose (Sigma Aldrich) gel electrophoresis in 1X Electrophoresis buffer (50X = 242g Tris-free-base, 18.61g Disodium EDTA, 57.1 mL Glacial Acetic Acid , dH_2O to 1L and then diluted to 1X) with Nippon gel ladder Wide2 (Nippon Gene – catalog #310-06971). Multiplate PCR plates 96 well clear (Biorad) or DNAse/RNAse free PCR tubes 0.2mL (Eppendorf) were used. When PCR products was contaminated with aspecific products or gel slices and PCR mixes to be purified, these were submitted to Wizard SV gel and PCR product Clean-up system (Promega – catalog #A9281).

Cloning

The following restriction enzymes were used to clone the target genes: EcoR1 (catalog #R0101), Xho1 (catalog #R0146S) and BamH1 (catalog #R0136S) from New England BioLabs with their respective buffer. The pMXS_hPDL1_Neo, pEGFP-C1 plasmids were already available in house. Both the vector and the target genes were cut through restriction enzymes, submitted to Wizard SV gel and PCR product Clean-up system (Promega – catalog #A9281) and then their concentration was evaluated with Nanovue (GE Healthcare). The consequent ligation step was done combining vectors and inserts 1:3, respectively, and calculating the volumes to use with the following rule :

Vector (ng) x Insert size (Kb)/ Vector size (Kb) x3 / Insert (ng/ µL) = Insert µL

Vector and Insert were combined with 2X Ligation buffer (Nippon gene – catalog #319-05961) and dH_2O to reach the volume of 20µL and the mix was then incubated at RT for 20-30 minutes. Afterwards, the ligation mix was transformed in *Escherichia coli* XL10-Gold Ultra-competent cells (Agilent – catalog #200314), following manufacturer's

instructions. Briefly, an aliquot of 100µL of competent cells for each transformation was thawed on ice for 15 minutes into a 1.5 mL microcentrifuge tube. 10µL pf each ligation mix were added to the cells and mixed gently. Tubes were incubated on ice for 20 minutes and then heat-shocked for 60 seconds in a 42°C heating block module (Eppendorf). Tubes were placed again on ice for 2 minutes. Afterwards, 300µL of pre-warmed sterilized LB medium (Miller LB broth - Sigma Aldrich – catalog #L3522) were added to each tube. Then 50µL and 300µL from each transformation were spreaded on pre-warmed selective plates for bacterial cultures (Fisher Scientific) previously prepared with Lennox LB broth with agar (Sigma Aldrich – catalog #L2897) and 100µg/mL Ampicillin (Ampicillin Sodium Salt - Shelton Scientific – catalog #171254) and incubated at 37°C O/N. The following day, several single colonies were spotted and analysed through Colony PCR as reported below (Table n.2):

Table n.2

Colony PCR MIX	**1X**
10X Buffer PCR (Invitrogen):	1.5 µL
dNTPs 2,5mM each (Invitrogen – catalog #R72501):	1.5µL
γTaq Polymerase (Invitrogen) :	0.2µL
Primer F :	1.5µL
Primer R :	1.5µL
Template :	1 spotted colony
Promega Nuclease free Water (Fisher Scientific – catalog #PR-P1193):	10.8µL
Volume to add per well	15µL

	95°C, 3 min	
.	95°C, 30 sec 58 °C, 30 sec 72°C, 1 min 40 sec	X 30 cycles
	72°C, 5 min	
	12°C, ∞	

The PCR results were verified by 1% Agarose gel electrophoresis in 1X Electrophoresis buffer with Nippon gel ladder Wide2. The colonies with the correct insert amplified through colony PCR were recovered and added to 4mL of LB medium with 100µg/mL Ampicillin in Falcon™ Round-Bottom Polypropylene Test Tubes (Fisher Scientific) and incubated at 37°C, O/N at 225rpm. The next day the culture was submitted to the plasmid extraction using QIAprep Spin Miniprep Kit (Qiagen – catalog #27104), following manufacturer's instructions. To quantify, plasmids were eluted in 50µL of Promega Nuclease free Water (Fisher Scientific – catalog #PR-P1193) and then the absorbances at 260 and 280nm were misured with Nanovue (GE Healthcare).
Alternatively we used the In-Fusion HD Cloning Kit (Clontech – Takara Bio – catalog #638920), following manufacturer's instructions.

CRISPR/CAS9

To create the gene specific KO cell lines we used the CRISPR/CAS9 system through Guide-It™ CRISPR/CAS9 system (Clontech – Takara Bio – catalog #632601/2) with pGuide-it-ZsGreen1 linear vector or lentiCRISPRv2 vector (Addgene – catalog #52961) with Genome-scale CRISPR Knock-Out (GeCKO) v2.0 pooled libraries (Gecko-ZhangLab), following manufacturer's instructions, respectively.

Sequencing

Sequencing was also done using BigDye™ Terminator v3.1 Cycle Sequencing Kit (Thermo Fisher – catalog #4337454), following manufacturer's instructions. Briefly, a

PCR amplification with given primers and template was done with the following reaction mix and program (Table n.3):

Table n.3

	1X **(10** µL)	**Conc**
• **5X Sequencing Buffer (Thermo Fisher – catalog #4336697) :**	1.75µL	1x
• **BigDye™ Terminator :**	0.5µL	
• **Primer :**	1.6µL	1µM
• **DNA Template:**	2µL	100-200ng
• **UltraPure™ DNase/RNase-Free Distilled Water (Invitrogen – catalog #10977035):**	4.14µL	
Total	10µL	

96°C, 1 min

96°C, 10 sec

50 °C, 5 sec — X 25 cycles

60°C, 4 min

16°C, ∞

For each 10µL PCR product from the above step, 45µL of SAM Solution (Thermo Fisher Scientific – catalog #4376497) and 10µL of X Terminator Solution (Thermo Fisher Scientific – catalog #4376493) were added and samples were vortexed for 30 minutes at 3000rpm. Samples were then centrifuged at 1000g for 2 minutes and then loaded in the 3130xl Genetic Analyzer machine (Thermo Fisher), following manufacturer's

instructions. Analysis of the sequences were made through the Sequencher software (Gene Codes Corporation).

Electroporation

Complete selected plasmids were transfected into cell lines using Amaxa Cell Line Nucleofector™ Kit V (Lonza – catalog #VCA1003) and the Nucleofector™ Device, following manufacturer's instructions. The day after the electroporation, the efficacy of the transfection was controlled through GFP emission, given by the control plasmid supplied by the kit, through fluorescence microscope or/and FACSCanto analysis. After 4 days of transfection, the selection agent was added (Neomycin or Puromycin were used, Sigma Aldrich – catalog #G418RO and Invivogen – catalog #ant-pr-1, respectively) to select the correct population holding plasmids containing the sequence providing resistance. Once reached an homogenous population (around 14-21 days after transfection), cells were used for further analysis.

Also plasmids containing directly GFP as reporter gene were created and cells were immediately sorted in GFP+ and GFP- through BD™ FACS Aria Cell Sorter (BD Biosciences).

Flow cytometry analysis

The following monoclonal antibodies (mAbs) were used to detect the respective antigens during FACS staining: CD8 (53–6.7 and SK1), CD279/PD-1 (29F.1A12 and EH12.2H7), CD152/ CTLA-4 (L3D10 and BNI3), CD366/Tim3 (RMT3-23 and F38-E2E), CD183/CXCR3 (G025-H7), γH2AX (2F3), Zombie Fixable Viability Sampler Kit (catalog #423117) from BioLegend; and TFX (the reference number has been hidden for confidentiality) from eBioscience. Annexin V-FITC Apoptosis Detection Kit (catalog # APOAF) from Sigma-Aldrich. Normal sera to block (catalog #31876 and #10410) from Invitrogen. All flow cytometry experiments were performed on a FACSCanto II (BD Biosciences), and analyzed using the FlowJo software (FLOWJO).

Intranuclear staining

For intranuclear staining, cells were fixed and permeabilized using the Foxp3 staining kit (Thermo Fisher Scientific, catalog #00-5523-00) following the manufacturer's instructions. After fixation and permeabilization, cells were incubated with the respective antibody for 15 min at 4°C in the dark, followed by washing with FACS buffer (PBS, 0.5–1% BSA or 5–10% FBS, 0.1% NaN3 sodium azide).

qRT-PCR

We isolated RNA from the experimental groups sorted through through BD™ FACS Aria Cell Sorter (BD Biosciences) with RNA isolation mini kit and synthesized cDNA by reverse transcription through RevertraAce qPCR RT Master Mix and Kit. The gene specific primer pairs used to perform quantitative real-time PCR (qRT-PCR) were designed and purchased from Eurofins Genomics. β-actin and HPRT were used as loading control.The thermal profile followed is reported below:

	50°C, 2 min	
	95°C, 2 min	
.	95 °C, 15 sec	X 40 cycles
	60°C, 1 min	
	16°C, ∞	

Data analysis was carried out with Prism Graphpad Software.

Measurement of oxygen consumption rates and extracellular acidification rate

The oxygen consumption rate (OCR) and extracellular acidification rate (ECAR) of wild type and treated cells were measured using an XF^e96 Extracellular Flux analyzer (Seahorse Biosciences, North Billerica, MA, USA). One day before the experiment, first

the XF^{e}96 plate was coated with CellTak solution as per the manufacturer's recommendation. On the day of the experiment, all chemicals (e.g. Oligomycin, FCCP, and Rotenone/Antimycin A) were prepared in OCR media as per the manufacturer's recommendation and the machine was calibrated using the calibrant buffer in the calibrant plate prior to the experiment. 400 thousand cells per well were seeded in the precoated XF^{e}96 plate and the OCR/ECAR was measured. Different parameters from the OCR graph were calculated. ATP turnover was defined as follows: (last rate measurement before oligomycin) - (minimum rate measurement after oligomycin injection). Maximal respiration was defined as follows: (maximum rate measurement after FCCP) - (non-mitochondrial respiration). Spare respiratory capacity (SRC) was calculated by subtracting basal respiration from maximal respiration. We measured the ECAR value in the same well, which contained an optimal glucose level so the basal ECAR (or glycolysis) value is the reading we obtained immediately before oligomycin injection. We prepared the assay medium as described in the XF cell Mito Stress Test Kit (Kit 103015–100). The glucose concentration in this medium is 10mM. In the classical glycolytic assay procedure (glucose-free media) the final concentration of glucose added to the port was 10mM while measuring flux. The basal ECAR value in this classical method is calculated by subtracting the last rate measurement before the glucose injection from the maximum rate measurement before the oligomycin injection. Glycolytic capacity was defined as the rate measured after the oligomycin injection. The glycolytic reserve was defined as follows: (glycolytic capacity) – (basal ECAR value).

Results

Graphic experimental workflow

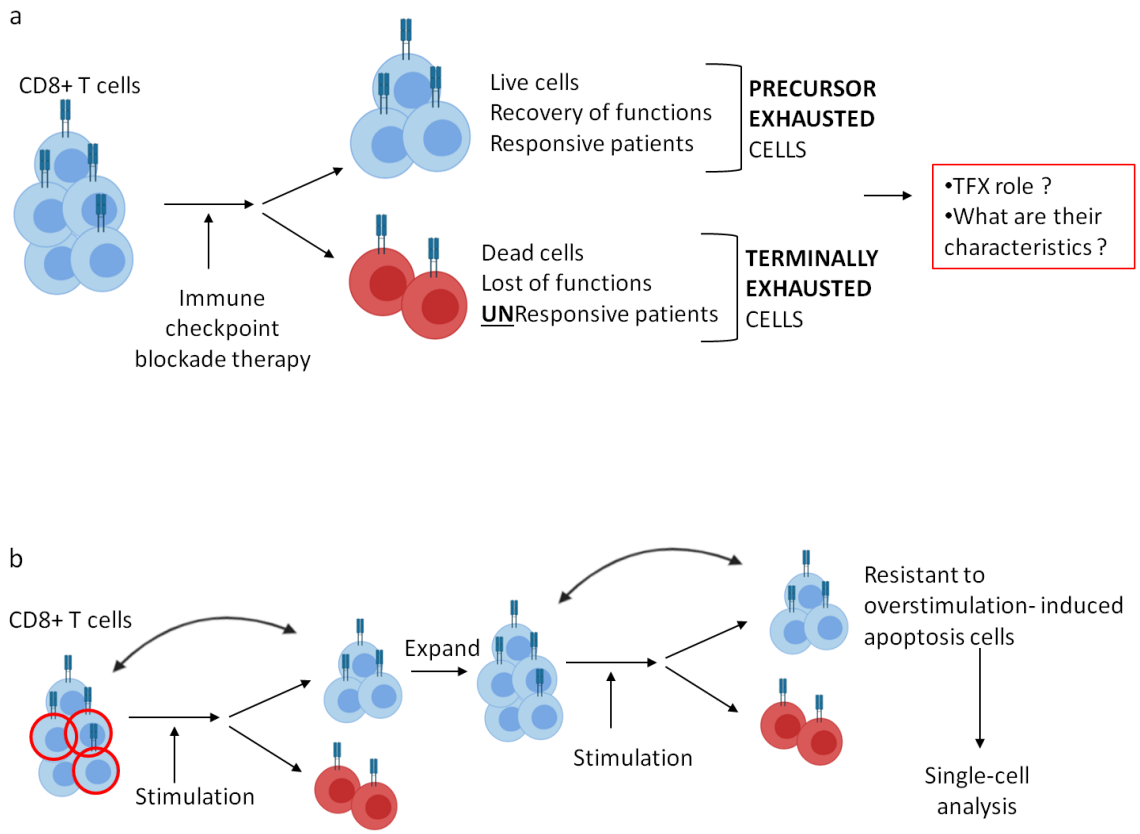

To better understand the role of TFX, two different cell lines were used: Jurkat for the human condition and TK-1 for the murine condition, with which two opposite systems of overexpression and KO were established.

Previously other groups already did these studies (not mentionables for confidentiality issues) and what was already known was that establishing the overexpression of TFX cells had:

- higher expression of inhibitory receptors;
- lower cytokines production;
- reduction of DNA damage response

and all these characteristics lead to the establishment of the exhausted phenotype of $CD8^+$ T cells.

As first step, the goal of the project was to replicate and to confirm published data and then establish the precise functional role of the transcription factor in $CD8^+$ T cells.

Overexpression of TFX

To establish the overexpression of *TFX*, *murineTFX* and *humanTFX* were cloned into pMXS-Neo vector, already available in house as pMXS-hPDL1-Neo.

MurineTFX and *humanTFX* genes were amplified via PCR from murine naïve $CD8^+$ T cells deriving from B6 wild-type mice and human total PBMC, respectively.

From the human sample also the *β-actin* gene was amplified to be used as control (Fig.1).

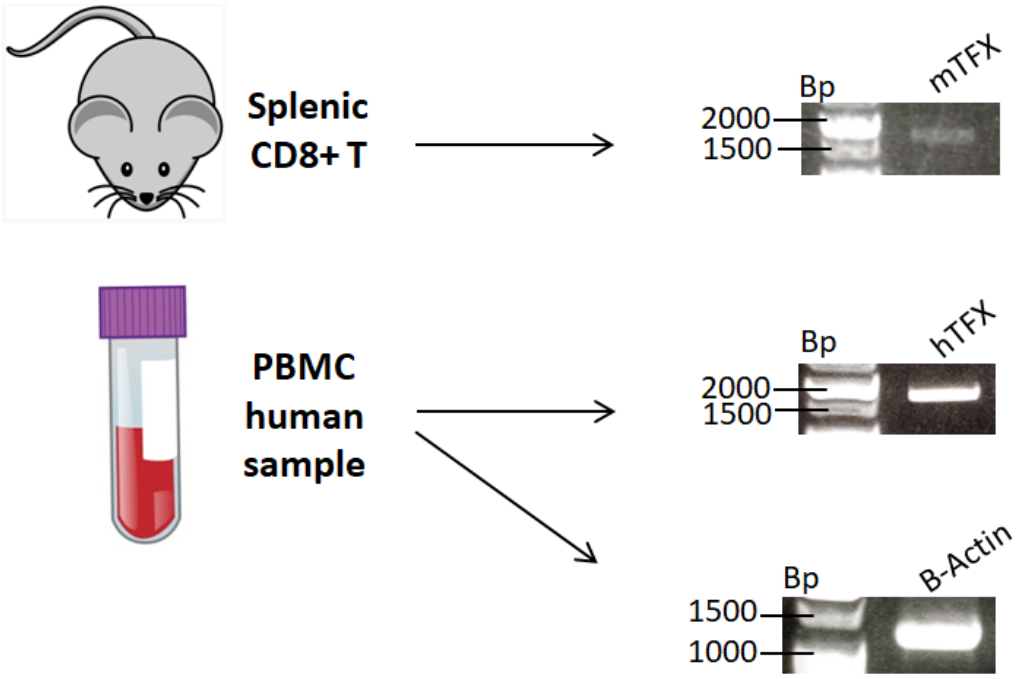

Fig. 1 *PCR results of the amplification of murineTFX, humanTFX and β-actin genes.*

Once amplified, the genes and pMXS-hPD-L1-Neo were all cut through EcoRI and XhoI restriction enzymes, thus hPD-L1 was replaced with *TFX* or *β-actin* genes, so three different vectors were cloned (Fig.2).

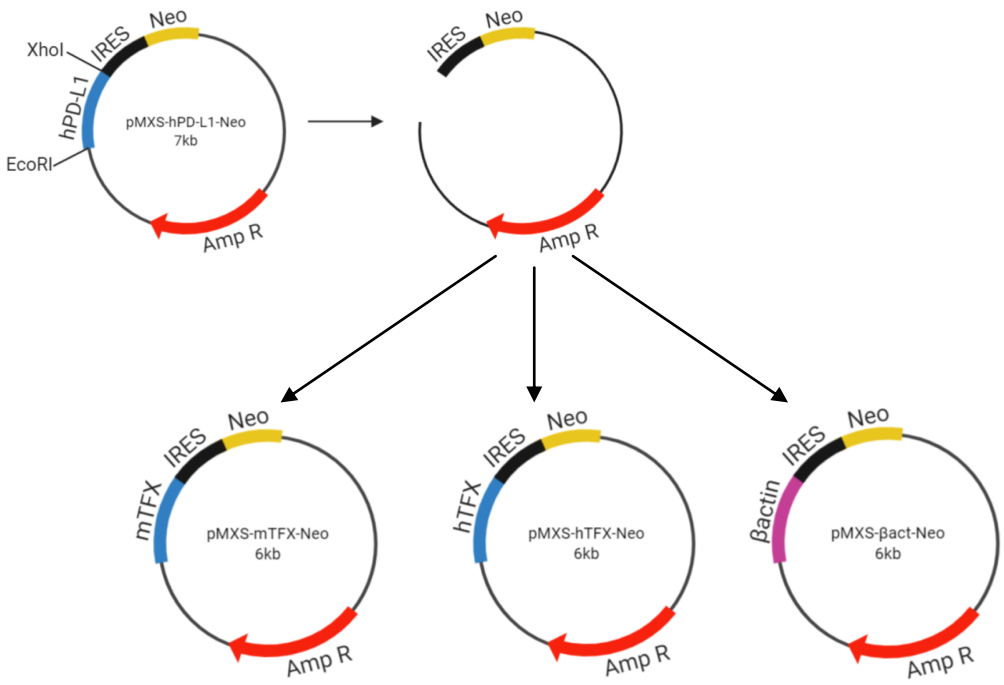

Fig.2 *Three pMXS-Neo vectors created with the addition of murine or human TFX or human β-actin genes.*

TFX genes contain many mutations

Going ahead with the sequencing step, which is expected during the cloning protocol, it was found that *TFX* genes contain many mutations. In particular, 20% of the analysed sequences were mutated in the murine vector, but 80% of the analysed sequences were mutated in the human one. Moreover, in this last one, the same mutation pattern in each analysis was found, as schematically reported in Fig.3.

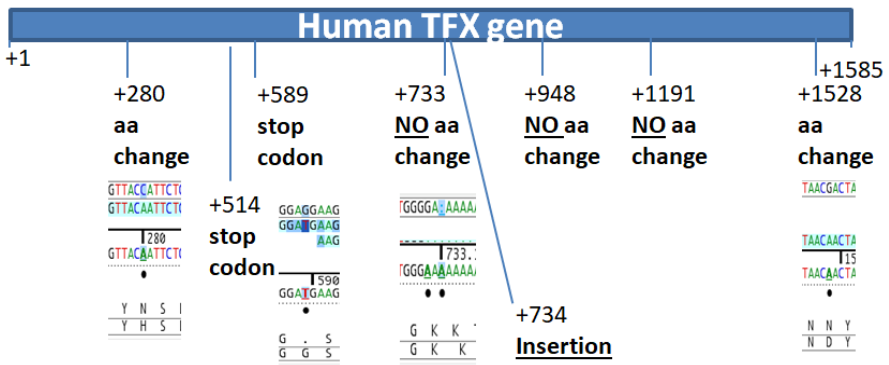

Fig.3 *Schematic representation of the mutation pattern found in the human TFX gene via sequencing analysis.*

The first explanation to this particular result was that maybe the polymerase enzyme during PCR amplification or the growth of bacteria introduced mutations. Thus, for these reasons, also the third vector holding the *β-actin* gene was analysed. Surprisingly, 0% of the analysed sequences were mutated.

To explain this result it was though that to amplify *TFX* and *β-actin* genes the total human PBMC population was taken. In this population only a low percentage of cells could express *TFX* and these presented mutations on the analysed sequences; while *β-actin,* as it is an housekeeping gene, it was expressed from the whole population in which the largest subgroup presented the right sequence of the gene. So on average the exctrated sequence of *β-actin* was correct.
If we were able to isolate only the *TFX* expressing cells, analysing all other genes it would be possible to find other mutation patterns, including in the *β-actin* gene.
These results led us to hypothesize a correlation between the expression of *TFX* genes and the accumulation of mutations. And whereas *TFX* expression is specific of exhausted T cells and its expression induced accumulation of mutations, so exhausted cells are more easily going to die.

To confirm this hypothesis, the overexpression of *TFX* was induced through the right vectors obtained from the cloning step reported before: 1x10^6 cells (Jurkat and TK-1) were electroporated; 4 days post transfection the selection agent was added (Neomycin) to select only the cells holding the correct vectors and then, between 14-21 days post transfection, the check for the establishment of the overexpression was done through PCR amplification, Western Blot and Flow cytometry analysis (Fig.4).
In all three tests the overexpression of *mTFX* was easily observable and confirmed, while for the human condition the PCR and Western Blot analysis showed a very similar expression of *hTFX* between the wt and the transfected cell lines, but then the Flow cytometry confirmed that the overexpression was successfull also in this cell line.

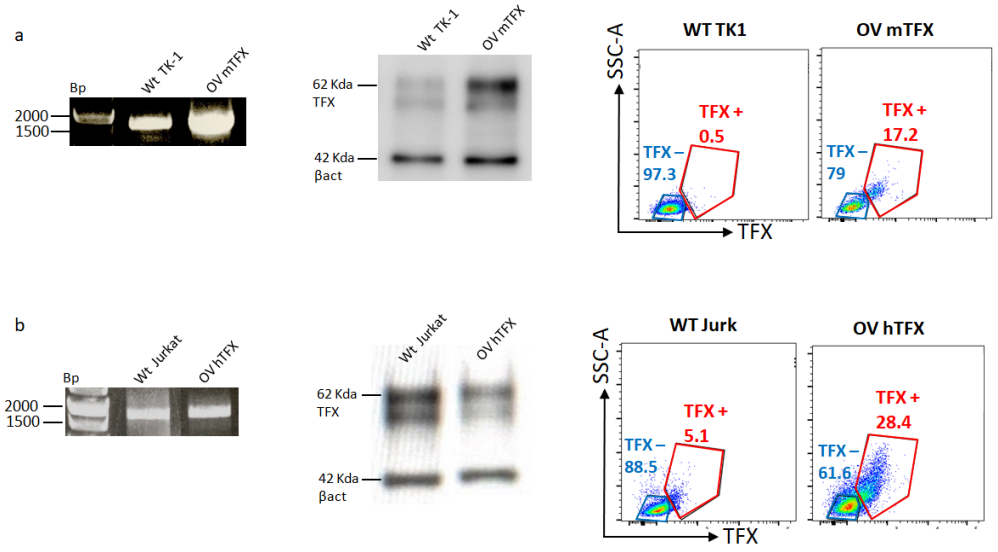

Fig.4 *PCR , Western Blot and FACS analysis results of the murine (a) and human (b) wild-type and overexpression conditions. FlowJo software was used for he analysis: gating strategy was done single cells.*

TFX overexpression uregulates inhibitory receptors expression

Once the overexpression of *TFX* was established, it was tested if the overexpression induced changes in the phenotypic expression of inhibitory receptors, as previous studies already reported.

As it is observable from Fig. 5, histograms of Flow cytometry analysis showed actually an upregulation in the expression of PD-1, TIM-3 and CXCR3 for the murine condition, while only PD-1 and TIM-3 for the human one. Meantime CTLA-4 doesn't demonstrate differences in the expression levels between the wild-type and the overexpressed cell lines.

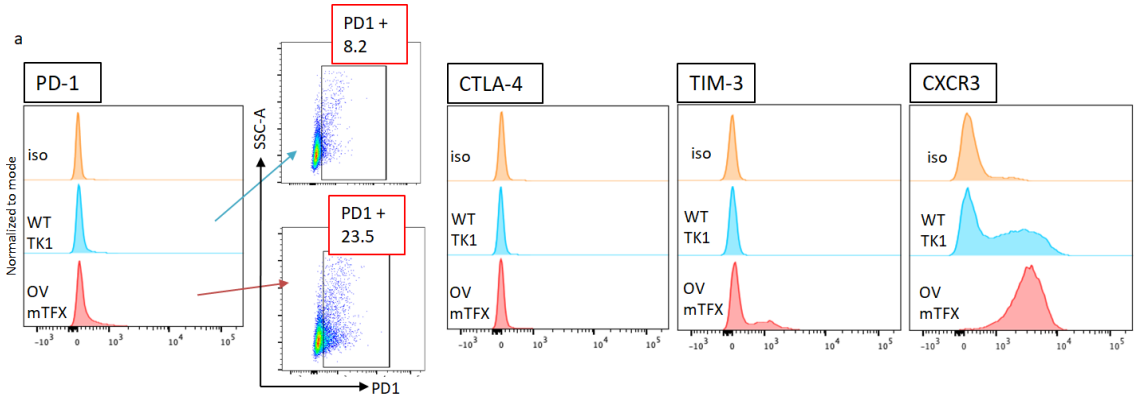

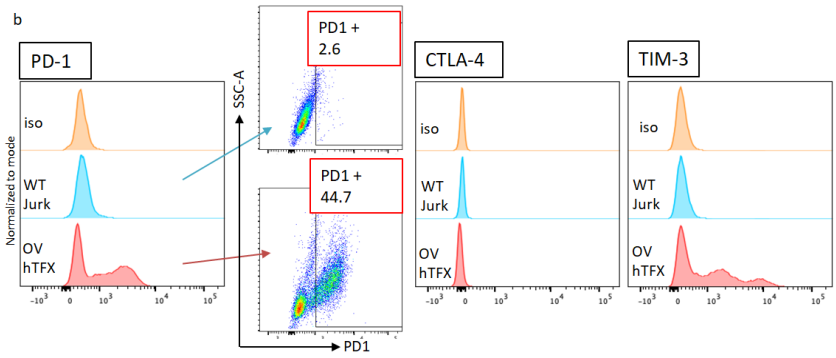

Fig.5 *Dot plots and histograms representing FACSCanto staining analysis of inhibitory receptors expression on wild-type and TFX overexpressing murine (a) and human (b) cell lines. FlowJo software was used for the analysis: gating strategy was done only on single cells.*

TFX overexpression correlates with PD-1, γH2AX and cell death

After having verified the establishment of the overexpression and that this condition really induced the phenotypic overexpression of inhibitory receptors, we went back to our previous hypothesis so to find out if TFX overexpression was correlated to exhaustion, apoptosis and the onset of mutations in the DNA, through PD-1, Zombie and γH2AX FACS staining, respectively. Thus cells were gated separately in TFX^+ and TFX^- and each group was tested first for PD-1 and Zombie: already in the wild-type cell line, the TFX^+ cells were also $PD\text{-}1^+$ and $Zombie^+$, while the TFX^- were double negative. This tendency was much more higher in the overexpressing cell line where again the TFX^- was double negative for PD-1 and Zombie staining but TFX^+ resulted double positive with a higher percentage than the wild type condition. This tendency is visible in both the murine and the human cell lines (Fig. 6a and b), confirming that there is a correlation between the expression of TFX, PD-1 and cell death.

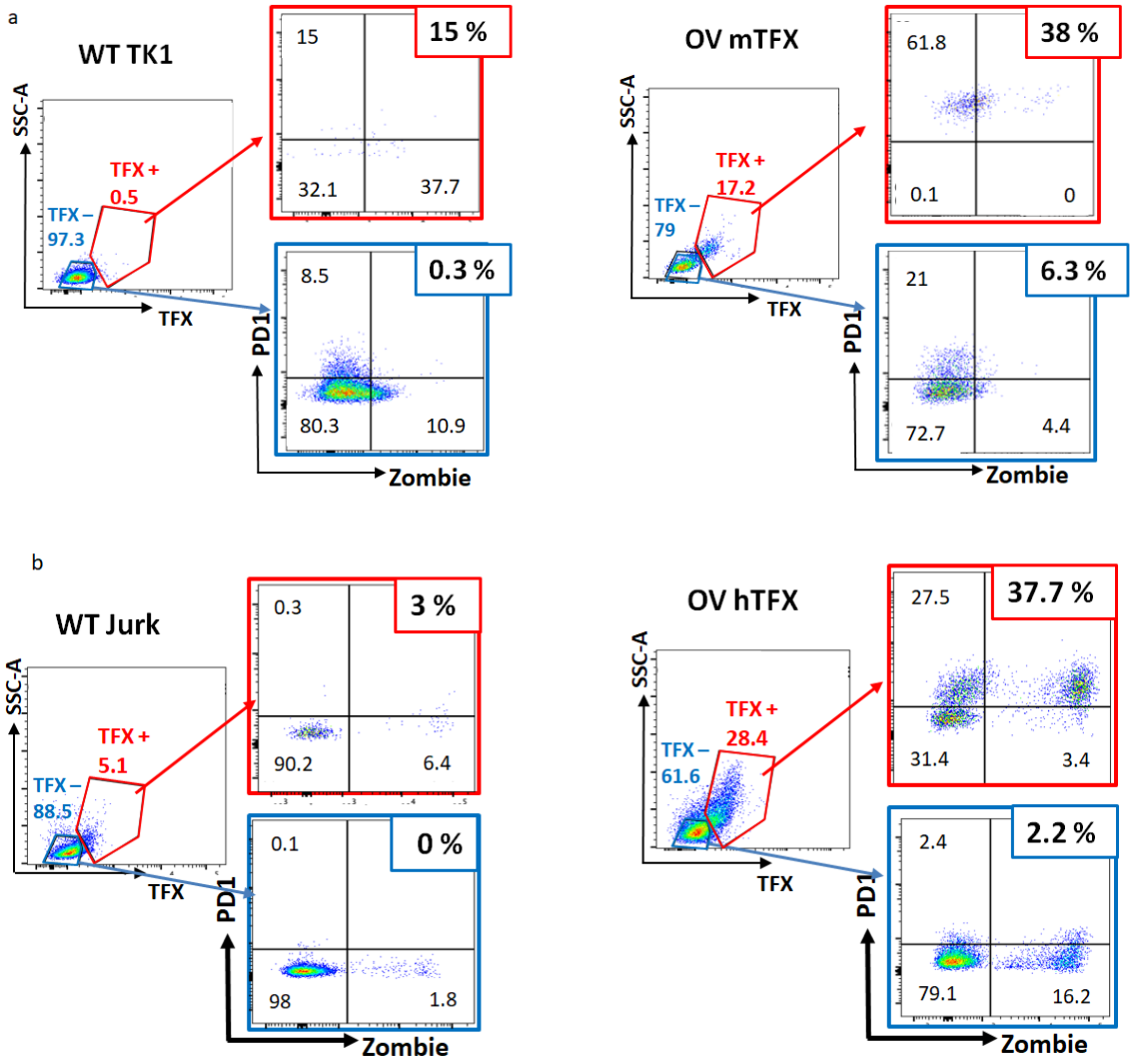

Fig.6 *Dot plots reporting FACSCanto staining analysis of TFX, PD-1 and Zombie (Live/Dead) expression on wild-type and TFX overexpressing murine (a) and human (b) cell lines. FlowJo software was used for the analysis: gating strategy was done only on single cells.*

For the human cell lines only the staining for γH2AX was done to evaluate the accumulation of mutations into the DNA. The results were the same as reported before for the cell death analysis: TFX expression was correlated to PD-1 but also to γH2AX, demonstrating so a tight link between TFX and the onset of mutations, which led and correlated to apoptosis (Fig.7).

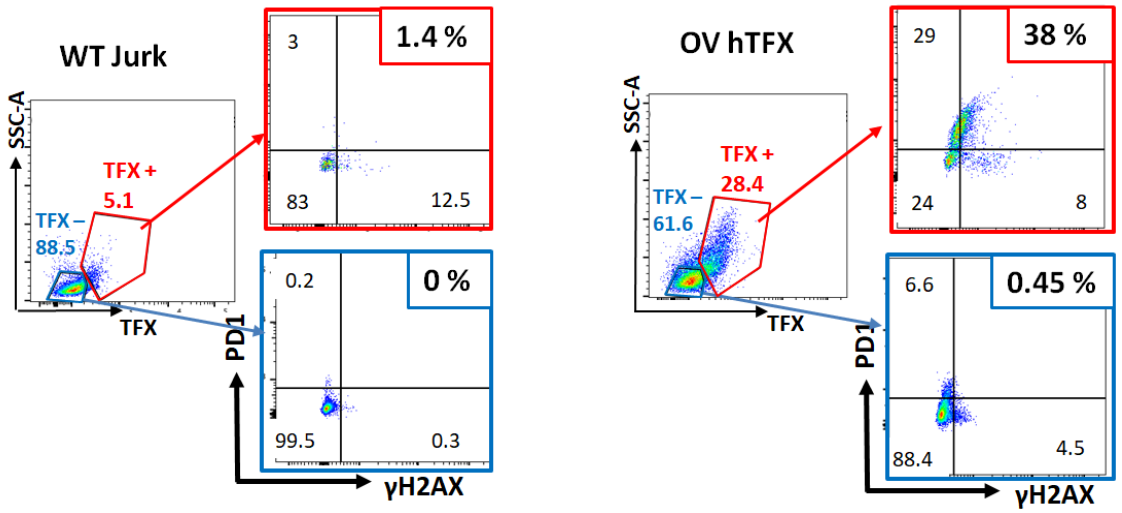

Fig.7 *Dot plots reporting FACSCanto staining analysis of TFX, PD-1 and* γH2AX *expression on wild-type and TFX overexpressing human cell lines. FlowJo software was used for the analysis: gating strategy was done only on single cells.*

Creation of pMXS-TFX-EGFP vectors

In summary, the overexpression of TFX induced an upregulation of inhibitory receptors expression, an accumulation of mutations into the DNA and induction of cell death. These results drove us to the onset of a major practical issue: long term colture of TFX overexpressing cell lines was difficult because the cells will undergo apoptosis.

For this reason new vectors pMSX-TFX-EGFP were generated, which included GFP as reporter gene, instead of the sequence which confers resistance against Neomycin agent, to get a faster selection of TFX overexpressing cells and to perform the analysis.

To create these new vectors two cloning steps were done: in the first one, EGFP sequence, extracted from pEGFP-C1 plasmid, already available in house, substituted the Neo-R sequence in the pMXS-hPD-L1-Neo plasmid (Fig.8a).

In the second step, *hPD-L1* sequence was removed with EcoRI and XhoI restriction enzymes and the two sequences of *mTFX* and *hTFX* were inserted, creating pMXS-mTFX-EGFP and pMXS-hTFX-EGFP plasmids (Fig. 8b).

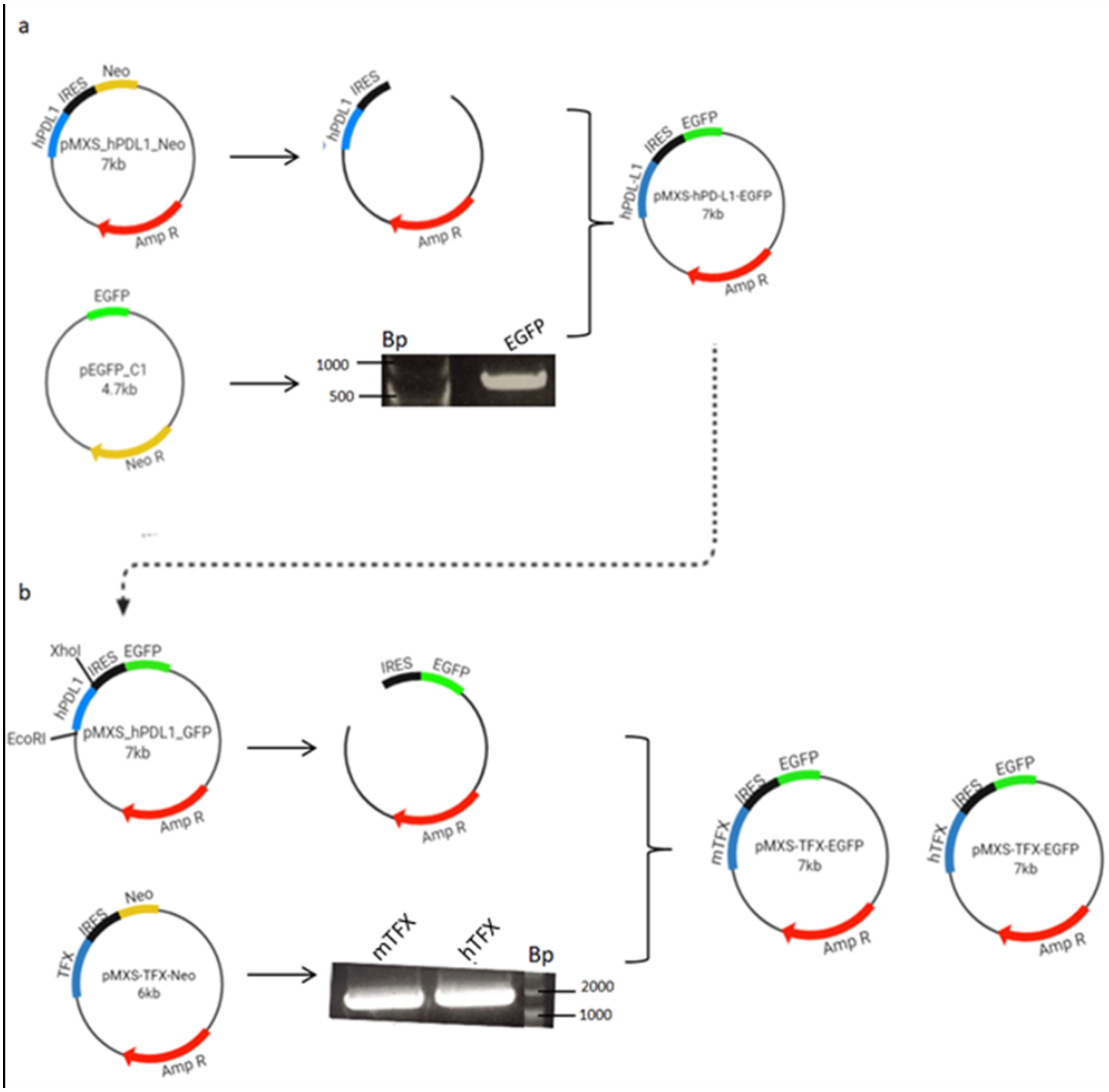

Fig.8 *Two steps of cloning to obtain pMXS-TFX-EGFP vectors.*

These plasmids will then be used to confirm the results previously obtained and to proceed with the metabolic and transcriptome analysis.

KO of TFX

To establish the KO of *TFX*, lentiviral CRISPR/CAS9 and single guide RNA were used. CRISPR (Clustered Regularly Interspaced Short Palindromic Repeats) is a microbial nuclease involved in defense against invading phages and plasmids. CRISPR loci in microbial hosts contain a combination of CRISPR-associated (CAS) genes as well as non-coding RNA elements capable of programming the specificity of the CRISPR-

mediated nucleic acid cleavage. Lentiviral CRISPR/Cas can infect a broad variety of mammalian cells by co-expressing a mammalian codon-optimized Cas9 nuclease along with a single guide RNA (sgRNA) to facilitate genome editing (*Sanjana et al*., 2014; *Shalem et al*., 2014).

The protocol used was with lentiCRISPRv2 system: this plasmid contains two expression cassettes, hSpCas9 and the chimeric guide RNA. The vector was digested using BsmBI and a pair of annealed oligos can be cloned into the single guide RNA scaffold. The oligos were designed based on the target sequences of the murine and the human *TFX* (Fig.9).

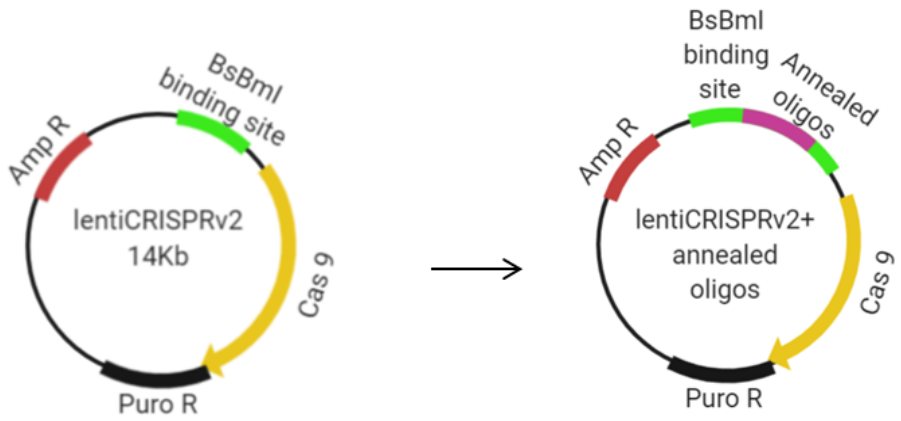

Fig.9 *Two lentiCRISPRv2 containing oligos against murine or human TFX.*

Then these vectors were inserted through electroporation in 1x10^6 cells (Jurkat and TK-1). Four days post transfection the selection agent was added (Puromycin) to select only the cells holding the correct vectors and then, between 14-21 days post transfection, the effective KO was tested by flow cytometry analysis (Fig.10).

From the analysis, the KO of the gene was successfull but, staining for Live/dead distinction with Zombie and Annexin V, the percentage of apoptotic cells was over 50% in Jurkat cells and over 90% in TK1 cell lines.

Once the resistant population was selected, the percentage of live cells should have increased. In contrast the amount of dead cells was still very high.

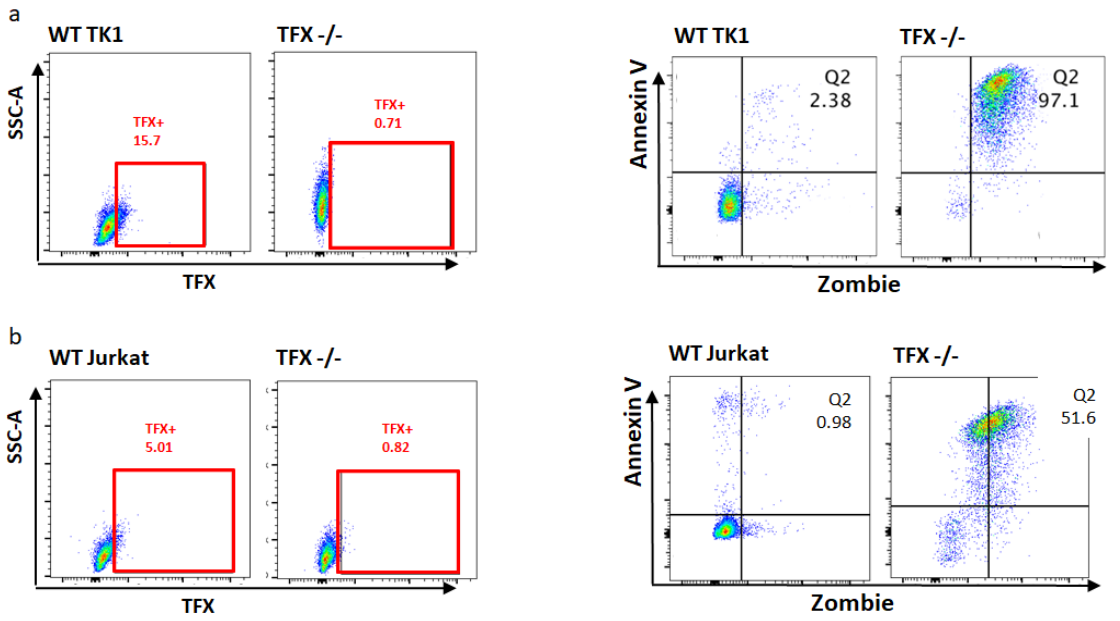

Fig.10 *Dot plots reporting FACSCanto staining analysis of TFX expression and apoptosis via Live/dead staining on wild-type and TFX -/- murine (a) and human (b) cell lines after 14-21 days post transfection. FlowJo software was used for the analysis: gating strategy was done only on single cells.*

Creation of pGuide-it-ZsGreen1 vectors

With these preliminary results it was impossible to understand if the high rate of apoptosis was due to the use of the selection agent in a not appropriate dose or to the nature of the KO condition. A previous study recently published (2019, not mentionable) demonstated that the removal of *TFX* gene blocked the cell cycle, together with the expression of caspases and induction of apoptosis.

These results were similar to the ones obtained with the overexpression condition: long term colture of TFX -/- cell lines was difficult because cells will undergo apoptosis.

For this reason we generated new vectors: pGuide-it-ZsGreen1-TFX, which included ZsGreen1 sequence, comparable to GFP, as reporter gene so it would be easier and faster to select TFX -/- and to proceed with the analysis.

To create these new vectors the linear ready-to-use pGuide-it-ZsGreen1 was used and annealed with oligos which targeted *TFX* genes (Fig. 11).

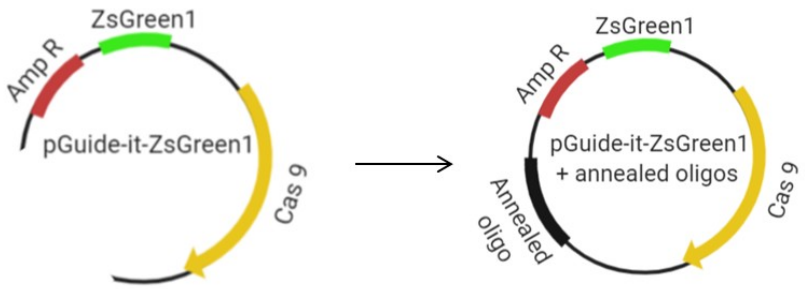

Fig.11 *Two pGuide-it-ZsGreen1 linear vectors encompassing oligos against murine or human TFX.*

Only the human cell line was kept. So the human vector was electroporated, following the protocol as before, but the selection of the right population was done immediately after (24h after transfection) through FACS sorting using FITC emission from ZsGreen1 sequence. Three different sets of oligos (thus three different plasmids were created) were used to establish the KO condition and in each of them more than 95% of cells were positive. Gating to distinguish FITC+ and FITC- groups were created and sorted via FACSAria (Fig.12).

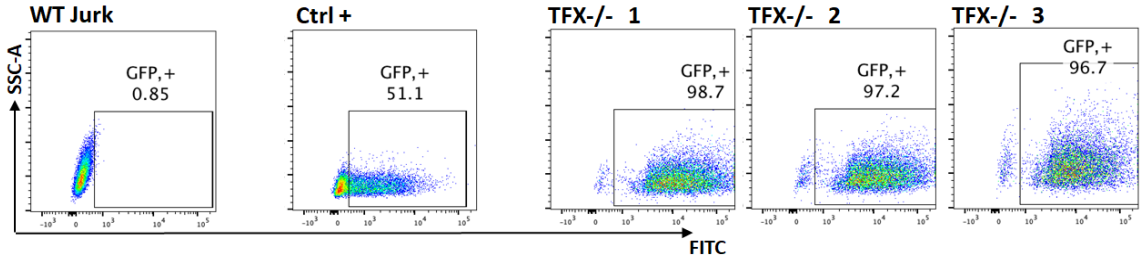

Fig.12 *Dot plots reporting FACSAria FITC emission on Jurkat cell line wild type and 24h after the transfection with GFP emitting vector as positive control (supplied by the kit) and pGuide-it-ZsGreen1 vector against human TFX gene. FlowJo software was used for the analysis: gating strategy was done on alive and single cells.*

GFP+ cells (corresponding to TFX-/- cells) were then tested to verify if the KO condition was successfull through qRT-PCR: in all three attempts there was the confirmation of the reduction of the gene expression in the KO conditions, in comparison with the wild type cell line which presented a higher basal expression of TFX (Fig. 13).

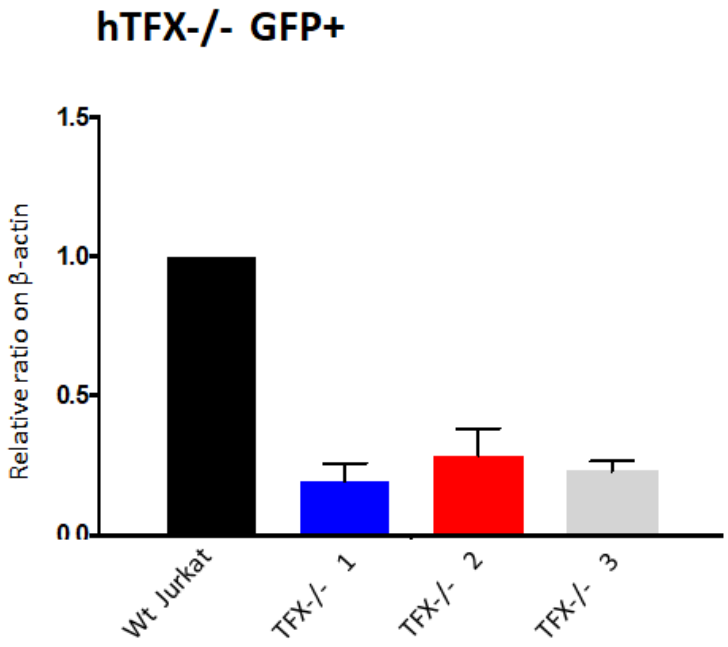

Fig.13 *Histograms representing qRT-PCR results of the relative expression of TFX in wild type and GFP+ sorted Jurkat cells. Data confirmed the reduction of TFX mRNA expression in all three transfected groups. β-actin and HPRT were used as as internal control to normalize the expression data. Data analysis was carried out with Prism Graphpad Software.*

TFX -/- doesn't change inhibitory receptors expression

Once the TFX-/- was established, it was tested if this condition induced changes in the phenotypic expression of inhibitory receptors, in correlation and comparison with the overexpression condition tested before. Fig. 14 shows the histograms from flow cytometry analysis: no significant differences in PD-1, CTLA-4 and TIM-3 expression between the wild type and TFX-/- were found. Therefore, as in the overexpression condition there was an upregulation of inhibitory receptors expression, conversely when the expression of TFX was almost completely downregulated the expression of inhibitory receptors didn't change.

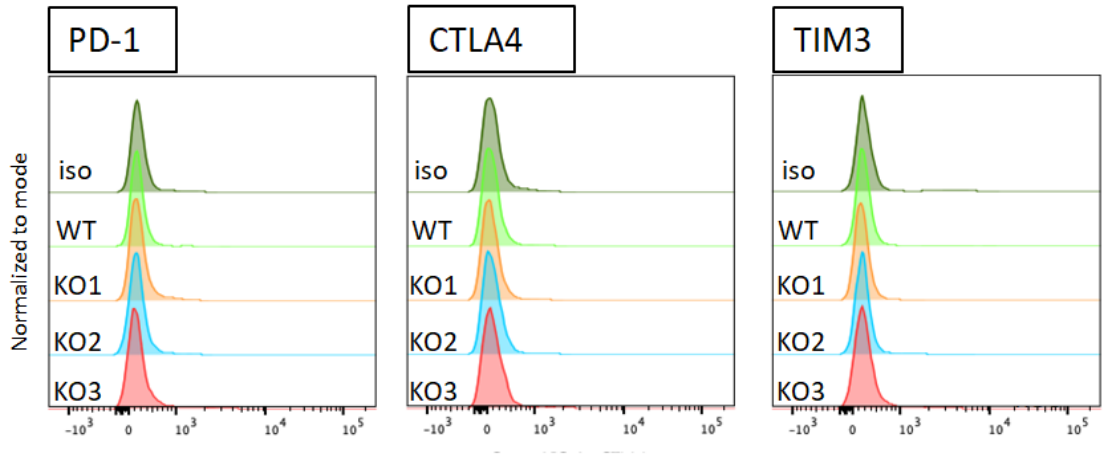

Fig.14 *Histograms representing FACSCanto staining analysis of inhibitory receptors expression on wild-type and TFX -/- (in triplicate) Jurkat cell line. FlowJo software was used for the analysis: gating strategy was done only on single cells.*

TFX reduction confirms a metabolic change in GFP+ sorted cells

A correlation between the metabolic status and the exhaustion cell phenotype has been shown. Indeed, the exhaustion phenotype could be linked to a lower mitochondrial respiration which confers to the cells a 'stand-by' condition where the cells could survive but would not recover their functions. Other groups had previously reported that TFX, as transcriptional factor, is able to bind to genes which can modulate metabolism directly or factors involved in metabolic pathways. These, in turn, are involved in the establishment of a more active or exhausted cell phenotypes. To determine whether there was an association between the TFX expression and mitochondrial activation, we measured several markers of mitochondrial activation using the Seahorse Analyzer (Fig. 15).

We found that TFX-/- Jurkat cells had significantly higher basal respiration, maximal respiration, spare respiratory capacity (SRC), and ATP turnover than the wild type (Fig. 16a). These results were then confirmed by the presentation of a higher level ECAR in the KO conditions (Fig.16b). Together, decreased TFX expression in Jurkat cells related to their activation status of mitochondria, thus a more active metabolic and in general status of cells.

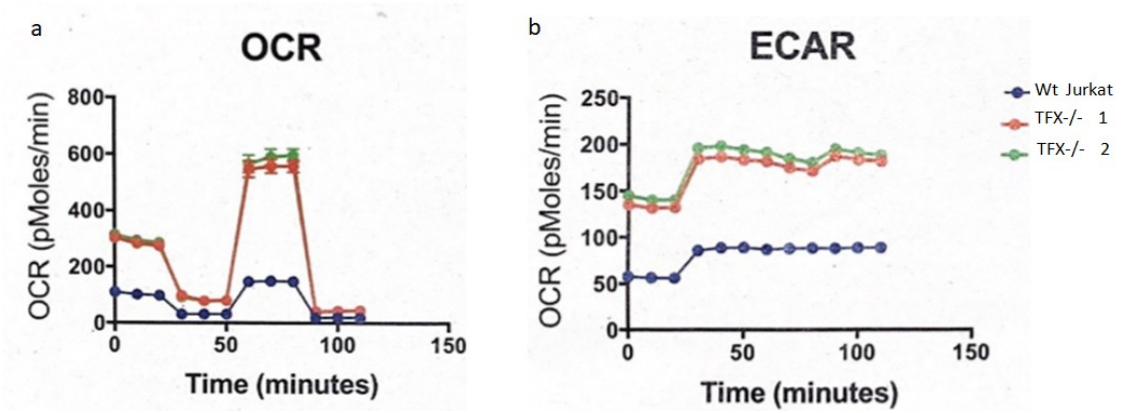

Fig.15 *Schematic representation of Oxygen consumption rates (OCR, in pMoles/min) and extracellular acidification rates (ECAR, in mpH/min) results. They were measured for wild type and TFX-/- cells (in duplicate). All measurements were normalized for cell count.*

The next plan will be to replicate and to confirm these results and, then, to proceed with the metabolic and transcriptome analysis

Discussion

Cancer biology is one of the research areas that greatly benefited from the application of single-cell omics. Thanks to this in-depth approach, it was possible to discover the mechanisms at the base of the immune checkpoint blockade and the development of treatments which have revoluzionized the way to deal to these pathologies.

However, despite the impressive success rate of PD-1 blockade therapy, still a significant fraction of patients (~40%) show unresponsiveness. Thus it is very urgent to elucidate the mechanisms for unresponsiveness and we must identify new biomarker(s) that predict this condition. The $CD8^+$ lymphocytes 'exhaustion' phenotype seems to be at the basis of the patients's unresponsiveness, which encompasses the expression of the TFX factor.

In the second study we demonstrated that the overexpression of TFX induces an upregulation of the inhibitory receptors's expression, an accumulation of mutations into the DNA and, consequently, a high rate of apoptosis, confirming the correlation between TFX expression and the loss of functionality of $CD8^+$ T lymphocytes. In the other hand, the opposite condition (TFX-/-) does not presents changes in the expression levels of inhibitory receptors in comparison with the wild type cell line, but there was the induction of an awakening of $CD8^+$ lymphocytes which recover their functions, according to a more active respiratory metabolism.

Given the central role of TFX expression in moderating various processes correlated with the exhaustion phenotype, the in-depth study of this factor, the pathways in which it is involved and the expression of which genes it is able to moderate, could be very useful to better understand the exhaustion phenotype and to discover new biomarkers.

The preliminary results that we have obtained open the way to further research work that could reveal the molecular mechanisms that are responsible of $CD8^+$ T cell exhaustion.

We aim to carry out experiments to confirm the previous results and then to perform bulk and single-cell RNA-seq analysis to focus on the discovery of new biomarkers as companion diagnostics in PD-1 new therapies.

BIBLIOGRAFY

- Alfei F., Kanev K., Hofmann M., Wu M., Ghoneim HE., Roelli P., Utzschneider DT., von Hösslin M., Cullen JG., Fan Y., Eisenberg V., Wohlleber D., Steiger K., Merkler D., Delorenzi M., Knolle PA., Cohen CJ., Thimme R., Youngblood B., Zehn D. "TFX reinforces the phenotype and longevity of exhausted T cells in chronic viral infection" *Nature* (2019);
- Altschuler SJ., Wu LF. "Cellular heterogeneity: do differences make a difference?" *Cell* (2010); **141**: 559-563;
- Aman P., Ehlin-Henriksson B., Klein G. "Eptein-Barr virus susceptibility of normal human B lymphocyte populations" *J Exp Med* (1984); **159**;
- Babcook JS., Leslie KB., Olsen OA., Salmon RA., Schrader JW. "A novel strategy for generating monoclonal antibodies from single, isolated lymphocytes producing antibodies of defined specificities" *Proc Natl Acad Sci U S A* (1996);
- Barber DL. et al. "Restoring function in exhausted CD8 T cells during chronic viral infection" *Nature* (2006); **439**: 682–687;
- Beerli RR., Rader C."Mining human antibody repertoires" *MAb*s (2010); **2**: 365-78 doi:10.4161/mAbs.12187
- Benner R., Hijmans W., Haaijman JJ. "The bone marrow: the major source of serum immunoglobulins, but still a neglected site of antibody formation" *Clin Exp Immunol* (1981); **46**:1 - 8;
- Biomarkers Definition Working Group "Biomarkers and surrogate endpoints: preferred definitions and conceptual framework" *Clin Pharmacol Therapeutics* (2001) **69**:89–95.;
- Bock C., Farlik M. and Sheffield NC. "Multi-omics of single cells: strategies and applications" *Trends Biotechnol*. (2016); **34**: 605–608. doi: 10.1016/j.tibtech.2016.04.004 ;
- Brahmer JR., Drake CG., Wollner I., Powderly JD., Picus J., Sharfman WH., Stankevich E., Pons A., Salay TM., McMiller TL., Gilson MM., Wang C., Selby M., Taube JM., Anders R., Chen L., Korman AJ., Pardoll DM., Lowy I., Topalian SL. "Phase I study of single-agent anti-programmed death-1 (MDX-

1106) in refractory solid tumors: safety, clinical activity, pharmacodynamics, and immunologic correlates" *Journal of Clinical Oncology* (2010); **28**:3167–3175; https://doi.org/10.1200/JCO.2009.26.7609;

- Brouzes E., Medkova M., Savenelli N., Marran D., Twardowski M., Hutchison JB., Rothberg JM., Link DR., Perrimon N., Samuels M.L. "Droplet microfluidic technology for single-cell high-throughput screening" *Proc. Natl. Acad. Sci. USA* (2009); **106**: 14195–14200;
- Bussard KM., Mutkus L., Stumpf K., Gomez-Manzano C., Marini FC. "Tumor-associated stromal cells as key contributo sto the tumor microenvironment" *Breast Cancer Res* (2016); **18**: 84;
- Carroll S., Al-Rubeai M. "ACSD labelling and magnetic cell separation: a rapid method of separating antibody secreting cells from non-secreting cells" *J Immunol Methods* (2005); **296**:171 - 8;
- Chen R. and Snyder M. "Promise of personalized omics to precision medicine. Wiley interdisciplinary reviews*" Systems biology and medicine*(2013); **5**(1), 73–82;
- Chen-Bettecken U., Wecker E., Schimpl A. "Transcriptional control of mu- and kappa-gene expression in resting and bacterial lipopolysaccharide-activated normal B cells" *Immunobiology* (1987); **174**:162 - 76;
- Cheung P. et al "Single-cell chromatin modification profiling reveals increased epigenetic variations with" *Aging Cell* (2018); **173:**1385–1397.e1314. https://doi.org/10.1016/j. cell.2018.03.079;
- Chihara N. et al. "Induction and transcriptional regulation of the co-inhibitory gene module in T cells" *Nature* (2018); **558**: 454–459;
- Chowdhury PS., Chamoto K., Honjo T "Combination therapy strategies for improving PD-1 blockade efficacy: a new era in Cancer immunotherapy" *Journal of Internal Medicine* (2018a); **283**:110–120. https://doi.org/10.1111/joim.12708
- Clargo A., Hudson A., Ndlovu W., Wootton R., Cremin L., O'Dowd V., Nowosad C., Starkie D., Shaw S., Compson J., White D., MacKenzie B., Snowden J., Newnham L., Wright M., Stephens P., Griffiths M., Lawson A., Lightwood D.

"The rapid generation of recombinant functional monoclonal antibodies from individual, antigen-specific bone marrow-derived plasma cells isolated using a novel fluorescence-based method". *mAbs* (2014); **6**(1): 143-159;

- Clargo AM., Hudson AR., Ndlovu W., Wootton RJ., Cremin LA., O'Dowd VL., Nowosad CR., Starkie DO., Shaw SP., Compson JE., et al. "The rapid generation of recombinant functional monoclonal antibodies from individual, antigen-specific bone marrow-derived plasma cells isolated using a novel fluorescence-based method" *mAbs* (2014); **6**:1, 143-159;
- Clark SJ., Lee HJ., Smallwood SA., Kelsey G., Reik W. !Single-cell epigenomics: powerful new methods for understanding gene regulation and cell identity" *Genome Biol* (2016); **17**: 72;
- Coronella JA., Telleman P., Truong TD., Ylera F., Junghans RP. "Amplification of IgG VH and VL (Fab) from single human plasma cells and B cells" *Nucleic Acids Res* (2000); **28**:E85;
- Di Carlo D., Wu LY., Lee LP. "Dynamic single cell culture array" *Lab Chip* (2006); **6**: 1445–1449;
- Di Niro R., Mesin L., Raki M., Zheng NY., Lund-Johansen F, Lundin KE, Charpilienne A, Poncet D, Wilson PC, Sollid LM. "Rapid generation of rotavirus-specific human monoclonal antibodies from small-intestinal mucosa" *J Immunol* (2010); **185**:5377 - 83; http://dx.doi.org/10.4049/jimmunol.1001587; PMID: 20935207;
- Dohmen SE., Mulder A., Verhagen OJ., Eijsink C., Franke-van Dijk ME., van der Schoot CE. "Production of recombinant Ig molecules from antigen-selected single B cells and restricted usage of Ig-gene segments by anti-D antibodies" *J Immunol Methods* (2005); **298**:9 - 20;
- ec.europa.eu/research/health/pdf/biomarkers-for-patient-stratification_en.pdf;
- Ecker S., Pancaldi V., Valencia A., Beck S., Paul DS. "Epigenetic and transcriptional variability shape phenotypic plasticity" *BioEssays* (2018); **40**:1700148. https://doi.org/10.1002/bies.201700148;

- Emmert-Buck MR., Bonner RF., Smith PD., Chuaqui RF., Zhuang Z., Goldstein SR., Weiss RA., Liotta LA. "Laser Capture microdissection" *Science* (1996); **274**: 998–1001. Int. J. Mol. Sci. 2015, 16 16916 23;
- Enge M., Arda HE., Mignardi M., Beausang J., Bottino R., Kim SK., Quake SR. "Single-cell analysis of human pancreas reveals transcriptional signatures of aging and somatic mutation patterns" *Cell* (2017); **171**:321–330. https://doi.org/10.1016/j.cell.2017.09.004;
- Espina V., Heiby M., Pierobon M., Liotta L.A. "Laser capture microdissection technology" *Expert Rev. Mol. Diagn*. (2007); **7**: 647–657;
- Esposito G. "Complementary techniques: Laser capture microdissection–increasing specificity of gene expression profiling of cancer specimens" *Adv. Exp. Med. Boil*. (2007); **593**: 54–65;
- Fairfax KA., Kallies A., Nutt SL., Tarlinton DM. "Plasma cell development: from B-cell subsets to long-term survival niches" *Semin Immunol* (2008); **20**:49 - 58;
- Fink L., Kwapiszewska G., Wilhelm J., Bohle M. "Laser-microdissection for cell type- and compartment-specific analyses on genomic and proteomic level" *Exp. Toxicol. Pathol*. (2006); **5**: 25–29;
- Frumkin D., Wasserstrom A., Kaplan S., Feige U., Shapiro E. "Genomic variabilità within an organism exposes its cell lineage tree" *PLoS Comput Biol* (2005); **1**: e50;
- Gallimore A., Hengartner H. & Zinkernagel R. "Hierarchies of antigen-specifc cytotoxic T-cell responses" *Immunol. Rev*. (1998); **164**: 29–32;
- Gambari R., Borgatti M., Altomare L., Manaresi N., Medoro G., Romani A., Tartagni M., Guerrieri R. "Applications to cancer research of "lab-on-a-chip" devices based on dielectrophoresis (DEP)" *Technol Cancer Res Treat* (2003); **2**: 31– 39;
- Gandini S, Massi D, Mandalà M "PD-L1 expression in cancer patients receiving anti PD-1/PD-L1 antibodies: A systematic review and meta-analysis" *Critical Reviews in Oncology/Hematology* (2016); **100**: 88–98. doi:10.1016/j.critrevonc.2016.02.001.

- Gawad C., Koh W., Quake SR. "Single-cell genome sequencing: current state of the science" *Nat Rev* (2016); **17**: 175-188;
- Ghoneim H E. et al. "De novo epigenetic programs inhibit PD-1 blockademediated T cell rejuvenation" *Cell* (2017); **170**: 142–157;
- Gomez-Sjoberg R., Leyrat AA., Pirone DM., Chen CS., Quake SR. "Versatile, fully automated, microfluidic cell culture system" *Anal.Chem.* (2007); **79**: 8557–8563;
- Grilo AL., & Mantalaris A. "The Increasingly Human and Profitable Monoclonal Antibody Market" *Trends in Biotechnology* (2018); doi:10.1016/j.tibtech.2018.05.014;
- Hafen E., Kossmann D., Brand A. "Health data cooperatives–citizen empowerment" *Methods Inf Med* (2014); **8**: 53;
- Han, Y., Liu, D., & Li, L. "PD-1/PD-L1 pathway: current researches in cancer" *American journal of cancer research* (2020); **10**(3): 727–742;
- Herzenberg, LA., Parks D., Sahaf B., Perez O., Roederer M., Herzenberg LA. "The history and future of the fluorescence activated cell sorter and flow cytometry: A view from Stanford" *Clin. Chem*. (2002); **48:** 1819–1827;
- Hodi FS., O'Day SJ., McDermott DF., Weber RW., Sosman JA., Haanen JB., Gonzalez R., Robert C., Schadendorf D., Hassel JC., Akerley W., van den Eertwegh AJ., Lutzky J., Lorigan P., Vaubel JM., Linette GP., Hogg D., Ottensmeier CH., Lebbé C., Peschel C., Quirt I., Clark JI., Wolchok JD., Weber JS., Tian J., Yellin MJ., Nichol GM., Hoos A., Urba WJ "Improved survival w*ith ipilimumab in patients with* metastatic melanoma" *New England Journal of Medicine* (2010); **363**:711–723. https://doi.org/10.1056/NEJMoa1003466;
- Hood L and Galas D"The digital code of DNA" Nature (2003); **421**:444–448;
- Hu Y., An Q., Sheu K., Trejo B., Fan S., Guo Y. "Single cell multi-omics technology: methodology and application" *Frontiers in Cell and Dev Biol* (2018); **6**: 28. Doi: 10.3389/fcell.2018.00028;
- Hurria A., Jones L., Muss HB. "Cancer treatment as an accelerated aging process: assessment, biomarkers, and interventions" *Am Soc Clin Oncol Educ Book* (2016); https://doi.org/10.1200/ EDBK_156160;

- Iwai Y., Hamanishi J., Chamoto K., Honjo T. "Cancer immunotherapies targeting the PD-1 signaling pathway" *J Biomed Sci.* (2017); **24**:26;
- J Couzin-Frankel "Breakthrough of the year 2013. Cancer immunotherapy" *Science* (2013); **342**:1432–1433. https://doi.org/10.1126/science.342.6165.1432
- Jahan-Tigh RR., Ryan C., Obermoser G., Schwarzenberger K. "Flow cytometry" *J. Investig. Dermatol*. (2012); **132**, doi:10.1038/jid.2012.282;
- Jin A., Ozawa T., Tajiri K., Obata T., Kishi H., Muraguchi A. "Rapid isolation of antigen-specific antibody-secreting cells using a chip-based immunospot array" *Nat Protoc* (2011); **6**:668 - 76;
- Jin A., Ozawa T., Tajiri K., Obata T., Kondo S., Kinoshita K., Kadowaki S., Takahas hi K., Sugiyama T., Kishi H., et al. "A rapid and efficient single-cell manipulation method for screening antigen-specific antibody-secreting cells from human peripheral blood" *Nat Med* (2009); **15**:1088 - 92;
- Kallies A., Zehn D., Utzschneider DT. "Precursor exhausted T cells: key to successful immunotherapy?" *Nat. Rev. Immunol*. (2019); **20**: 128-136;
- Kamies R., Martinez-Jimenez "Advances of single.cell genomics and epigenomics in human disease: where are we now?" Mammalian Genome (2020); 31: 170-180;
- Kodituwakku AP., Jessup C., Zola H., Roberton DM. "Isolation of antigen-specific B cells" *Immunol Cell Biol* (2003); **81**:163 - 70;
- Köhler G., Milstein C. "Continuous cultures of fused cells secreting antibody of predefined specificity" *Nature* (1975); **256**: 495-7;
- Kozbor D., Lagarde E., Roder JC. "Human hybridomas constructed with antigen-specific Epstein-Barr virus transformed cell lines" *Proc Natl Acad Sci USA* (1982); **79**: 6651-5;
- Kumar A., Chamoto K., Chowdhury PS., Honjo T." Tumors attenuating the mitochondrial activity in T cells escape from PD-1 blockade therapy" . *eLife Immunology and Inflammation* (2020); **9**:e52330. DOI: https://doi.org/10.7554/eLife.52330;

- Kwakkenbos MJ., Diehl SA., Yasuda E., Bakker AQ., van Geelen CM., Lukens MV., van Bleek GM., Widjojoatmodjo MN., Bogers WM., Mei H., et al. "Generation of stable monoclonal antibody-producing B cell receptor-positive human memory B cells by genetic programming" *Nat Med* (2010); **16**:123 - 8;
- Lagerkvist AC., Furebring C., Borrebaeck CA. "Single, antigen-specific B cells used to generate Fab fragments using CD40-mediated amplification or direct PCR cloning" *Biotechniques* (1995); **18**:862 - 9;
- Laifenfeld D., Drubin DA., Catlett NL., Park JS., Van Hooser AA., Frushour BP., de Graaf D., Fryburg DA., Deehan R. "Early patient stratification and predictive biomarkers in drug discovery and development: a case study of ulcerative colitis anti-TNF therapy" *Adv Exp Med Biol* (2012); **736**:645-53;
- Lambrechts D., Wauters E., Boeckx B., Aibar S., Nittner D., Burton O., Bassez A., Decaluwé H., Pircher A., Van den Eynde K. Et al. " Phenotype molding of stromal cells in the lung tumor microenvironment" *Nat Med* (2018); **24**: 1277-1289;
- Langreth R.,Waldholz M. "New era of personalized medicine: Targeting drugs for each unique genetic profile" *The Oncologist* (1999); **4**:426–427;
- Lapin M., Tjensvoll K., Oltedal S., Javie M., Smaaland R., Gilje B., Nordgard O. "Single-cell mRNA profiling reveals transcriptional heterogeneity among pancreatic circulating tumour cells" *BMC Cancer* (2017); **17**: 390;
- Lecault V., White AK., Singhal A., Hansen CL."Microfluidic single cell analysis: From promise to practice" *Curr. Opin. Chem. Biol*. (2012); **16**: 381–390;
- Lehrach H "Virtual clinical trials, an essential step in increasing the effectiveness of the drug development process" *Public Health Genomics* (2015); **18**(6):366–371;
- Lehrach H. "Virtual clinical trials, an essential step in increasing the effectiveness of the drug development process" *Public Health Genomics* (2015); **18**(6):366–371;

- Leyens L., Horgan D., Lal JA., Steinhausen K., Satyamoorthy K., Brand A. "Working towards personalization in medicine: main obstacles to reaching this vision from today's perspective" *Per Med* (2014); **11**(7):641–649;
- Lightwood D., O'Dowd V., Carrington B., Veverka V., Carr MD., Tservistas M., He nry AJ., Smith B., Tyson K., Lamour S., et al. "The discovery, engineering and characterisation of a highly potent anti-human IL-13 fab fragment designed for administration by inhalation" *J Mol Biol* (2013); **425**:577 - 93;
- Lightwood DJ., Carrington B., Henry AJ., McKnight AJ., Crook K., Cromie K., Laws on AD. "Antibody generation through B cell panning on antigen followed by in situ culture and direct RT-PCR on cells harvested en masse from antigen-positive wells" *J Immunol Methods* (2006); **316**:133 - 43;
- Lim BN., Tye GJ., Choong YS., Ong EBB., Ismail A., Lim TS. "Principles and application of antibody libraries for infectious diseases" *Biotechnol Lett* (2014); **36**: 2381-92 doi: 10.1007/s10529-014-1635-x
- Liu A. "Laser capture microdissection in the tissue biorepository" *J. Biomol. Tech*. (2010); **21**: 120–125:
- Ljunggren HG, Jonsson R, Hoglund P. Seminal immunologic discoveries with direct clinical implications: the 2018 nobel prize in physiology or medicine honours discoveries in cancer immunotherapy. Scand J Immunol. 2018;88:e12731;
- Lotta von Boehmer "Sequencing and cloning of antigen-specific antibodies from mouse memory B cells". *Nature protocols (2016);*
- Love JC., Ronan JL., Grotenbreg GM., van der Veen AG., Ploegh HL. "A microengraving method for rapid selection of single cells producing antigen-specific antibodies" *Nat Biotechnol* (2006); **24**:703 - 7;
- Mahoney KM., Rennert PD., Freeman GJ "Combination Cancer Immunotherapy and new immunomodulatory targets" *Nature Reviews Drug Discovery* (2015); **14**:561–584. https://doi.org/10.1038/nrd4591;
- Manaresi N., Romani A., Medoro G., Altomare L., Leonardi A., Tartagni M., Guerrieri R. "A CMOS chip for individual cell manipulation and

detection" *IEEE J. Solid-State Circuits* (2003); **38**: 2297–2305. https://doi.org/10.1109/JSSC.2003.819171;

- Manz R., Assenmacher M., Pflüger E., Miltenyi S., Radbruch A. "Analysis and sorting of live cells according to secreted molecules, relocated to a cell-surface affinity matrix" *Proc Natl Acad Sci U S A* (1995); **92**:1921 - 5;
- Manz RA, Hauser AE, Hiepe F, Radbruch A "Maintenance of serum antibody levels". *Annu Rev Immunol* (2005); **23**:367 - 86; http://dx.doi.org/10.1146/annurev.immunol.23.021704.115723;
- Manz RA., Hauser AE., Hiepe F., Radbruch A. "Maintenance of serum antibody levels" *Annu Rev Immunol* (2005); **23**:367 - 86;
- Manz RA., Thiel A., Radbruch A. "Lifetime of plasma cells in the bone marrow" *Nature* (1997); **388**:133 - 4;
- Mathur S. and Mathur S. "Personalized medicine could transform healthcare" Biomed Rep (2017); **7**: 3-5;
- McLane LM., Abdel-Hakeem MS., Wherry EJ. " CD8 T cell exhaustion during chronic viral infection and cancer" *Annu. Rev. Immunol*. (2019); **37**:457-495;
- McMillan R, Longmire RL, Yelenosky R, Lang JE, Heath V, Craddock CG "Immunoglobulin synthesis by human lymphoid tissues: normal bone marrow as a major site of IgG production". *J Immunol* (1972); **109**:1386 - 94;
- Meijer PJ., Andersen PS., Haahr-Hansen M., Steinaa L., Jensen A., Lantto J., Oleksiewicz MB., Tengbjerg K., Pouls en TR., Coljee VW., et al. "Isolation of human antibody repertoires with preservation of the natural heavy and light chain pairing" *J Mol Biol* (2006); **358**:764 - 72;
- Messenheimer DJ., Jensen SM., Afentoulis ME., Wegmann KW., Feng Z., Friedman DJ., Gough MJ., Urba WJ., Fox BA. "Timing of PD-1 blockade is critical to effective combination immunotherapy with anti-OX40" *Clin Cancer Res*. (2017); **23**:6165–6177;
- Mike Fan "Global Markets for Research Antibodies" BCC Research Report Overview (2018); BIO141B;

- Mitra AK., Mukherjee UK., Harding T., Jang JS., Stessman H., Li Y., Abyzov A., Jen J., Kumar S., Rajkumar V. Et al. "Single-cell analysis of targeted transcriptome predicts drug sensitivity of single cells within human myeloma tumors" *Leukemia* (2016); **30**: 1094-1102;
- Nakamura N., Ruebel K., Jin L., Qian X., Zhang H., Lloyd R.V. "Laser capture microdissection for analysis of single cells" *Methods Mol. Med*. (2007); **132**: 11–18;
- Naldini L. "Gene therapy returns to centre stage" *Nature* (2015); **526**: 351–360;
- Navin N., Kendall J., Troge J., Andrews P., Rodgers L., McIndoo J., Cook K., Stepansky A., Levy D., Esposito D., et al. "Tumour evolution enferred by single-cell sequencing" *Nature* (2011); **472**: 90-94;
- Ogunniyi AO., Story CM., Papa E., Guillen E., Love JC. "Screening individual hybridomas by microengraving to discover monoclonal antibodies" *Nat Protoc* (2009); **4**:767 - 82;
- Ortega MA., Poirion O., Zhu X., Huang S., Wolfgruber TK., Sebra R., et al. "Using single-cell multiple omics approaches to resolve tumor heterogeneity" *Clin. Transl. Med*. (2017); **6**:46. doi: 10.1186/s40169-017-0177-y;
- Ozawa T., Piao X., Kobayashi E., Zhou Y., Sakurai H., Andoh T., Jin A., Kishi H., M uraguchi A. "A novel rabbit immunospot array assay on a chip allows for the rapid generation of rabbit monoclonal antibodies with high affinity" *PLoS One* (2012); 7:e52383;
- Park S., Han J., Kim W., Lee GM., Kim HS. "Rapid selection of single cells with high antibody production rates by microwell array" *J Biotechnol* (2011); **156**:197 - 202;
- Pauken KE. et al. "Epigenetic stability of exhausted T cells limits durability of reinvigoration by PD-1 blockade" *Science* (2016); **354:** 1160–1165;
- Philip M. et al. "Chromatin states defne tumour-specifc T cell dysfunction and reprogramming" Nature (2017); **545:** 452–456;
- Polzer B., Medoro G., Pasch S., Fontana F., Zorzino L., Pestka A., Andergassen U., Meier-Stiegen F., Czyz ZT., Alberter B., et al. "Molecular profiling of single

circulating tumor cells with diagnostic intention" *EMBO Mol Med* (2014); **6**: 1371– 1386;

- Qian M., Wang DC., Chen H., Cheng Y. "Detection of single cell heterogeneity in cancer" *Semin Cell Dev Biol* (2017); **64**:143–149. https ://doi.org/10.1016/j.semcdb.2016.09.003;
- Radbruch A., Muehlinghaus G., Luger EO., Inamine A., Smith KG., Dörner T., Hie pe F. "Competence and competition: the challenge of becoming a long-lived plasma cell" *Nat Rev Immunol* (2006); **6**:741 - 50;
- Radpour R., Forouharkhou F. "Single-cell analysis of tumors: creating new value for molecular biomarker discovery of cancer stem cells and tumor-infltrating immune cells" *World J Stem Cells* (2018); **10:**160–171. https://doi.org/10.4252/wjsc.v10.i11.160;
- Ramskold D., Luo S., Wang YC., Li R., Deng Q., Faridani OR., Daniels GA., Khrebtukova I., Loring JF., Laurent LC. Et al. " Full-lenght mRNA-Seq from single-cell levels of RNA and individual circulating tumor cells" *Nat Biotechnol* (2012); **30**: 777-782;
- Reddy ST., Ge X., Miklos AE., Hughes RA., Kang SH., Hoi KH., Chrysostomou C., H unicke-Smith SP., Iverson BL., Tucker PW., et al. "Monoclonal antibodies isolated without screening by analyzing the variable-gene repertoire of plasma cells" *Nat Biotechnol* (2010); **28**:965 - 9;
- Redmond MJ., Leyritz-Wills M., Winger L., Scraba DG. "The selection and characterization of human monoclonal antibodies to human cytomegalovirus*" J Virol Methods* (1986); **14**: 9-24;
- Reichert JM. "Marketed therapeutic antibodies compendium" *MAbs* (2012); **4**:413 - 5; http://dx.doi.org/10.4161/mabs.19931; PMID: 22531442;
- Rial DV, Ceccarelli EA "Removal of DnaK contamination during fusion protein purification"*. Protein Expression and Purification (2002)*;
- Roden DM. "Cardiovascular pharmacogenomics: current status and future directions" *J Hum Genet* (2015); **61**(1):79–85;

- S O'Gorman, D T Fox, G M Wahl "Recombinase-mediated gene activation and site-specific integration in mammalian cells". *Science (1991);* Mar 15;**251**(4999):1351-5. doi: 10.1126/science.1900642;
- Sacher AG., Gandhi L. "Biomarkers for the clinical use of PD-1/PD-L1 inhibitors in non-small-cell lung cancer: a review" *JAMA Oncol*. (2016); **2**:1217–1222;
- Sadée W. and Dai Z. "Pharmacogenetics/genomics and personalized medicine" *Hum Mol Genet*. (2005); **14**:R207–R214;
- Saggy I., Wine Y., Shefet-Carasso L., Nahary L., Georgiou G., Benhar I. "Antibody isolation from immunized animals: comparison of phage display and antibody discovery via v gene repertoire mining" *Protein Eng Des Sel* (2012); **25**: 539-49 doi: 10.1093/protein/gzs060
- Sairamesh J and Rossbach M. "An economic perspective on personalized medicine"*HUGO J*. **7:**12013;
- Salmaninejad A., Valilou SF., Shabgah AG., Aslani S., Alimardani M., Pasdar A., Sahebkar A. "PD-1/PD-L1 pathway: basic biology and role in cancer immunotherapy" *J Cell Physiol* (2019); **234**:16824–16837;
- Sanjana NE., Shalem O., Zhang F. "Improved lentiviral vectors and genome-wide libraries for CRISPR screening" *Nature Methods* (2014);
- Sant GR., Knopf KB., Albala DM. "Live-single-cell phenotypic cancer biomarkers-future role in precision oncology?" *NPJ Precis Oncol* (2017); **1**:21. https://doi.org/10.1038/s41698-017-0025-y;
- Scheid JF., Mouquet H., Feldhahn N., Seaman MS., Velinzon K., Pietzsch J et al. "Broad diversity of neutralizing antibodies isolated from memory B cells in HIV-infected individuals" *Nature* (2009); **458**: 636-640;
- Scheid JF., Mouquet H., Feldhahn N., Walker BD., Pereyra F., Cutrell E., Seaman MS., Mascola JR., Wyatt RT., Wardemann H., et al."A method for identification of HIV gp140 binding memory B cells in human blood" *J Immunol Methods* (2009); **343**:65 - 7;
- Schietinger A. & Greenberg PD. "Tolerance and exhaustion: defning mechanisms of T cell dysfunction" *Trends Immunol*. (2014); **35:** 51–60 ;

- Shalek AK, Benson M. “Single-cell analyses to tailor treatments” *Sci Transl Med* (2017); **9**:eaan4730. https://doi.org/10.1126/ scitranslmed.aan4730;
- Shalem O., Sanjana NE., Hartenian E., Shi X., Scott DA., Mikkelsen T., Hecki D., Ebert BL., Root DE., Doench JG., Zhang F. “Genome-scale CRISPR-Cas9 Knockout screening in human cells” *Science* (2014); **343**: 83-87;
- Shapiro-Shelef M., Calame K. “Regulation of plasma-cell development” *Nat Rev Immunol* (2005); **5**:230 - 42;
- Slifka MK, Ahmed R. “Long-lived plasma cells: a mechanism for maintaining persistent antibody production”. *Curr Opin Immunol* (1998); **10**:252 - 8; http://dx.doi.org/10.1016/S0952-7915(98)80162-3;
- Slifka MK, Antia R, Whitmire JK, Ahmed R “Humoral immunity due to long-lived plasma cells”. *Immunity* (1998); **8**:363 - 72; http://dx.doi.org/10.1016/S1074-7613(00)80541-5;
- Slifka MK., Ahmed R. “Long-lived plasma cells: a mechanism for maintaining persistent antibody production” *Curr Opin Immunol* (1998); **10**:252 - 8;
- Slifka MK., Antia R., Whitmire JK., Ahmed R. “Humoral immunity due to long-lived plasma cells” *Immunity* (1998); **8**:363 - 72;
- Smith K., Garman L., Wrammert J., Zheng NY., Capra JD., Ahmed R., Wilson PC. “ Rapid generation of fully human monoclonal antibodies specific to a vaccinating antigen” *Nat Protoc* (2009); **4**:372 - 84;
- Smith KG., Light A., Nossal GJ., Tarlinton DM. “The extent of affinity maturation differs between the memory and antibody-forming cell compartments in the primary immune response” *EMBO J* (1997); **16**:2996 - 3006;
- Speiser DE. et al “T cell diferentiation in chronic infection and cancer: functional adaptation or exhaustion?” *Nat. Rev. Immunol*. (2014); **14**: 768–774;
- Stahli C., Staehelin T., Miggiano V., Schmidt J., Haring P. “High frequencues of antigen-specific hybridomas: dependence on immunization parameter and prediction by spleen cell analysis” *I Immunol Methods* (1980); **32:** 297-304;
- Staszewski R. “Cloning by limiting dilution: An improved estimate that an interesting culture is monoclonal” *Yale J. Biol. Med*. (1984); **57**: 865–868;

- Steinitz M., Klein G., Koskimies S., Makel O. “EB virus-induced B lymphocyte cell lines producing specific antibody” *Nature* (1977); **269**: 420-422;
- Striebich CC., Miceli RM., Schulze DH., Kelsoe G., Cerny J. “ Antigen-binding repertoire and IG H chain usage among B cell hybridomas from normal and autoimmune mice” *J Immunol* (1990); **144**;
- Strohl W. “Antibody Discovery: Sourcing of monoclonal antibody variable domains” *Curr Druf Discov Technol* (2014); **11**:3-19 doi:10.2174/1570163810666131120150043
- Strzelecka PM., Ranzoni AM., Cvejic A. “ Dissecting human disease with single-cell omics: application in model systems and in the clinic” *The Company of Biologists* (2018); **11**: dmm036525. Doi:10.1242/dmm.036525;
- Strzelecka PM., Ranzoni AM., Cvejic A. “Dissecting human disease with single-cell omics: application in model systems and in the clinic” *Dis Models Mech* (2018); **11**:36525. https://doi.org/10.1242/ dmm.036525;
- Svensson V., Natarajan KN., Ly LH., Miragaia RJ., Labalette C., MacAulay IC., et al. “Power analysis of single-cell RNA-sequencing experiments” *Nat. Methods* (2017); **14**: 381–387. doi: 10.1038/nmeth.4220;
- Syn N., Teng M., Mok T., Soo R. "De-novo and acquired resistance to immune checkpoint targeting" *The Lancet Oncology* (2017); **18** (12): e731–e741. doi:10.1016/s1470-2045(17)30607-1;
- Tarlinton DM., Smith KG. “Apoptosis and the B cell response to antigen” *Int Rev Immunol* (1997); **15**:53 - 71;
- Tarlinton DM., Smith KG. “Dissecting affinity maturation: a model explaining selection of antibody-forming cells and memory B cells in the germinal centre” *Immunol Today* (2000); **21**:436 - 41;
- Tenny S., Varacallo M. “Evidence-based Medicine” StatPearls [Internet]. Treasure Island (FL): StatPearls Publishing; 2020 Jan-. Available from: https://www.ncbi.nlm.nih.gov/books/NBK470182/;
- Tiller T. “Single B cell antibody technologies” *N Biotechnol* (2011); **28**:453 - 7; http://dx.doi.org/10.1016/j.nbt.2011.03.014;

- Tirosh I., Suvà ML. "Deciphering human tumor biology by singlecell expression profling" *Annu Rev Cancer Biol* (2019); **3**:151–166. https ://doi.org/10.1146/annurev-cancerbio-030518-055609;
- Topalian SL., Drake CG., Pardoll DM "Immune checkpoint blockade: a common denominator approach to Cancer therapy" *Cancer Cell*(2015); **27**:450–461; https://doi.org/10.1016/j.ccell.2015.03.001;
- Townsend SE., Goodnow CC., Cornall RJ. "Single epitope multiple staining to detect ultralow frequency B cells" *J Immunol Methods* (2001); **249**:137 - 46;
- Trusheim MR., Burgess B., Xinghua Hu S., Long T., Averbuch SD., Flynn AA., Lieftucht A., Mazumder A., Milloy A., Shaw AP., Swank D., Wang J., Berndt ER., Goodsaid F., Palmer MC. "Quantifying factors for the success of stratified medicine*" Nature Reviews Drug Discovery* (2011); **10**:11;
- Underwood AP., Bean PA. "Hazards of the limiting-dilution method of cloning hybridomas" *J. Immunol. Methods* (1988); **107:** 119–128;
- Utzschneider DT. et al. "T cells maintain an exhausted phenotype after antigen withdrawal and population reexpansion" *Nat. Immunol*. (2013); **14**: 603–610;
- Van den Brink SC., Sage F., Vértesy A., Spanjaard B., Peterson-Maduro J., Baron CS., Robin C., van Oudenaarden A. "Single-cell sequencing reveals dissociation-induced gene expression in tissue subpopulations" *Nat Methods* (2017); **14**: 935-936;
- Vogenberg FR., Barash C., Isaacson and Pursel M. "Personalized medicine: Part 1: Evolution and development into theranostics" *P T.* (2010); **35**:560–576. PubMed/NCBI Vogenberg FR., Barash CI. and Pursel M. "Personalized medicine: Part 2: Ethical, legal, and regulatory issues" *P T.* (2010); **35**:624–642. PubMed/NCBI
- Wang J., Song Y. "Single cell sequencing: a distinct new feld" *Clin Transl Med* (2017); **6**:10–10. https://doi.org/10.1186/s4016 9-017-0139-4;
- Wang X, Teng F, Kong L, Yu J "PD-L1 expression in human cancers and its association with clinical outcomes". *OncoTargets and Therapy* (2016). **9**: 5023–39. doi:10.2147/OTT.S105862.

- Wang Y. and Navin NE. “Advances and applications of single-cell sequencing technologies” *Mol. Cell* (2015); **58**, 598–609. doi: 10.1016/j.molcel.2015.05.005;
- Weber J "Immune checkpoint proteins: a new therapeutic paradigm for cancer--preclinical background: CTLA-4 and PD-1 blockade". *Seminars in Oncology* (2010); **37** (5): 430–9. doi:10.1053/j.seminoncol.2010.09.00;
- Wherry EJ. “T cell exhaustion” *Nat. Immunol (2011);* **12**: 492–499;
- Wieland D. et al. “TCF1+ hepatitis C virus-specifc CD8+ T cells are maintained after cessation of chronic antigen stimulation” Nat. Commun. (2017); **8**: 15050
- Yoshimoto N., Kida A., Jie X., Kurokawa M., Iijima M., Niimi T., Maturana AD., Ni kaido I., Ueda HR., Tatematsu K., et al. “An automated system for high-throughput single cell-based breeding” *Sci Rep* (2013); **3**:1191;
- Youngblood B. et al. “Chronic virus infection enforces demethylation of the locus that encodes PD-1 in antigen-specifc CD8+ T cells” *Immunity* (2011); **35**: 400–412;
- Yu X., McGraw PA., House FS., Crowe JE Jr. “ An optimized electrofusion-based protocol for generating virus-specific human monoclonal antibodies” *J Immunol Methods* (2008); **336**:142 - 51;
- Zhang K., Han X., Li Y., Li SY., Zu Y., Wang Z., Qin L. “Hand-held and integrated single-cell pipettes” *J. Am. Chem. Soc.* (2014); **136**: 10858–10861;

ACKNOLEDGEMENTS

I would like to remember all those who helped me in the drafting with suggestions, criticisms and observations: my gratitude goes to them, even if I bear the responsibility for every error contained in this work.

Fist of all, I would like to thank my tutors Prof.ssa Ottavia Spiga, Dott.ssa Cristina Tinti and Prof.ssa Paola Ricciardi-Castagnoli for welcoming me into the PhD and Research worlds, for the precious teachings they gave me during my years of study and for their wise guidance.
I would like to thank also Luigi Ricciardi for the support he always gave me.

Special thanks go to the TLS Foundation who hosted me in their building and laboratories. All people gave me life- and science-lessons and they made long days in the lab more carefree.

A special thanks goes to the TLS lab members Andrea Avati, Erika Bellini, Vittoria Cicaloni, Ilaria Maffei, Marco Rossi, Laura Salvini, Laura Tinti and Silvia Valensin, for the example they gave me that I consider unforgettable, of how it is possible to love and make people love the study of science, through dialogues and comparisons that are never trivial but, indeed, always constructive. It is an important baggage that I will take everywhere with me. They soon became friends, to whom I hope to be able to carry out all their projects in the workplace and in the personal one. I love you.

Thanks to Distinguished Prof. Tasuku Honjo and Prof. Kenji Chamoto and to all the lab members Alok Kumar, Keiko Yurimoto, Yoko Kitawaki, Yuka Nakajima, Muna Al-Habsi, Maryam Akrami, Rosie Menzies, Tomoko Hirano, Kana Yamasaki, Moto Shimazaki. Thanks for hosting me in their lab, for the support and affection that they have been able to give me in a short time and for always supporting and encouraging each other. Thank you for the precious teachings and for sharing with me the achievement of this

goal. I really hope to have the opportunity to see you and to work with you again very soon.

I turn to thank my family. Thanks to my uncles, Beatrice, Riccardo, Grazia and Sandro, and to my cousin-sister Linda, for always encouraging me and for their discreet but always present and caring attention. I thank in a special way my grandmother Attilia who has always been by my side, even when there was mid-globe between us, and who contributed, in her own way, to achieving this result.

A heartfelt thanks then goes to the Triade, Patcha and Dani, great listeners and supporters. Our bond is so strong that it would have been impossible not to mention you in these aknoledgements. We have always supported each other, in good and bad times, both during the hardships and despair that characterized our path, and in the moments of joy and satisfaction. I love you.

Thanks to Lise, sister not by blood but by choice, whose great strength, energy and charisma she manages to transmit to me. Thank you for the self-esteem you are able to instill in me and for always holding my hand on this path.

All new and old friends (all but absolutely all!) have had a decisive role in achieving this result, the point of arrival and at the same time the starting point of my life. Thanks to all the girls of the gym, to Serena, Kenta, Giuseppe and Luigi with who I shared my amazing experience in Kyoto and to all-time friends Gabriele, Benedetta, Giuditta for sharing the most important experiences with me over the years. I love you.

Finally, my heartfelt thanks go to my parents who, with their sweet and tireless support, have allowed me to get here in front of you today, contributing to my personal formation and to have such of once-in-a-lifetime experiences. Thanks to my father, who even though he may not yet have understood what I am doing, has always observed and watched over me and always understood without many words. Finally, thanks to

my mother that, even it wasn't a simply period to be so distant, she was always there supporting me. Thanks because I know that every time I thought of giving up, she gave me her strength and her courage to carry on. You are my myth and I want to fight to reach what I really want from life too, as you have always taught me.